Science with Spectral Distortions of the Cosmic Microwave Background

CUSO Lectures 2014

Jens Chluba (Johns Hopkins University)

October 24, 2014

Contents

1 Overview and motivation **5**
- 1.1 Why are spectral distortions interesting today? . . . 5
- 1.2 Overview of the different lectures and their goals . . . 7

2 Blackbody radiation **9**
- 2.1 What is a blackbody? . . . 9
- 2.2 Photon occupation number, energy and number density . . . 11
- 2.3 What do we need to do to change the blackbody temperature? . . . 12

3 Formulation of the thermalization problem **15**
- 3.1 What is the thermalization problem all about? . . . 15
- 3.2 General conditions and assumption . . . 15
  - 3.2.1 Which epochs do we need to worry about? . . . 17
  - 3.2.2 Perturbation in the cosmic fluid and spectral distortions . . . 18
  - 3.2.3 Electron temperature and ordinary matter distribution functions . . . 19
- 3.3 Photon Boltzmann equation in the expanding Universe . . . 21
  - 3.3.1 Liouville operator and gravitational effects . . . 21
  - 3.3.2 Photon collision term . . . 23
  - 3.3.3 Compton scattering . . . 23
  - 3.3.4 Bremsstrahlung . . . 27
  - 3.3.5 Double Compton scattering . . . 30
- 3.4 Final set of evolution equations . . . 36

4 Simple Analytic Approximations **39**
- 4.1 Compton-y distortion and the thermal Sunyaev-Zeldovich effect . . . 39
  - 4.1.1 Scattering of CMB photons in the limit of small y. . . . 39
  - 4.1.2 Thermal Sunyaev-Zeldovich effect . . . 41
- 4.2 Chemical potential or μ-distortion . . . 42
  - 4.2.1 Compton equilibrium solution . . . 42
  - 4.2.2 Definition of the μ-distortion . . . 43
  - 4.2.3 Simple zeroth order description of primordial distortions . . . 45
- 4.3 Evolution of the photon distribution by Compton scattering . . . 46
  - 4.3.1 Doppler-dominated scattering . . . 46
  - 4.3.2 Recoil-dominated scattering . . . 46
  - 4.3.3 Background-induced stimulated scattering . . . 47
- 4.4 Evolution under free-free absorption only . . . 50
- 4.5 Inclusion of photon production and the distortion visibility function . . . 51
  - 4.5.1 Quasi-stationary solution for the shape of the chemical potential distortion at $x \ll 1$ . . . 52

4.5.2 Single energy release and the distortion visibility function 54
4.5.3 Improved description of primordial distortions 56
4.6 Refined computation of the distortion visibility function 56

5 Green's function method **57**
5.1 Spectral distortion in the transition between the μ and y-eras 57

Chapter 1

Overview and motivation

Cosmology is now a precise scientific discipline, with detailed theoretical models that fit a wealth of very accurate measurements. Of the many cosmological data sets, the cosmic microwave background (CMB) temperature and polarization anisotropies provide the most stringent and robust constraints to theoretical models, allowing us to determine the key parameters of our Universe and address fundamental questions about inflation and early-universe physics. Clearly, by looking at the statistics of the CMB anisotropies with different experiments over the past decades we have learned a lot about the Universe we live in, establishing the *era of precision cosmology*, establishing the ΛCDM concordance model [2, 41].

But the hunt continues. Today we are in the position to ask exciting questions about extensions of the standard cosmological model. For instance, what do the CMB anisotropies tell us about the era of Big Bang Nucleosynthesis (BBN), most importantly about the primordial helium abundance, $Y_{\rm p}$? How many neutrino species are there in our Universe, a question that often is addressed through the effective number of relativistic degree's of freedom, $N_{\rm eff}$. What are the neutrino masses and their hierarchy? Are there some decaying or annihilating particles? What about dark radiation? And regarding the initial conditions of our Universe: what is the running of the power spectrum of curvature perturbations? How about the gravitational wave background, parametrized in form of the tensor-to-scalar ratio, r, which determines the energy scale of inflation, at least when assuming the standard inflation scenario. And to top it up, what about dark energy and the accelerated expansion of our Universe?

All these questions are very exciting and define todays cutting-edge research in cosmology, driving present-day theoretical and experimental efforts. The CMB anisotropies in combination with large-scale structure, weak lensing and supernova observations deliver ever more precise answers to these questions. But the CMB holds another, complementary and independent piece of invaluable information: its *frequency spectrum*. Departures of the CMB frequency spectrum from a pure blackbody – commonly referred to as *spectral distortion* – encode information about the thermal history of the early Universe (from when it was a few month old until today). Since the measurements with COBE/FIRAS in the early 90's, the average CMB spectrum is known to be extremely close to a perfect blackbody at a temperature $T_0 = (2.726 \pm 0.001)$K [23, 22] at redshift $z = 0$, with possible distortions limited to one part in 10^5. This impressive measurement was awarded the Nobelprize in Physics 2006 and already rules out cosmologies with extended periods of significant energy release, disturbing the thermal equilibrium between matter and radiation in the Universe.

1.1 Why are spectral distortions interesting today?

So far no spectral distortion of the average CMB spectrum were found. Then, why is it at all interesting to think about spectral distortions now? First of all, there is a long list of processes that could lead to spectral distortions. These include: *reionization* and *structure formation*; *decaying* or *annihilating particles*; *dissipation*

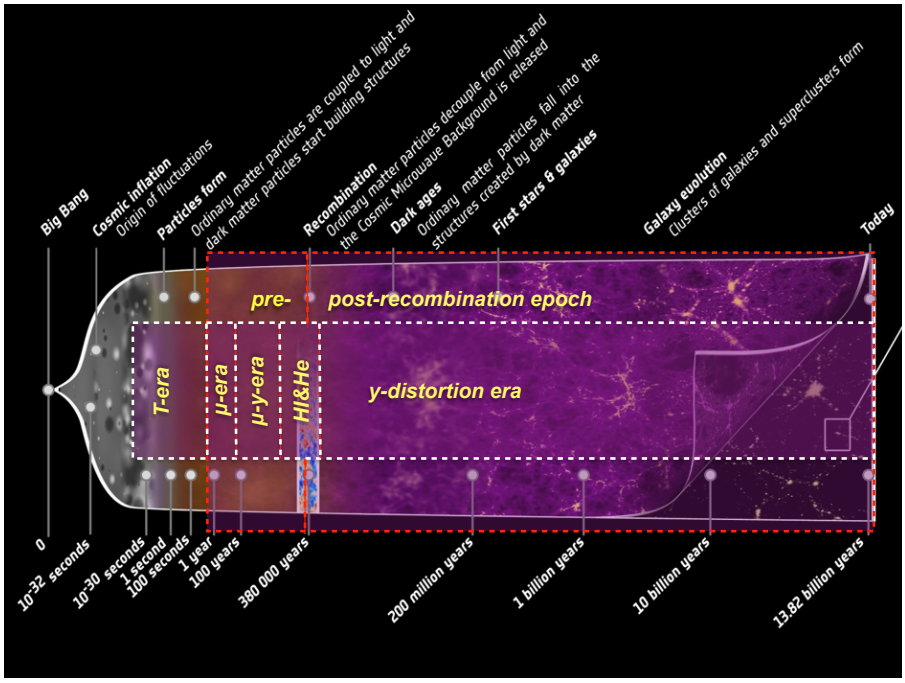

Figure 1.1: CMB spectral distortions probe the thermal history of the Universe at many stages during the pre- and post-recombination era. Energy release at $z \gtrsim$ few $\times\, 10^6$ only causes a change of the CMB temperature. A μ-type distortion arises from energy release at $3 \times 10^5 \lesssim z \lesssim$ few $\times\, 10^6$, while a y-type distortions is created at $z \lesssim 10^4$. The signal caused during the μ/y-transition era ($10^4 \lesssim z \lesssim 3 \times 10^5$) is described by a superposition of μ- and y-distortion with some small *residual* distortion that allows probing the time-dependence of the energy-release mechanism. In the recombination era ($10^3 \lesssim z \lesssim 10^4$), additional spectral features appear due to atomic transitions of hydrogen and helium. These could allow us to distinguish pre- from post-recombination y-distortions (Figure adapted from [1]).

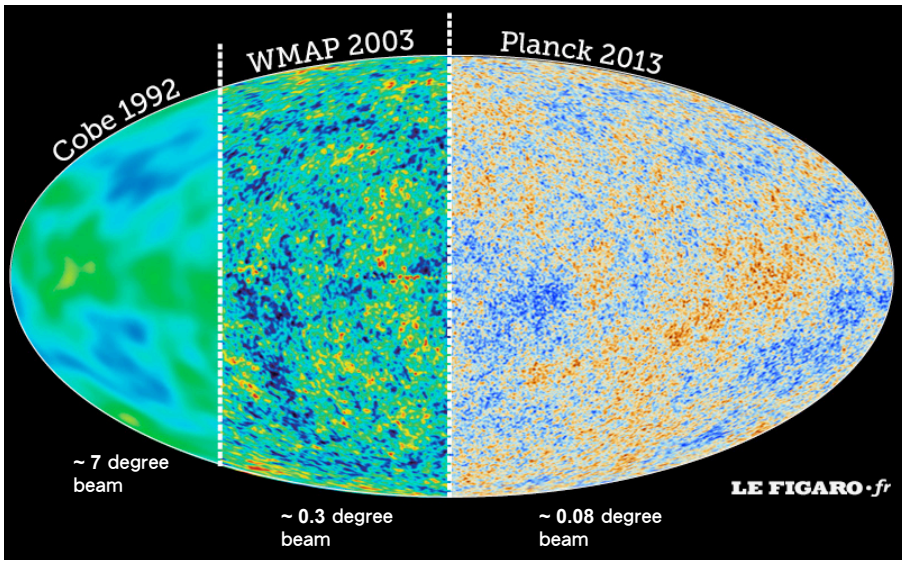

Figure 1.2: Over the past decades CMB experiments have seen a dramatic improvement in sensitivity and angular resolution, here illustrated with a comparison of COBE, WMAP and PLANCK. In contrast, CMB spectral distortion measurements are still in the state of some 20+ years ago, with COBE/FIRAS still being the standard.

of primordial density fluctuations; *cosmic strings*; *primordial black holes*; *small-scale magnetic fields*; the *adiabatic cooling of matter*; *cosmological recombination*; and several new physics examples [e.g., see 8, for overview]. This certainly makes theorists very happy, but most importantly, many of these processes (e.g., reionization and cosmological recombination) are part of our standard cosmology and therefore should lead to guaranteed signals to search for. This shows that studies of spectral distortions offer both the possibility to *constrain well-known physics* but also to open up a *discovery space* for non-standard physics and adding *time-dependent information* to the picture (Fig. 1.1).

The second reason for spectral distortion being interesting is due to technological advances. Although measurements of the CMB temperature and polarization anisotropies have improved significantly in terms of angular resolution and sensitivity since COBE/DMR, our knowledge of the CMB spectrum is still in a similar state as more than 20 years ago (Fig. 1.2). This could change dramatically in the future with experimental concepts like PIXIE [35] and PRISM [1] being discussed. These types of experiments could possibly improve the limits of COBE/FIRAS by more than three orders of magnitude, providing a unique way to learn about processes that are otherwise hidden from us. At this stage, CMB spectral distortion measurements are furthermore only possible from space, so that in contrast to B-mode polarization science competition from the ground is largely excluded, making CMB spectral distortions a unique target for future CMB space missions [48]. This immense potential of spectral distortions was also recently in the NASA 30-year Roadmap study, where improved characterization of the CMB spectrum was declared as one of the future targets [37].

1.2 Overview of the different lectures and their goals

The main goal of the lectures is to convince you that CMB spectral distortion studies will provide us with a new and immensely rich probe of early-universe physics, making it an exciting future direction of cosmology. In the first lecture, introduces a few simple relations for blackbody radiation and then focusses on deriving the evolution equations for the photon field and ordinary matter (electrons + baryons). In the second lecture, simple analytic solutions and the different types of spectral distortions will be introduced. The distortion visibility function and approximate representations of the distortions will be discussed as well as fast but precise numerical schemes. The third lecture will provide and overview for different sources of distortions. Particular attention will be payed to the dissipation of small-scale perturbations and decaying particle scenarios. In the fourth and final lecture, the physics of recombination and the recombination radiation will be discussed as well as computation of Sunyaev-Zeldovich signals from clusters and what one may be able to learn from this.

Chapter 2

Blackbody radiation

2.1 What is a blackbody?

When hearing the term 'blackbody', one usually thinks of an insulated cavity (German: *Hohlraum*) with perfectly absorbing walls that is internally in thermodynamic equilibrium at a fixed temperature T. In this case, the radiation field inside the cavity (viewed through a *tiny* hole) is described by a blackbody spectrum, $B_\nu(T)$, which only has one free parameter, the thermodynamic temperature T (Fig. 2.1).

A theoretical explanation for the precise energy/frequency dependence of $B_\nu(T)$ caused much confusion at the end of the nineteenth century. The shape of $B_\nu(T)$ was known experimentally, but the problem was that thinking of the cavity being filled with a bunch of electromagnetic waves (modes) and performing simple mode counting with $E = kT$ per mode gives a divergent result for the photon energy density. *Max Planck* eventually solved the problem in 1901 by quantizing the photon energy[1], $E = h\nu$, yielding *Planck*'s law:

$$B_\nu(T) = \frac{2h}{c^2}\frac{\nu^3}{\mathrm{e}^{h\nu/kT} - 1}. \tag{2.1}$$

Planck's law determines the intensity of photons per unit frequency. Intensity has units

$$[B_\nu(T)] = \mathrm{ergs\,sec^{-1}\,cm^{-2}Hz^{-1}sr^{-1}} = 10^{17}\,\mathrm{MJy\,sr^{-1}}. \tag{2.2}$$

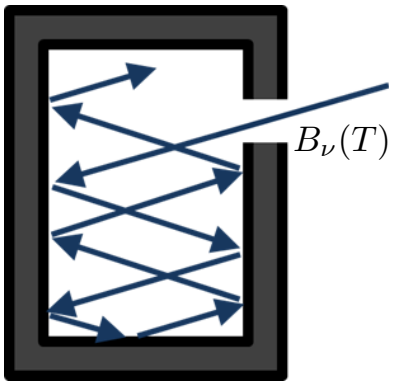

Figure 2.1: Blackbody cavity – The radiation field inside this ideal cavity is given by the Planck law once sufficient time has passed to reach equilibrium.

The spectrum of the Sun is approximately represented by this expression (let's be a theorist and forget about all the Fraunhofer lines and existence of the atmosphere with all its absorption bands) with a temperature $T_{\mathrm{ph}} \simeq 6000\,\mathrm{K}$ (photosphere). Also, we already heard about the CMB blackbody spectrum, which is really unbelievably close to a blackbody with $T_0 = 2.725\,\mathrm{K}$ [23].

The shape of the blackbody spectrum for different temperatures is illustrated in Fig. 2.2. We can see that at low frequencies, the blackbody spectrum scales as

$$B_\nu(T) \overset{h\nu \ll kT}{\approx} \frac{2\nu^2}{c^2} kT \propto \nu^2 T, \tag{2.3}$$

which is also known as *Rayleigh-Jeans* law, while in the other extreme the blackbody spectrum falls off exponentially, following the *Wien* law:

$$B_\nu(T) \overset{h\nu \gg kT}{\approx} \frac{2h\nu^3}{c^2}\mathrm{e}^{-h\nu/kT}. \tag{2.4}$$

[1] Planck found this relation empirically but *Albert Einstein* later explained it in connection with the photoelectric effect.

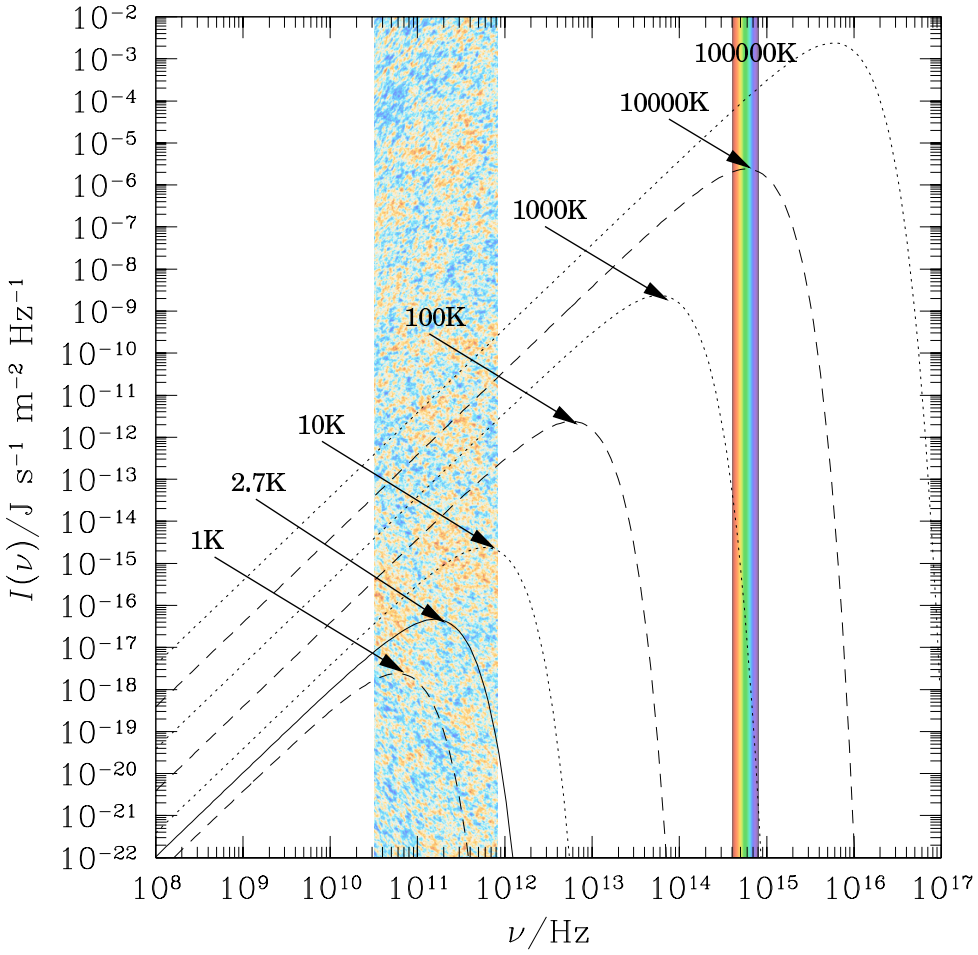

Figure 2.2: Blackbody spectrum for different temperatures. The intensity maximum is roughly at $\nu_{\max} \approx 58.8\,\mathrm{GHz\,K^{-1}}\,T$, which for the CMB blackbody today is $\nu_{\max} \simeq 160\,\mathrm{GHz}$ or at 2 mm wavelength. For $T \simeq 10^4\,\mathrm{K}$ the intensity maximum is in the visible part of the electromagnetic spectrum.

The Rayleigh-Jeans law also follows from simple mode-counting, but it vastly overestimates the blackbody intensity at high frequencies, leading to an *ultraviolet catastrophe*. In this case, the discrete quantum nature of the photons must be taken into account. The Wien law, on the other hand, can be guessed when you think of moving thermal charges emitting radiation: the velocity distribution (Maxwell-Boltzmann distribution) cuts off exponentially so that the highest frequency photon distribution should also show this energy dependence. The Planck law does the trick in both regimes.

Wien's displacement law For a blackbody spectrum, the maximum of the intensity *per unit wavelength* $[I_\lambda = I_\nu(\,\mathrm{d}\nu/\,\mathrm{d}\lambda) = I_\nu/(c\lambda^2)]$ according to *Wien's displacement law* is located at

$$\lambda_{\max} \approx \frac{2.898\,\mathrm{K\,mm}}{T}. \tag{2.5}$$

In terms of intensity per unit frequency (which we will use), from Eq. (2.1) one can find

$$\nu_{\max} \approx 58.8\,\mathrm{GHz\,K^{-1}}\,T \approx 160\,\mathrm{GHz}\left[\frac{T}{2.725\,\mathrm{K}}\right], \tag{2.6}$$

$$\lambda_{\max} \approx \frac{5.10\,\mathrm{K\,mm}}{T} \approx 1.87\,\mathrm{mm}\left[\frac{T}{2.725\,\mathrm{K}}\right]^{-1}, \tag{2.7}$$

which shows that the CMB spectrum peaks at about 2 millimeter wavelength or a frequency of about 160 GHz.

2.2 Photon occupation number, energy and number density

The Planck law specifies the spectral intensity of a blackbody. If we multiply this by $1/c$, we have the specific energy density of photons, $U_\nu = B_\nu/c$ (definition of energy $\mathrm{d}E = U_\nu\,\mathrm{d}V\,\mathrm{d}\Omega\,\mathrm{d}\nu$ with $\mathrm{d}V = c\,\mathrm{d}A\,\mathrm{d}t$ versus $\mathrm{d}E = I_\nu\,\mathrm{d}A\,\mathrm{d}t\,\mathrm{d}\Omega\,\mathrm{d}\nu$). This corresponds to $U_\nu \equiv$ (photon energy $\times$ specific state density $\times$ mean occupation number). The photon energy is $E = h\nu$ and the specific density of states is[2] $2\nu^2/c^3$, where the factor of 2 accounts for the two polarizations of the photon. Thus the *photon occupation number for a blackbody* is

$$n_{\mathrm{Pl}} = \frac{c^3 U_\nu(T)}{2h\nu^3} = \frac{c^2 B_\nu(T)}{2h\nu^3} = \frac{1}{\mathrm{e}^{h\nu/kT} - 1} = \frac{1}{\mathrm{e}^x - 1}, \tag{2.8}$$

where for convenience we introduced $x = h\nu/kT$ ($x = 1$ corresponds to $\nu \approx 56.8$ GHz). For a blackbody, the occupation number drops exponentially in the Wien tail and diverges as $n_{\mathrm{Pl}} \simeq 1/x$ in the Rayleigh-Jeans part of the spectrum. The '$-$' sign in the denominator of Eq. (2.8) shows that photon follow *Bose-statistics* (they are social and bunch up in phase space) with zero chemical potential (photons do not have a rest mass). Similarly, for general photon distribution, with intensity $I_\nu(\boldsymbol{x}, \hat{\boldsymbol{\gamma}})$ at location $\boldsymbol{x}$ and in different directions $\hat{\boldsymbol{\gamma}}$, the *photon occupation number* is given by

$$n_\nu(\boldsymbol{x}, \hat{\boldsymbol{\gamma}}) = \frac{c^2 I_\nu(\boldsymbol{x}, \hat{\boldsymbol{\gamma}})}{2h\nu^3}. \tag{2.9}$$

The photon occupation number is very useful, since it is Lorentz-invariant, $n'_{\nu'} \equiv n_\nu$, in two inertial frames S and S' moving relative to each other. The specific intensity transforms as $(I'_{\nu'}/\nu'^3) \equiv (I_\nu/\nu^3)$ [Exercise 1].

[2] $2\,\mathrm{d}^3k/(2\pi)^3 = 2/(2\pi)^3 \times k^2\,\mathrm{d}k\,\mathrm{d}\Omega = 2/(2\pi)^3(2\pi/\lambda)^2\,\mathrm{d}(2\pi/\lambda)\,\mathrm{d}\Omega = 2(\nu/c)^2\,\mathrm{d}(\nu/c)\,\mathrm{d}\Omega = (2\nu^2/c^3)\,\mathrm{d}\nu\,\mathrm{d}\Omega$

Photon energy and number density To obtain the photon energy density, we just need to integrate the specific energy density over all directions and frequencies,

$$\rho_\gamma = \int U_\nu \,\mathrm{d}\nu\,\mathrm{d}\Omega = \frac{2}{c^3}\int E\,\nu^2 n_\nu \,\mathrm{d}\nu\,\mathrm{d}\Omega \equiv \int E\,f\,\mathrm{d}^3p, \tag{2.10}$$

where $p = E/c = h\nu/c$ is the photon momentum. Similarly, for the number density we have

$$N_\gamma = \int \frac{U_\nu}{h\nu}\,\mathrm{d}\nu\,\mathrm{d}\Omega = \frac{2}{c^3}\int \nu^2 n_\nu \,\mathrm{d}\nu\,\mathrm{d}\Omega \equiv \int f\,\mathrm{d}^3p. \tag{2.11}$$

For blackbody radiation this simply gives

$$\begin{aligned}\rho_\gamma^{\rm Pl} &= \frac{2h}{c^3}\int \frac{\nu^3}{\mathrm{e}^x-1}\,\mathrm{d}\nu\,\mathrm{d}\Omega = \frac{8\pi h}{c^3}\left(\frac{kT}{h}\right)^4\int\frac{x^3\,\mathrm{d}x}{\mathrm{e}^x-1} = \frac{8\pi^5(kT)^4}{15\,c^3h^3}\\ &= a_R T^4 \approx 5.10\times10^{-7}\,m_{\rm e}c^2{\rm cm}^{-3}\left(\frac{T}{2.725{\rm K}}\right)^4 \approx 0.26\,{\rm eV}\left(\frac{T}{2.725{\rm K}}\right)^4 \end{aligned}\tag{2.12}$$

$$\begin{aligned}N_\gamma^{\rm Pl} &= \frac{2}{c^3}\int \frac{\nu^2}{\mathrm{e}^x-1}\,\mathrm{d}\nu\,\mathrm{d}\Omega = \frac{8\pi}{c^3}\left(\frac{kT}{h}\right)^3\int\frac{x^2\,\mathrm{d}x}{\mathrm{e}^x-1} = \frac{16\pi\zeta_3(kT)^3}{c^3h^3}\\ &= b_R T^3 \approx 410\,{\rm cm}^{-3}\left(\frac{T}{2.725{\rm K}}\right)^3, \end{aligned}\tag{2.13}$$

where ζ_i denotes the Riemann ζ-function. Here, $a_R = 4\sigma/c \approx 7.566\times10^{-15}\,{\rm ergs\,cm^{-3}\,K^{-4}}$ is the *radiation constant*, where σ is the *Stefan-Boltzmann constant*. We also have the useful relation $\rho_\gamma^{\rm Pl} \approx 2.701kTN_\gamma^{\rm Pl}$. In particular, we have $\rho_\gamma^{\rm Pl}\propto T^4$ and $N_\gamma^{\rm Pl}\propto T^3$.

2.3 What do we need to do to change the blackbody temperature?

Blackbody radiation is fully characterized by one number, its temperature T. Thus, one simple question is, *what do we have to do to change the temperature to $T'\neq T$*. Let's suppose we increase the temperature by adding some energy to the photon field (let's say we just move all photons upwards in frequency in some way; no change of the volume or photon number), $\epsilon = \Delta\rho_\gamma/\rho_\gamma^{\rm Pl}(T) \equiv (T'/T)^4 - 1$, then the expected change in the photon temperature is

$$\frac{\Delta T}{T} = (1+\epsilon)^{1/4} - 1 \approx \frac{1}{4}\frac{\Delta\rho_\gamma}{\rho_\gamma^{\rm Pl}}. \tag{2.14}$$

Clearly, if we stopped here, the new spectrum cannot be a blackbody anymore, since we did not change the photon number density. To keep the blackbody relation $N_\gamma^{\rm Pl}\propto T^3$ unchanged we *simultaneously* need to add

$$\frac{\Delta N_\gamma}{N_\gamma^{\rm Pl}} = (T'/T)^3 - 1 = (1+\epsilon)^{3/4} - 1 \approx 3\frac{\Delta T}{T} \quad\Longrightarrow\quad \frac{\Delta N_\gamma}{N_\gamma^{\rm Pl}} \equiv \frac{3}{4}\frac{\Delta\rho_\gamma}{\rho_\gamma^{\rm Pl}} \tag{2.15}$$

of photons to avoid creating a non-blackbody spectrum. This condition is *necessary but not sufficient*, since it does not specify *how* the missing photons are distributed in energy! Let us assume we add photons to the blackbody spectrum at one frequency only. Then $\Delta\rho_\gamma = h\nu\Delta N_\gamma$ and $\epsilon = (h\nu/2.701kT)\,\Delta N_\gamma/N_\gamma^{\rm Pl}$, so that to satisfy the condition Eq. (2.15), we just need to tune the frequency to $h\nu/kT \equiv (4/3)\,2.70 \approx 3.60$. Clearly, a blackbody spectrum with a single line at $h\nu \simeq 3.6\,kT$ is no longer a blackbody even if Eq. (2.15) is satisfied.

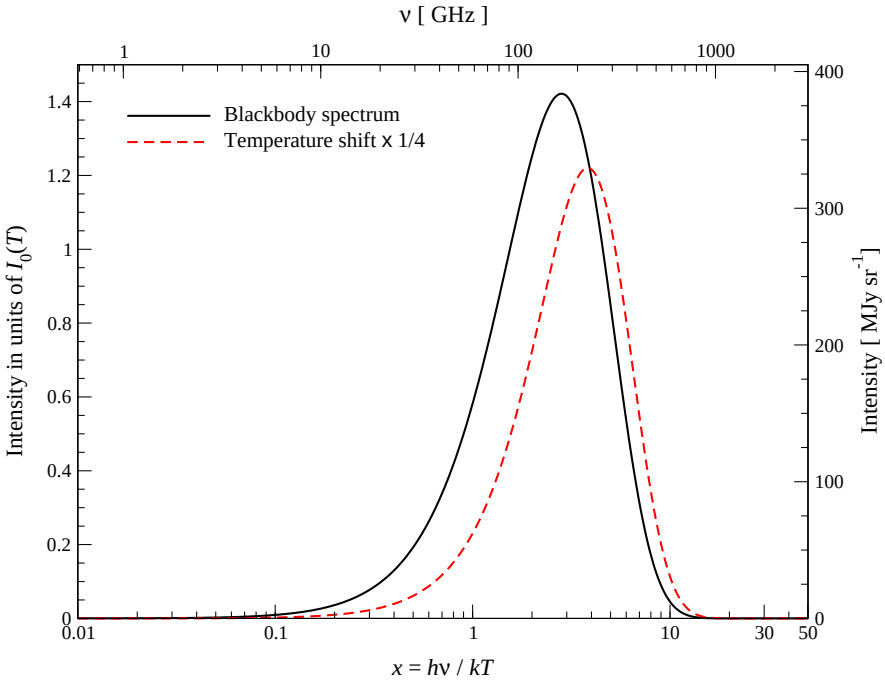

Figure 2.3: Blackbody spectrum and the spectrum of a temperature shift, $T\partial_T B_\nu = I_0(T)\, x^3 G(x) = -I_0(T)\, x^4 \partial_x n_{\rm Pl}(x)$. For convenience, we plot the spectrum as a function of $x = h\nu/kT$ and normalize the left y-axis by $I_0(T) = (2h/c^2)(kT/h)^3 \approx 270\,{\rm MJy\,sr^{-1}}(T/2.725{\rm K})^3$ [the shown curves are basically $x^3/({\rm e}^x - 1)$ and $x^3 G(x)$]. The maximum of the blackbody is at $x \approx 2.821$ ($\equiv$ 160GHz), while the maximum of the temperature shift is at $x \simeq 3.830$ ($\equiv$ 217GHz). The upper x-axis and right y-axis also give the corresponding frequency and spectral intensity for $T = 2.725\,{\rm K}$.

To go from one blackbody to another we need to have a change of the photon occupation number by

$$\Delta n_\nu = n_{\rm Pl}(T') - n_{\rm Pl}(T) = \frac{1}{{\rm e}^{x'} - 1} - \frac{1}{{\rm e}^x - 1} = -x\partial_x n_{\rm Pl}\,\frac{\Delta T}{T} + O(\Delta T/T)^2 = \frac{x{\rm e}^x}{({\rm e}^x - 1)^2}\,\frac{\Delta T}{T} + O(\Delta T/T)^2 \quad (2.16)$$

with $x' = x\,T/T'$. In what follows, we will frequently use the definition

$$G(x) = -x\partial_x n_{\rm Pl} = \frac{x\,{\rm e}^x}{({\rm e}^x - 1)^2} \approx \begin{cases} \frac{1}{x} & \text{for} \quad x \ll 1 \\ x{\rm e}^{-x} & \text{for} \quad x \gg 1. \end{cases} \quad (2.17)$$

which determines the *spectrum of a temperature shift*, $T\partial_T B_\nu \propto x^3 G(x)$, for small $\Delta T/T$. Its spectral shape is shown in Fig. 2.3.

Let's check if Eq. (2.16) really plays out. We first define the integrals (we already know them from above)

$$G_k^{\rm Pl} = \int \frac{x^k\,{\rm d}x}{{\rm e}^x - 1} = k!\zeta(k+1) \quad (2.18)$$

$$G_2^{\rm Pl} = \int \frac{x^2\,{\rm d}x}{{\rm e}^x - 1} = 2\zeta_3 \approx 2.4041 \quad (2.19)$$

$$G_3^{\rm Pl} = \int \frac{x^3\,{\rm d}x}{{\rm e}^x - 1} = 6\zeta_4 = \frac{\pi^4}{15} \approx 6.4939, \quad (2.20)$$

with the Riemann ζ function, $\zeta(k)$, and compare with $\Delta G_3 = \int x^3 G(x)\,{\rm d}x = 4G_3^{\rm Pl}$ and $\Delta G_2 = \int x^2 G(x)\,{\rm d}x = 3G_2^{\rm Pl}$, implying $\Delta\rho_\gamma/\rho_\gamma^{\rm Pl} = 4(\Delta T/T)$ and $\Delta N_\gamma/N_\gamma^{\rm Pl} = 3(\Delta T/T)$, which certainly satisfies Eq. (2.15).

Adjusting the volume but leaving the photon number unchanged Let us go back to the example in which we just move photons upwards in energy, say by some constant fractional amount (think of a batter that hits all the photons but is more aggressive for the energetic ones), $\nu' = \nu f$. The kinetic *Sunyaev-Zeldovich* effect [53] acts somewhat like this, resulting in Doppler boosts $\Delta\nu/\nu \simeq v_{\rm p,\parallel}/c = $ const, but the kSZ effect is not as democratic and only affect a small fraction, $\tau \simeq 0.01$, of the CMB photons. Let us also fix the number of photons inside a given volume V. If we assume that the number of photons in each hit is not changed, after the batting the new distribution ($N_\nu = I_\nu/[h\nu]$)

$$V N'_\nu = \frac{2}{c^3}\frac{V}{f^3}\frac{\nu^2}{e^{h\nu/kTf}-1} \equiv V'\frac{2}{c^3}\frac{\nu^2}{e^{h\nu/kT'}-1} \tag{2.21}$$

would be described by a blackbody at temperature $T' = Tf > T$, if the photons are confined to a smaller volume $V' = V/f^3$. Without readjusting the volume, the energy density of the new distribution would be $\rho'_\gamma = f\rho^{\rm Pl}_\gamma(T) = \rho^{\rm Pl}_\gamma(Tf^{1/4}) > \rho^{\rm Pl}_\gamma(T)$ but the number density did not change, $N'_\gamma \equiv N^{\rm Pl}_\gamma(T)$. After also readjusting the volume $V \to V'$, we have $\rho'_\gamma = (V/V')\, f\rho^{\rm Pl}_\gamma(T) = f^4\rho^{\rm Pl}_\gamma(T) = \rho^{\rm Pl}_\gamma(T')$ and $N'_\gamma = (V/V')N^{\rm Pl}_\gamma(T) = N^{\rm Pl}_\gamma(T')$, so that the spectrum is a blackbody again at the higher temperature $T' = Tf$ inside a smaller volume $V' = V/f^3$.

Entropy and adiabatic changes of a blackbody Assuming that the photon distribution at all stages is given by a blackbody (in detail this may actually be pretty hard), we can also apply standard thermodynamics for a photon gas. Combining the first and second law of thermodynamics we have

$$T\,{\rm d}S_\gamma = {\rm d}E_\gamma + P_\gamma\,{\rm d}V = {\rm d}(V\rho^{\rm Pl}_\gamma) + \frac{\rho^{\rm Pl}_\gamma}{3}\,{\rm d}V = V\,{\rm d}\rho^{\rm Pl}_\gamma + \frac{4}{3}\rho^{\rm Pl}_\gamma\,{\rm d}V = V\,{\rm d}(a_R T^4) + \frac{4}{3}(a_R T^4)\,{\rm d}V, \tag{2.22}$$

where S_γ is the photon entropy, $E_\gamma = V\rho^{\rm Pl}_\gamma$ the total internal energy and $P_\gamma = \rho^{\rm Pl}_\gamma/3$ the photon pressure (Exercise 2). From this, we have

$${\rm d}S_\gamma = V\,4a_R T^2 + \frac{4}{3}(a_R T^3)\,{\rm d}V = V\,{\rm d}\left(\frac{4}{3}a_R T^3\right) + \frac{4}{3}(a_R T^3)\,{\rm d}V = {\rm d}\left(\frac{4}{3}\,a_R T^3 V\right) \Longrightarrow \frac{S_\gamma}{V} = \frac{4}{3}\frac{\rho^{\rm Pl}_\gamma}{T}. \tag{2.23}$$

This expression implies that for *adiabatic changes* of a blackbody ($S_\gamma \equiv$ const) we have $V T^3 = $ const. This just means that if you increase the temperature by a factor of f you need to decrease the confining volume by a factor of $1/f^3$, as we already argued above. Recasting this expression in terms of $PV^\gamma = $ const we find the adiabatic index of photons $\gamma = 4/3$. For comparison, a monoatomic ideal gas has $\gamma = 5/3$ and for diatomic idea gases one has $\gamma = 7/5$.

Taking a spherical volume, $V \propto R^3$, that is filled with non-relativistic electrons and radiation and increasing the radius of the sphere to $R' > R$, we directly have $T_\gamma \propto R/R'$, while for the electrons with $P_{\rm e} = N_{\rm e}kT_{\rm e} \propto T_{\rm e}/V$ we find $T_{\rm e} \propto V^{1-\gamma} \propto (R/R')^2$. This means that the electron temperature drops faster than the radiation temperature if you adiabatically expand the volume. A similar process occurs in the expanding Universe but the cooling electrons are continuously up-scattered by the CMB photons, so that they *extract* energy from the photon field. This actually causes a small but *inevitable* spectral distortion [7, 17], as we will see below. Also, there would be no distortion if the Universe were only filled with photons!

Exercises

Exercise 1 Show that the phase space distribution function, f, is invariant under Lorentz transformation. Start by looking at the number of particles ${\rm d}N \propto f(\boldsymbol{x},\boldsymbol{p})\,{\rm d}^3x\,{\rm d}^3p \equiv f'(\boldsymbol{x}',\boldsymbol{p}')\,{\rm d}^3x'\,{\rm d}^3p' = {\rm d}N'$.

Exercise 2 Argue that the pressure of an isotropic photon field is given by $P_\gamma = \rho_\gamma/3$. You can use the definition of the pressure based on the distribution function, for example by starting with the energy-momentum tensor, $T^{\mu\nu} = c\int {\rm d}^3p\, p^\mu\, p^\nu f(x,p)/p^0$.

Chapter 3

Formulation of the thermalization problem in the expanding Universe

3.1 What is the thermalization problem all about?

When considering the cosmological thermalization problem we are basically asking: *how was the present CMB spectrum really created?* Assuming that everything starts off with a pure blackbody spectrum, we will see that the uniform adiabatic expansion of the Universe (absolutely no collisions and spatial perturbations here!) leaves this spectrum unchanged – a blackbody thus remains a blackbody at all times. However, if some energy is transferred to or extracted from the photon field or if photons are injected or absorbed by some process, then this inevitably creates a *momentary* spectral distortion. Then be big question is: *was there enough time from the creation of the distortion until today to fully restore the blackbody shape below any observable level?* – The last part of the question depends somewhat on our experimental sensitivity and the first part on all the interactions of the matter in the Universe with the photon field. By understanding the thermalization problem, we can then also ask: *what can we learn about different early-universe processes and the thermal history of our Universe by studying the CMB spectrum in fine detail?*

Ok, so *what do we need to thermalize a distortion?* We already discussed some of the requirements to conserve a blackbody spectrum. First of all, if we transfer some energy $\Delta\rho_\gamma/\rho_\gamma \ll 1$ to the photon field, we also need to change the number density by $\Delta N_\gamma/N_\gamma \approx (3/4)\Delta\rho_\gamma/\rho_\gamma$. Assuming that the volume occupied by the photon field does not change, this means we really need to *add/create photons*! Two of the important processes here are thermal *Bremsstrahlung* (BR) and *double Compton emission* (DC). As we will see below, these processes are only efficient at low frequencies, but exponentially inefficient in the Wien tail of the CMB. We therefore need another process that *transports* photons over frequency, so that low frequency BR or DC photons can reach the high frequency part more efficiently. This is achieved by *Compton scattering* (CS), which works pretty well in the pre-recombination era ($z > 10^3$). Bottom line, if any process in the early Universe creates a CMB spectral distortion, we need to *readjust* the number of photons and *redistribute* them in energy to really restore full equilibrium; the crucial processes are BR, DC emission and CS, for which we need to understand when they work efficiently and how long they take to complete the thermalization process.

3.2 General conditions and assumption

In the early Universe, photons undergo many interactions with the other particles. If we would attempt to follow the whole evolution of the photon field from day one of the Universe, including its spatial structure in detail this would clearly be a difficult endeavor. But we can simplify things, since it is clear that at very early times, the thermalization process is extremely fast, so that no distortion can survive until today. We therefore start with the minimal assumptions and then see afterwards if things work out[1].

[1] This type of reverse engineering always goes on, even if people do not often present it that way.

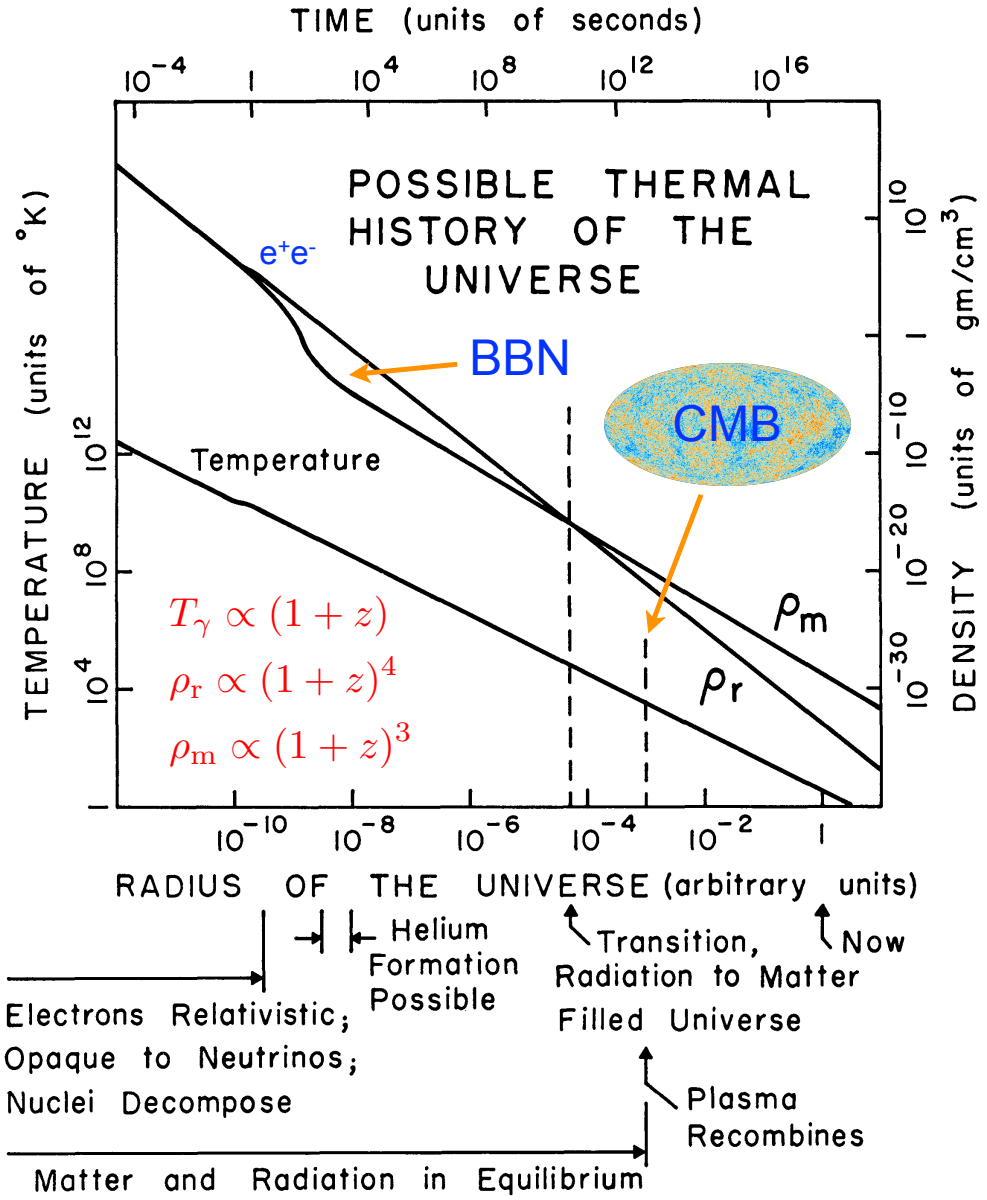

Figure 3.1: Sketch of the thermal history of our Universe from the paper of Dicke et al. [20], published in the same issue with the CMB discovery paper of Penzias & Wilson [40] in 1965. Parts of this picture were already worked out by Gamow, Alpher and Herman years earlier, but the value of $T_0 \simeq 3.5\,\mathrm{K}$ fixed the energy scale for radiation. Neutrinos decoupled at a temperature $kT_\gamma \simeq 1.5\,\mathrm{MeV} - 2\,\mathrm{MeV}$, while electron-positron annihilation finished around $kT_\gamma \simeq 0.5\,\mathrm{MeV}$. The light elements produced in the Big Bang Nucleosynthesis (BBN) era froze out at $kT_\gamma \lesssim 0.1\,\mathrm{MeV}$.

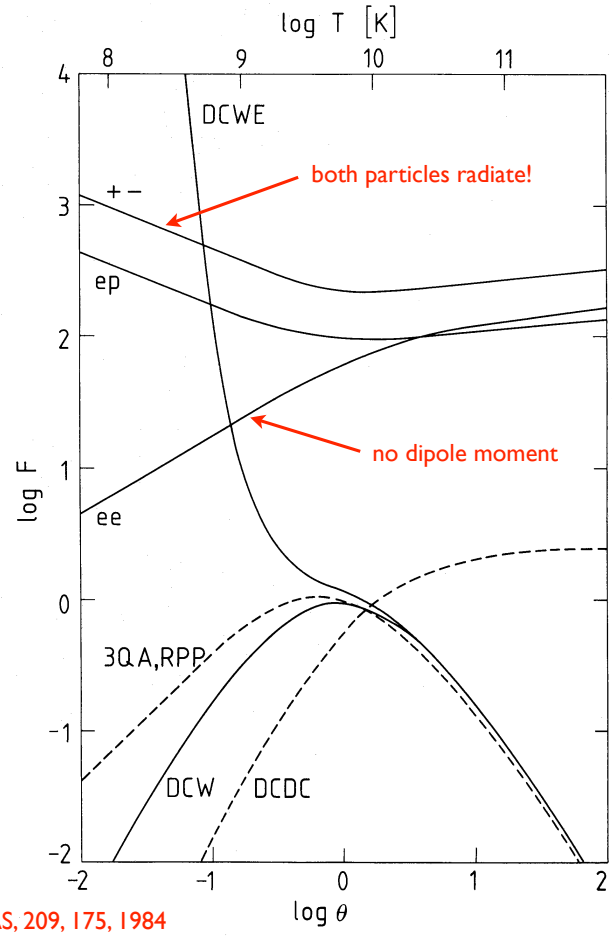

Svensson, MNRAS, 209, 175, 1984

The dimensionless emissivity $F(x = 10^{-6}, \theta) \equiv \dot{n}\,(x,\ \theta)\ x/(n_1 n_2 c r_e^2 \alpha)$ in the soft photon limit ($x \ll \theta$). The process and $n_1 n_2$ for each curve are $+-$: e^+e^- bremsstrahlung, $n_+ n_-$; ep: ep bremsstrahlung, $(n_+ + n_-)n_p$; ee: $e^{\pm}e^{\pm}$ bremsstrahlung, $n_+^2 + n_-^2$; DCW: double Compton from a Wien distribution, $n_\gamma(n_+ + n_-)$; DCDC: double Compton from a double Compton distribution, $N_\gamma(n_+ + n_-)$; DCWE: double Compton in pair-dominated Wien equilibrium, $n_\pm^2$; 3QA: three quantum annihilation, $n_+ n_-$; RPP: radiative pair production in Wien equilibrium, $n_+ n_-$, respectively. $F(x, \theta)$ depends on x (logarithmically) for bremsstrahlung only. See Appendix A for definition of N_γ and further details.

Figure 3.2: Photon emissivities for different Bremsstrahlung and double Compton cases [55].

3.2.1 Which epochs do we need to worry about?

A sketch of the standard thermal history is shown in Fig. 3.1. We are already far after the *inflation* epoch and also past the time of *reheating* and the *quark-gluon phase transition*, which all happen at much higher redshifts. We all know that the light elements were cooked in the BBN era, when the Universe was around 3 minutes old. Just before that, electron-positron pairs became non-relativistic and dropped out of equilibrium with the photon field, causing a difference between the temperature of the neutrino background ($T_\nu \simeq 1.9\,\mathrm{K}$ today) and the CMB due to *entropy production*.

Electron-positron annihilation was certainly associated with plenty of energy release, and it is actually not trivial to really compute the possible residual distortion from this era! The big problem is that with all these electron-positron pairs one has to deal with several Bremsstrahlung processes (e.g., e^-p, e^+e^-, $e^{\pm}e^{\pm}$) and photons from annihilations, all transitioning from the relativistic to non-relativistic regime (e.g., see Fig. 3.2). In the pair-dominated plasma, thermalization was definitely very efficient! But what is important for us is that even if you do the thermalization calculation assuming that electron-positron pairs are long gone, you find

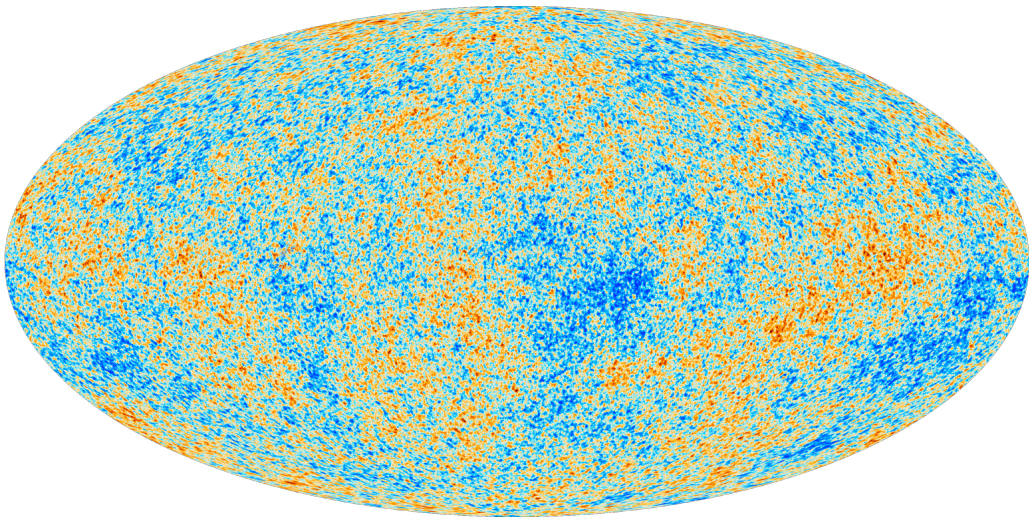

Figure 3.3: CMB temperature anisotropies as seen by the Planck satellite [41]. The CMB monopole and motion-induced dipole were removed (as well as all the real life things like foregrounds and our galaxy).

that any distortion should be tiny today if you inject energy at $z \gtrsim$ few $\times\, 10^6$ (you will see this below). We can therefore forget about searching for distortions from before $z \simeq 10^7$. Electron-positron pairs are thus never important for our problem. At that point, the temperature of the plasma had dropped below $kT \simeq 2\,\mathrm{keV}$, and we are just dealing with non-relativistic electrons, protons and helium nuclei immersed in a bath of photons from the CMB. We can neglect the traces of other light elements for the thermalization problem and also neutrinos and dark matter are only important for determining the expansion rate of the Universe.

3.2.2 Perturbation in the cosmic fluid and spectral distortions

For the evolution of primordial spectral distortions, the fluctuations in density of the cosmic medium can be neglected. This greatly simplifies the computations of the thermalization problem, but to understand this let us take a step back and just think about the CMB temperature and polarization anisotropies. We know that inflation sets the Universe up with tiny spatial fluctuations in the cosmic fluid (photons, baryons, neutrinos, dark matter...). These initial perturbations then evolve under gravity to form the structure we see today. At the time of recombination ($z \simeq 10^3$), the perturbations are all still tiny and reflected by the CMB temperature and polarization anisotropies. Because from the CMB observations we know that the CMB temperature perturbations around the CMB monopole temperature, $T_0 = 2.726\,\mathrm{K}$, are $\Delta T_\gamma/T_\gamma \simeq 10^{-5} - 10^{-4}$ (see Fig. 3.3), also the CMB spectrum should vary at a similar level only. That is, however, relative to the average distortion, just like the CMB temperature perturbations are with respect to the average CMB temperature! Because COBE/FIRAS shows that the average distortion can be no larger than $\Delta I_\nu/I_\nu \simeq 10^{-5} - 10^{-4}$, this implies that spatial variations of the CMB spectrum at most could be visible at the level $\Delta I_\nu/I_\nu \simeq 10^{-10} - 10^{-9}$, at least when we are only thinking about perturbations in the cosmic fluid as source of the fluctuations. Observing fluctuations of the CMB spectrum at this level is very futuristic.

There is a couple of ways this could be different. For example, if the source of the distortion is highly anisotropic (think of a SZ cluster of galaxies) one can see local distortions that are much larger than the average all-sky limit! Similarly, if you think about annihilating dark matter, then the energy release scales like $\propto N_{\rm X}^2 \langle\sigma v\rangle$, so that high density regions forming at the later stages could locally produce much larger distortions. For the thermalization calculation we will consider homogeneous energy release scenarios only.

Finally, we mention that the dissipation of primordial perturbations in the photon field by Thomson scattering creates a uniform spectral distortion due to the mixing of blackbodies of different temperatures. This

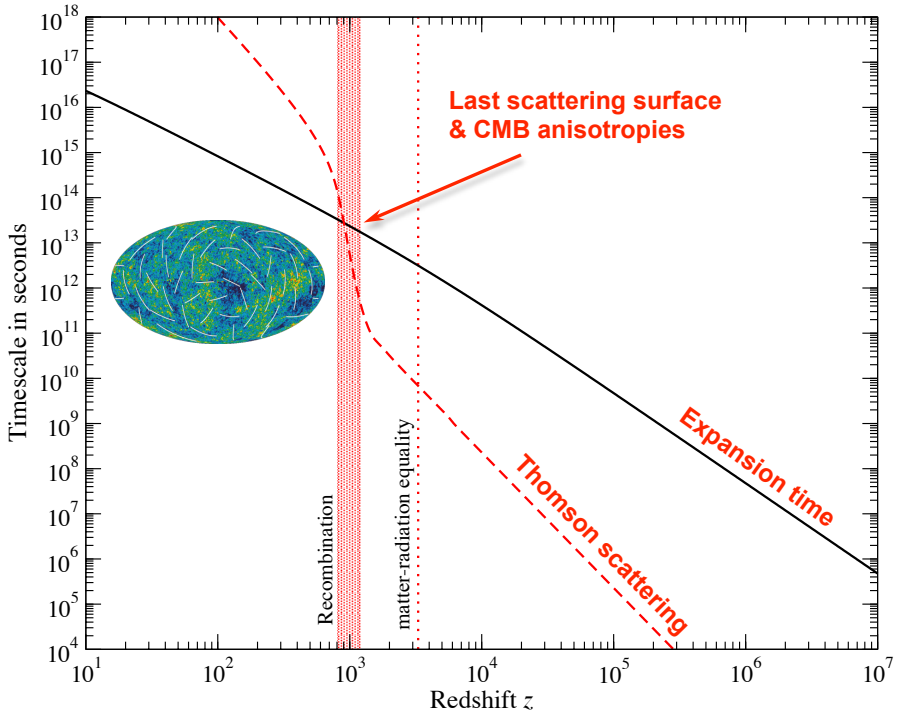

Figure 3.4: Comparison of the Thomson scattering time-scale with the Hubble expansion time-scale.

process allows us to constrain the small-scale power spectrum using future CMB spectral distortion measurements. In this sense, perturbations can be important for the *creation* of an average distortion, but they only give tiny corrections when it comes to describing the thermalization of the average distortion.

3.2.3 Electron temperature and ordinary matter distribution functions

Also the electron and ordinary matter distributions functions turn out to be simple, so that one need not worry about departures from equilibrium, describing all the matter using thermal Maxwell-Boltzmann distribution at one common temperature, $T = T_{\rm e}$. This approximation works very well even until very late stages $z \simeq 10$! To understand this a little better let us look at some characteristic time-scales. One useful time-scale is the Thomson scattering time-scale, $t_{\rm T} = (\sigma_{\rm T} N_{\rm e} c)^{-1}$. It will appear many times and describes on what time-scale photons scatter with electrons. For the standard cosmology with 24% of helium (by mass), we have

$$t_{\rm T} = (\sigma_{\rm T} N_{\rm e} c)^{-1} \simeq 2.7 \times 10^{20}\, X_{\rm e}^{-1} (1+z)^{-3}\ \text{sec} \simeq 4.0 \times 10^{4} \left[\frac{X_{\rm e}}{0.16}\right]^{-1} \left[\frac{z}{1100}\right]^{-3}\ \text{years}, \tag{3.1}$$

where $X_{\rm e} = N_{\rm e}/N_{\rm H}$ is the free electron fraction relative to the number of hydrogen nuclei. This sounds like a long time between scatterings, $\simeq$ 40 000 years at recombination! To put this into perspective we have to compare with the typical expansion time-scale given by the inverse Hubble rate:

$$t_{\rm exp} = H^{-1} \simeq \begin{cases} 4.8 \times 10^{19}\, (1+z)^{-2}\ \text{sec} & \text{(radiation domination)} \\ 8.4 \times 10^{17}\, (1+z)^{-3/2}\ \text{sec} & \text{(matter domination)}, \end{cases} \tag{3.2}$$

where the transition between matter and radiation (photons + neutrinos) domination occurs around $z_{\rm eq} \simeq 3400$. From Fig. 3.4 we see that the Thomson scattering rate (shorter time-scales) is much higher than the Hubble expansion rate until after decoupling. But even then, the time-scale for scattering only exceeds the expansion time by a factor of $\simeq 10^2 - 10^4$.

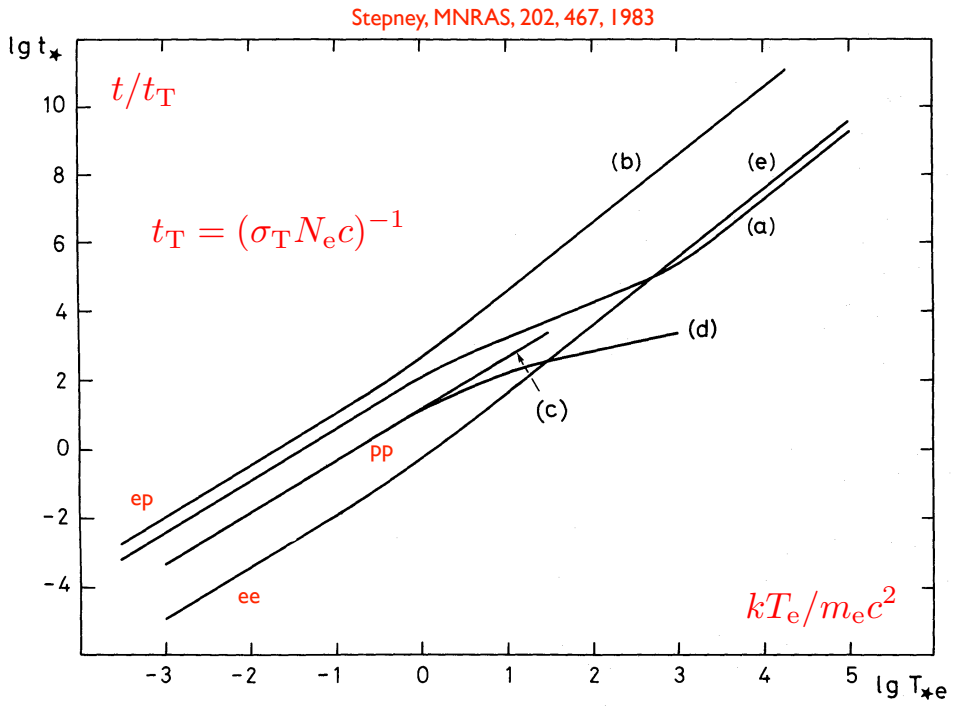

Two-body relaxation time-scales (putting $N_e = N_p$, $\ln\Lambda = 20$). (a) Electron –proton relaxation, $T_p = T_e$. (b) Electron–proton relaxation, $T_p = m_p T_e/m_e$. (c) Pure Coulomb proton–proton relaxation. (d) Proton–proton relaxation including nuclear scattering. (e) Electron–electron relaxation.

Figure 3.5: Relaxation times-scales for relativistic thermal plasma [50]. While electrons and photons are coupled, in our Universe we have $\theta_e = kT_e/m_e c^2 \simeq 4.6\times10^{-10}(1+z) \simeq 5.1\times10^{-7}[(1+z)/1100]$.

We can now turn to the question of the distribution functions for electrons and protons. For this not only the scattering rates are important, since scattering itself just means isotropization of the medium. What you really need is scattering events with energy exchange between the particles. Just like for thermalization of CMB spectral distortions we need Compton scattering (rather than just Thomson scattering) to redistribute photons in energy. Since we are already in the post-BBN era, the particle numbers are all fixed, so we have non-zero chemical potentials which fixes the normalization of the distribution functions.

To estimate the efficiency of energy exchange one has to compute the energy transfer from the differential cross sections. For two-particle interactions, this gives expressions of the form [e.g., 50]

$$\frac{\mathrm{d}E_1}{\mathrm{d}t} = f(T_1,T_2)[kT_2 - kT_1] \equiv -\frac{\mathrm{d}E_2}{\mathrm{d}t}, \tag{3.3}$$

where T_1 could denote the temperature of the electrons and T_2 the one of protons, for instance. The function $f(T_1,T_2) > 0$ describes the details of the interaction. If $T_1 > T_2$, heat flows from particles N_1 to N_2. To get a time-scale over which things equilibrate we just look at the total out-of-equilibrium thermal energy, $\Delta E = (3/2)N(kT_2 - kT_1)$ (non-relativistic limit and $N \equiv N_1 = N_2$), and compute

$$t_{12} = \left|\frac{\Delta E}{\mathrm{d}E_1/\,\mathrm{d}t}\right| = \frac{(3/2)N}{f(T_1,T_2)}. \tag{3.4}$$

In Fig. 3.5, we can see the comparison of different relaxation time-scales up to the relativistic regime. The results are all expressed in terms of the Thomson time-scale, t_T. The slowest process is the electron-proton relaxation, but even that is orders of magnitudes faster than Thomson scattering, in particular for the non-relativistic regime ($kT_e \ll m_e c^2$) that is relevant to us.

An estimate of how efficiently free electrons and protons are thermally coupled can be obtained with the Spitzer formula [49]

$$t_{\rm ep} \approx \sqrt{\frac{\pi}{2}}\frac{m_{\rm p}}{m_{\rm e}}\frac{t_{\rm T}}{\ln\Lambda}\,\theta_{\rm e}^{3/2} \simeq 1.1\times10^{-12}\,t_{\rm T}\,(1+z)^{3/2} \simeq 4.1\times10^{-8}\,t_{\rm T}\left[\frac{(1+z)}{1100}\right]^{3/2} \tag{3.5}$$

Here, we assumed $N_{\rm e} \approx N_{\rm p}$ and also $T_{\rm e} \approx T_{\rm p}$. The Coulomb logarithm, $\ln\Lambda$, is determined by the minimum momentum transfer possible (plasma frequency) and we used $\ln\Lambda \approx 20$ for the estimate.

Clearly, for free electrons and protons the thermalization timescale is very short. Thus their distributions are expected to be given by Maxwell-Boltzmann distributions and one common temperature $T_{\rm e} \simeq T_{\rm p}$. For neutral hydrogen and helium atoms the thermalization is slower but we have many orders of magnitudes of buffer here. Also, the statement of equilibration is not just a simple energy independent aspect, but for our computation the bulk of electrons and protons is important, so we are safe. Finally, for very non-thermal electrons (e.g., due to some particle decay) many energy loss mechanisms allow degrading their energy (for example Compton cooling) to more manageable energies in very short time. Overall, the simplest approximation for the ordinary matter distributions functions is well-justified.

3.3 Photon Boltzmann equation in the expanding Universe

The study of the formation and evolution of CMB fluctuations in both real and frequency space begins with the radiative transport, or Boltzmann equation for the phase space distribution, $f(x^\mu, p^\mu)$. The photon Boltzmann equation, written in abstract form as

$$\frac{{\rm d}f}{{\rm d}t} = {\rm C}[f], \tag{3.6}$$

contains a collisionless part ${\rm d}f/{\rm d}t$, which includes the effects of gravity, and collision terms ${\rm C}[f]$, which account for its interactions with other species in the Universe. The collision terms in the Boltzmann equation have several important effects. Most importantly, Compton scattering couples the photons and baryons, keeping the two close to kinetic equilibrium. Bremsstrahlung and double Compton emission allow adjusting the photon number and are especially fast at low frequencies, we explain now.

3.3.1 Liouville operator and gravitational effects

Neglecting collisions, we deal with the Vlasov-equation for the photon field. This only includes effects related to gravity, such as *gravitational redshifting* due to spatial fluctuation in the density and the *cosmological redshifting* due to the Hubble expansion ('stretching' of the metric). The photon phase space distribution function depends on the photon four vectors, $x^\mu = (ct, \boldsymbol{x})$ and $p^\mu = (E/c, \boldsymbol{p})$, so that we can write (sum over indices)

$$\frac{{\rm d}f}{{\rm d}t} = \frac{\partial f}{\partial x^\mu}\frac{{\rm d}x^\mu}{{\rm d}t} + \frac{\partial f}{\partial p^\mu}\frac{{\rm d}p^\mu}{{\rm d}t} = \frac{\partial f}{\partial t} + \frac{\partial f}{\partial x^i}\frac{{\rm d}x^i}{{\rm d}t} + \frac{\partial f}{\partial p}\frac{{\rm d}p}{{\rm d}t} + \frac{\partial f}{\partial \gamma^i}\frac{{\rm d}\gamma^i}{{\rm d}t} \equiv 0. \tag{3.7}$$

The gravitational effects are all hidden inside ${\rm d}p^\mu/{\rm d}t$. Let's do perturbation theory, but since we are interested in the average CMB spectrum, only up to zeroth order. Because, $\partial f^{(0)}/\partial x^i = \partial f^{(0)}/\partial \gamma^i = 0$, we have

$$\frac{\partial f^{(0)}}{\partial t} + \frac{\partial f^{(0)}}{\partial p}\frac{{\rm d}p^{(0)}}{{\rm d}t} \equiv 0, \tag{3.8}$$

which is quite simple. We only need to compute ${\rm d}p^{(0)}/{\rm d}t$, which we can obtain from the geodesic equation [e.g., see 21]. In zeroth order of perturbations, no fluctuations in the density are present, so that no gravitational redshifting (differences in the gravitational potential) or effects from fluctuations in the local curvature arise. We

are thus only left with the cosmological redshifting effect, $\mathrm{d}p^{(0)}/\,\mathrm{d}t = -H\,p$, which arises from the stretching of the coordinate system by the Hubble expansion, $p \propto (1+z) \propto 1/a$. The Hubble factor $H = \dot{a}/a\,(= 8\pi G\rho/3 - \kappa)$ is given by

$$H^2 = \left(\frac{\dot{a}}{a}\right)^2 = H_0^2\left[\Omega_\mathrm{r}(1+z)^4 + \Omega_\mathrm{m}(1+z)^3 + \Omega_\mathrm{k}(1+z)^2 + \Omega_\Lambda\right], \tag{3.9}$$

where $H_0 \simeq 70\,\mathrm{km\,s^{-1}Mpc^{-1}}$ and $\Omega_i = \rho_i(z=0)/\rho_\mathrm{cr}$ gives the energy density of the different universal constituents (i.e., relativistic species, matter, curvature and cosmological constant) relative to the critical density

$$\rho_\mathrm{cr} = \frac{3H_0^2}{8\pi G} \simeq 1.879\times10^{-29}h^2\,\mathrm{g\,cm^{-3}} \simeq 1.054\times10^4 h^2\mathrm{eV\,cm^{-3}} \simeq 1.123\times10^{-5}\,h^2 m_\mathrm{p}\,\mathrm{cm^{-3}}, \tag{3.10}$$

where $h \equiv H_0/[100\,\mathrm{km\,s^{-1}Mpc^{-1}}]$. For the standard concordance cosmology we have $\Omega_\mathrm{r} \simeq 7.4\times10^{-5}$, $\Omega_\mathrm{m} \simeq 0.32$, $\Omega_\mathrm{k} \simeq 0$ and $\Omega_\Lambda \simeq 0.68$ [41]. Then Eq. (3.8) reads

$$\frac{\partial f^{(0)}}{\partial t} - H\,p\frac{\partial f^{(0)}}{\partial p} \equiv 0, \tag{3.11}$$

where $f \equiv f(t,p)$. With this expression we can prove several properties of the average photon field. First of all, Eq. (3.11) shows that without collisions the photon distribution function does not change its shape so that a blackbody spectrum always remains a blackbody spectrum. By integrating the equation over d^3p [to obtain the photon number density, Eq. (2.11)], we obtain

$$\frac{\partial N_\gamma}{\partial t} + 3HN_\gamma = \frac{\mathrm{d}(a^3N_\gamma)}{a^3\,\mathrm{d}t} \equiv 0, \tag{3.12}$$

which shows that the average photon number scales as $N_\gamma \propto (1+z)^3$. With the blackbody law this directly implies $T_\gamma = T_0(1+z)$. Similarly, by integrating over $E\,\mathrm{d}^3p$ [to obtain the photon energy density, Eq. (2.10)], we obtain

$$\frac{\partial \rho_\gamma}{\partial t} + 4H\rho_\gamma = \frac{\mathrm{d}(a^4\rho_\gamma)}{a^4\,\mathrm{d}t} \equiv 0, \tag{3.13}$$

which shows that the average photon energy density scales as $\rho_\gamma \propto (1+z)^4$. The r.h.s. of both Eq. (3.12) and (3.13) will depart from zero if collisions are present. In this case, photon number and also energy density are not conserved but depend on the energy exchange with other constituents of the Universe (e.g., electrons).

Remark: For electrons and protons, the equivalent of Eq. (3.12), $\mathrm{d}(a^3N_i)/\,\mathrm{d}t = 0$, holds at the redshifts we are interested in, reflecting that the number of particles is conserved. The energy density equation for baryons is a little different. A more general form of Eq. (3.13) is [Exercise 1]

$$\frac{\partial \rho_i}{\partial t} + 3H\,(\rho_i + P_i) = 0, \tag{3.14}$$

which reduces to Eq. (3.13) for $P_\gamma = \rho_\gamma/3$. For electron and baryons this gives $\mathrm{d}(a^3\rho_i)/\,\mathrm{d}t \approx 0$, since the pressure, P_i, is subdominant. For ordinary matter we have $P_i = N_i k T_i$, which implies that this condition is correct when $kT_i \ll M_i c^2$ (thermal energy much less important than rest mass energy), which is precisely the regime we are considering. Again, when including collisions, there can be heat transfer between different species (which enforces $T_i \equiv T_\mathrm{e}$ but also allows matter to be heated by photons or energy release), so that we can derive an evolution equation for the matter temperature when considering both rest mass energy density and thermal energy density, $\rho_i \approx M_i c^2 N_i + \frac{3}{2}kT_iN_i$, as we show below.

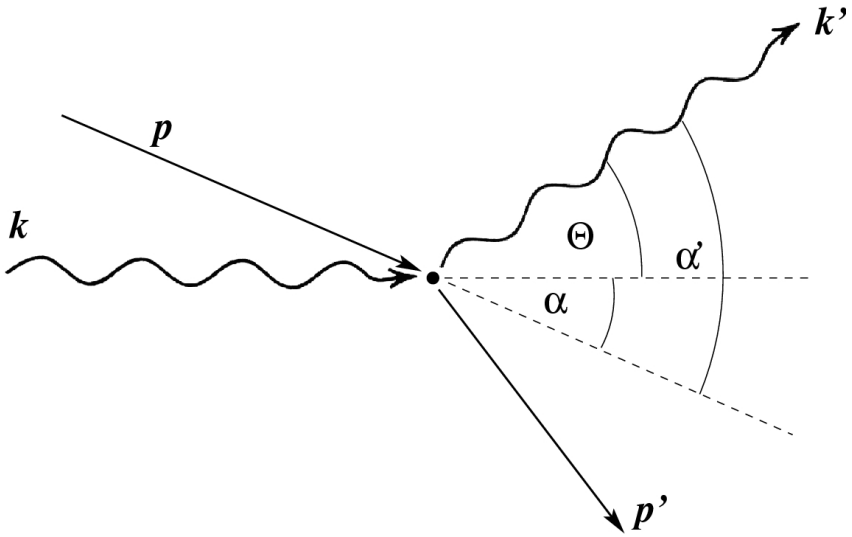

Figure 3.6: Compton scattering angles.

3.3.2 Photon collision term

In the early Universe, photons undergo many interactions with free electrons. The most important processes are Compton scattering (CS), double Compton (DC) scattering and Bremsstrahlung (BR), but there can also be non-standard processes (e.g., decaying particles) that add a photon source term. Among these processes, for most times Compton scattering is the fastest, while in particular DC and BR are only important early on. Including these processes, the photon collision term takes the form

$$\mathrm{C}[f] = \mathrm{C}[f]|_{\mathrm{CS}} + \mathrm{C}[f]|_{\mathrm{DC}} + \mathrm{C}[f]|_{\mathrm{BR}} + \mathrm{C}[f]|_{\mathrm{S}}\,. \tag{3.15}$$

The collision term describes local real changes to the photon distribution. We are only interested in the photon intensity but ignore polarization effects. Below we now consider each contribution separately.

3.3.3 Compton scattering

We already know that Compton scattering is responsible for redistributing photons in energy. This problem has been studied a lot in connection with X-rays from compact objects [42, 52] and the cosmological context [59, 54]. In reality, electron-photon scattering also helps isotropizing the photon field (Thomson scattering limit), although for this energy exchange is not as crucial [12, 11]. The reaction we are considering is

$$e(p) + \gamma(k) \longleftrightarrow e(p') + \gamma(k') \tag{3.16}$$

with the kinematic constraints between the four-momenta $p + k = p' + k'$. It is pretty straightforward to show (using $p^2 = p'^2 = m_{\mathrm{e}}c^2$ and $k^2 = k'^2 = 0$) that for given angles and energies between the scattering particles this implies

$$\frac{\nu'}{\nu} = \frac{1-\beta\mu}{1-\beta\mu' + \frac{h\nu}{\gamma m_{\mathrm{e}}c^2}(1-\mu_{\mathrm{sc}})}, \tag{3.17}$$

where $\beta = v/c$, $\gamma = 1/\sqrt{1-\beta^2}$, $\mu = \cos\alpha$, $\mu' = \cos\alpha'$ and $\mu_{\mathrm{sc}} = \cos\Theta$ (see Fig. 3.6 for illustration).

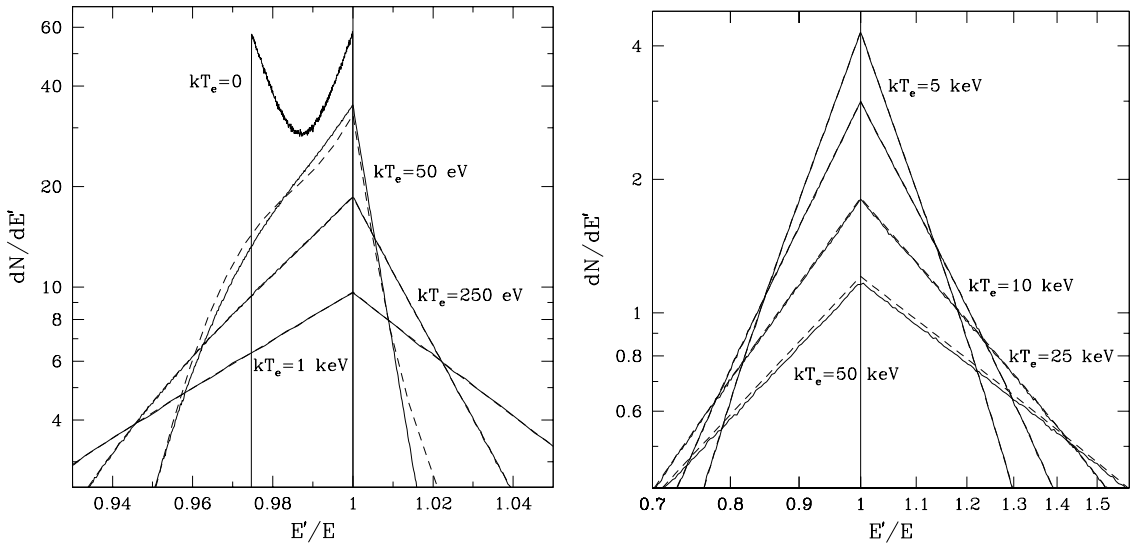

Figure 3.7: Compton scattering kernel for $E = h\nu = 6.7\,\mathrm{keV}$ photons. The left panel shows cases for cold ($h\nu \gg kT_\mathrm{e}$) electrons. In this case the redistribution process has significant contributions from recoil, although even for $kT_\mathrm{e} \simeq 0.01 h\nu$ the Doppler broadening already becomes important. The right panel shows examples for hot ($h\nu \ll kT_\mathrm{e}$) electrons, where the redistribution is dominated by Doppler broadening and boosting. Dashed lines show analytic approximations for the kernel. The figure was taken from Sazonov & Sunyaev [47].

Recoil dominated scattering event (Compton effect). Assuming that the scattering electron is at rest ($\beta = 0$ and $\gamma = 1$) from Eq. (3.17) we have the relation

$$\frac{\nu'}{\nu} \approx \frac{1}{1+\frac{h\nu}{m_\mathrm{e}c^2}(1-\mu_\mathrm{sc})} \overset{h\nu \ll m_\mathrm{e}c^2}{\underset{\approx}{\downarrow}} 1 - \frac{h\nu}{m_\mathrm{e}c^2}(1-\mu_\mathrm{sc}). \tag{3.18}$$

If the photon scatters in the forward direction ($\mu_\mathrm{sc} = 1$) there is no change in the incoming photon energy, while for backward scattering ($\mu_\mathrm{sc} = -1$), the effect is largest giving $\frac{\Delta\nu'}{\nu} \simeq -2\frac{h\nu}{m_\mathrm{e}c^2}$, with the photon giving a significant kick (*recoil effect*) to the electron. While the incoming photon looses energy, the initially resting electron is now moving in the forward direction, with kinetic energy $E'_e = 2(h\nu)^2/(m_\mathrm{e}c^2)$ or at a velocity $\beta' \approx 2h\nu/m_\mathrm{e}c^2$. On average the photon looses $\left\langle\frac{\Delta\nu'}{\nu}\right\rangle \simeq -\frac{h\nu}{m_\mathrm{e}c^2}$ for all possible scattering angles.

Doppler dominated scattering. If we are in the regime when $h\nu \ll m_\mathrm{e}c^2$ but electrons are moving fast, then from Eq. (3.17) we have the other extreme

$$\frac{\nu'}{\nu} \approx \frac{1-\beta\mu}{1-\beta\mu'} \overset{\beta \ll 1}{\underset{\approx}{\downarrow}} 1 - \beta(\mu-\mu') - \beta^2(\mu-\mu')\mu' + O(\beta^3). \tag{3.19}$$

In this regime, photons can both loose energy in the scattering event but also gain energy (Doppler boost). At lowest order in β, no net effect remains when you average over all possible angles and assume that the electron distribution is isotropic, but at second order in β one finds $\left\langle\frac{\Delta\nu'}{\nu}\right\rangle \simeq \frac{\langle\beta^2\rangle}{3}$. Assuming a normal Maxwell-Boltzmann distribution for the electron velocity distribution, one has $\left\langle\beta^2\right\rangle = 3kT_\mathrm{e}/m_\mathrm{e}c^2$, so that $\left\langle\frac{\Delta\nu'}{\nu}\right\rangle \simeq kT_\mathrm{e}/m_\mathrm{e}c^2 \equiv \theta_\mathrm{e}$. While for the recoil dominated case this simple procedure gave the correct result, for the Doppler dominated case one also has to include the dependence of the scattering probably (scattering cross section) on the angles and electron velocity, so that the net gain do to *Doppler boosting* in fact is $\left\langle\frac{\Delta\nu'}{\nu}\right\rangle \simeq 4\theta_\mathrm{e}$. In addition, we will see that an initially narrow photon distribution broadens due to electron scattering. These two effects can be described using a diffusion approximation.

Compton collision term. Let us take a look at the Compton collision term. The general starting point is

$$\mathrm{C}[f]|_{\mathrm{CS}} = \frac{1}{2E}\int \mathrm{D}p\,\mathrm{D}p'\,\mathrm{D}k'\,(2\pi)^4\delta^{(4)}(p+k-p'-k')\,|M|^2\,\mathcal{F}(p,k,p',k'), \tag{3.20}$$

where $\mathrm{D}p = \frac{\mathrm{d}^3p}{(2\pi)^3 2E(p)}$ and so on. The δ-function ensure energy and momentum conservation in the process, $|M|^2$ denotes the Lorentz-invarant matrix element of the Compton process, and $\mathcal{F}(p,k,p',k')$ is the statistical factor, which for non-degenerate electrons (no Fermi-blocking) reads

$$\mathcal{F}(p,k,p',k') = f_{\mathrm{e}}(\boldsymbol{p}')f(\boldsymbol{k}')[1+f(\boldsymbol{k})] - f_{\mathrm{e}}(\boldsymbol{p})f(\boldsymbol{k})[1+f(\boldsymbol{k}')]. \tag{3.21}$$

Here, the factors $\propto (1+f)$ account for the effect Bose-bunching of photons, which leads to *induced scattering*. Also, $f_{\mathrm{e}}(\boldsymbol{p})$ is the isotropic Maxwell-Boltzmann distribution function for electrons. By eliminating the d^3p' and $k'\,\mathrm{d}k'$ integrals[2] this equation can be recast in terms of the differential Compton cross section

$$\mathrm{C}[f]|_{\mathrm{CS}} = c\int \frac{\mathrm{d}\sigma}{\mathrm{d}\Omega}\,\mathcal{F}(\boldsymbol{p},\boldsymbol{k},\hat{\boldsymbol{\gamma}}')\,\mathrm{d}^3p\,\mathrm{d}^2\hat{\gamma}', \tag{3.22}$$

where $\hat{\boldsymbol{\gamma}}'$ denotes the direction of the scattered photon. For explicit expressions of $\mathrm{d}\sigma/\,\mathrm{d}\Omega$ see for example Appendix C2 of Chluba et al. [12], but in general this is not very illuminating; especially because analytic expression for different orders in the energy exchange and electron temperature can be obtained using computer algebra programs. If the scattering electron is at rest and the energy exchange can be neglected, we have the simple Thomson cross section

$$\frac{\mathrm{d}\sigma}{\mathrm{d}\Omega} \approx \frac{3\sigma_{\mathrm{T}}}{16\pi}(1+\mu_{\mathrm{sc}}^2), \tag{3.23}$$

which shows the characteristic $\cos^2\Theta$ angle-dependence of the scattering. Beyond this limit, the expressions become complicated. However, we can just proceed and try to understand which integrals over the scattering cross section are actually needed when we assume that the change in the energy of the scattered photon is small and that the distribution functions are all smooth functions of the energies only. This gives us a Fokker-Planck approximation for the Compton collision term.

Let us start by rewriting the statistical factor, $\mathcal{F}$. We have $f_{\mathrm{e}}(E') = f_{\mathrm{e}}(E)\,\mathrm{e}^{-(E'-E)/kT_{\mathrm{e}}} = f_{\mathrm{e}}(E)\,\mathrm{e}^{h(\nu'-\nu)/kT_{\mathrm{e}}}$, because of energy conservation, so that

$$\mathcal{F}/f_{\mathrm{e}} = \mathrm{e}^{\Delta x_{\mathrm{e}}}\,f(\nu')[1+f(\nu)] - f(\nu)[1+f(\nu')] = (\mathrm{e}^{\Delta x_{\mathrm{e}}}-1)\,f(\nu')[1+f(\nu)] + f(\nu') - f(\nu), \tag{3.24}$$

with $\Delta x_{\mathrm{e}} = h(\nu'-\nu)/kT_{\mathrm{e}}$. We now assume that $\Delta\nu/\nu \ll 1$ (the change in the photon energy per scattering is small), which gives

$$\begin{aligned}\mathcal{F}/f_{\mathrm{e}} &\approx f + \nu\partial_\nu f\Delta + \frac{1}{2}\nu^2\partial_\nu^2 f\Delta^2 - f + \left(\Delta x_{\mathrm{e}}(f(\nu)+\nu\partial_\nu f\Delta) + \frac{\Delta x_{\mathrm{e}}^2}{2}\,f\right)[1+f]\\ &\approx x_{\mathrm{e}}\partial_{x_{\mathrm{e}}} f\Delta + \frac{1}{2}x_{\mathrm{e}}^2\partial_{x_{\mathrm{e}}}^2 f\Delta^2 + x_{\mathrm{e}}\left(f\,\Delta + x_{\mathrm{e}}\partial_{x_{\mathrm{e}}} f\Delta^2 + x_{\mathrm{e}}\frac{\Delta^2}{2}\,f\right)[1+f],\end{aligned} \tag{3.25}$$

with $\Delta = \Delta\nu/\nu$ and $x_{\mathrm{e}} = h\nu/kT_{\mathrm{e}}$. To obtain the final result, we need the averages of Δ and Δ^2 over the scattering cross section and velocity distribution function ('moments' of the energy shift). This is a little cumbersome, but one can find [e.g., 47]

$$\langle\Delta\rangle \approx 4\frac{kT_{\mathrm{e}}}{m_{\mathrm{e}}c^2} - \frac{h\nu}{m_{\mathrm{e}}c^2} = \theta_{\mathrm{e}}(4-x_{\mathrm{e}}) \tag{3.26}$$

$$\left\langle\Delta^2\right\rangle \approx 2\frac{kT_{\mathrm{e}}}{m_{\mathrm{e}}c^2} = 2\theta_{\mathrm{e}} \tag{3.27}$$

[2] Especially for the $k'\,\mathrm{d}k'$ integral one has be careful with the δ-function.

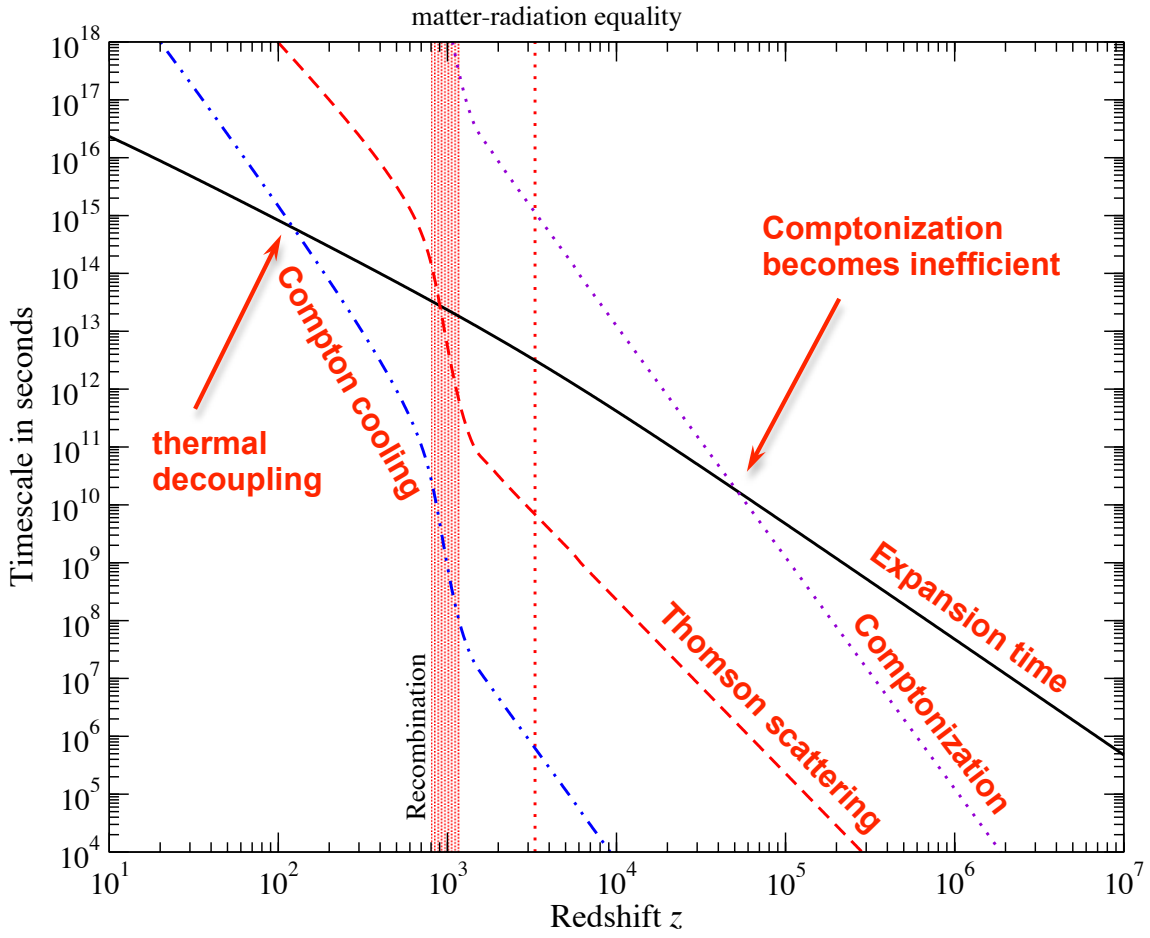

Figure 3.8: Comparison of the Comptonization and Compton cooling time-scale with the Hubble expansion time-scale.

at lowest order in $\theta_{\rm e} = kT_{\rm e}/m_{\rm e}c^2$ and $h\nu/m_{\rm e}c^2$. These expressions are per $\Delta\tau = c\sigma_{\rm T}N_{\rm e}\Delta t$, which defines the Thomson optical depth, τ. Inserting this into Eq. (3.25), with $x = h\nu/kT_\gamma$ we obtain [Exercise 2]

$$\left.\frac{\partial f}{\partial \tau}\right|_{\rm CS} \approx \frac{\theta_{\rm e}}{x_{\rm e}^2}\frac{\partial}{\partial x_{\rm e}}x_{\rm e}^4\left[\frac{\partial}{\partial x_{\rm e}}f + f(1+f)\right] \equiv \frac{\theta_{\rm e}}{x^2}\frac{\partial}{\partial x}x^4\left[\frac{\partial}{\partial x}f + \frac{T_\gamma}{T_{\rm e}}f(1+f)\right], \tag{3.28}$$

which is the famous *Kompaneets equation* [36]. It can be used to describe the repeated scattering of photons by thermal electrons in the isotropic medium. The first term in the brackets describes *Doppler broadening* and *Doppler boosting* and the last term accounts for the *recoil effect* and *stimulated recoil*. These terms are especially important for reaching full equilibrium in the limit of many scatterings.

We will discuss various analytic solutions of the Kompaneets equation in Chapter 4. Here, a couple of words about limitations of this equation. First of all, we assumed that the change in the energy of the photon by the scattering is small. For hot electrons this is no longer correct and one has to go beyond the lowest orders in Δ. This is for example important for the *Sunyaev-Zeldovich effect* of very hot clusters [29, 46, 6], but this procedure only converges *asymptotically* [e.g., 13, 18]. The second limitation is that if the photon distribution has very sharp features (more narrow than the width of the scattering kernel) then the shape of the scattered photon distribution is not well represented with the diffusion approximation. In this case, a scattering kernel approach can be used to describe the scattering problem [e.g., 47], although efficient numerical scheme for many scatterings are cumbersome.

Comptonization and Compton cooling. Some of the simple properties of Compton scattering are directly reflected by the Kompaneets equation. For example, scattering conserves the number of photons and it is straightforward to show that $\mathrm{d}N_\gamma/\,\mathrm{d}t|_{\rm CS} \propto \int x^2\,\mathrm{d}f/\,\mathrm{d}t|_{\rm CS}\,\mathrm{d}x = 0$, as it should be. The second aspect is energy exchange between electrons and photons. Computing $\mathrm{d}\rho_\gamma/\,\mathrm{d}t|_{\rm CS} \propto \int x^3\,\mathrm{d}f/\,\mathrm{d}t|_{\rm CS}\,\mathrm{d}x$ one finds

$$\left.\frac{\partial\rho_\gamma}{\partial\tau}\right|_{\rm CS} \approx 4\theta_{\rm e}\rho_\gamma\left[1-\frac{T_{\rm e}^{\rm eq}}{T_{\rm e}}\right] \qquad \text{with} \qquad T_{\rm e}^{\rm eq} = T_\gamma\frac{\int x^4 f(1+f)\,\mathrm{d}x}{4\int x^3 f\,\mathrm{d}x} \equiv \frac{h}{k}\frac{\int \nu^4 f(1+f)\,\mathrm{d}\nu}{4\int \nu^3 f\,\mathrm{d}\nu}, \tag{3.29}$$

where $T_{\rm e}^{\rm eq}$ defines the so called *Compton equilibrium temperature* [58] in a given radiation field $f(x)$. If $T_{\rm e}^{\rm eq} > T_{\rm e}$, electrons are heated and photons loose energy. No energy exchange happens if $T_{\rm e}^{\rm eq} = T_{\rm e}$, which does not necessarily mean that the photon field is a blackbody though. If $f(x) = 1/(\mathrm{e}^x-1)$ then $T_{\rm e}^{\rm eq} = T_\gamma$. The time-scale on which electrons transfer energy to the photons is

$$t_{\rm e\gamma} = \frac{t_{\rm T}}{4\theta_{\rm e}} \simeq 4.9\times10^5\,t_{\rm T}\left[\frac{1+z}{1100}\right]^{-1} \simeq 1.2\times10^{29}(1+z)^{-4}\ \mathrm{sec}\,. \tag{3.30}$$

Comparing this with the Hubble rate one finds that at $z_{\rm K} \simeq 5\times10^4$, *Comptonization* becomes inefficient (see Fig. 3.8). At this redshift, the characteristic of spectral distortions changes, as we will see below.

The Comptonization time-scale is is quite long compared to the time-scale over which electrons are heated by photons. The big difference is that every electron has $\simeq 1.9\times10^9$ photons to scatter with, making the number of interactions much larger. From $\rho_{\rm th} = (3/2)\sum_i N_i k T_{\rm e} = (3/2)N_{\rm H}(1+f_{\rm He}+X_{\rm e})\,kT_{\rm e}$ for the thermal energy of the plasma we have

$$t_{\gamma{\rm e}} = \frac{\rho_{\rm th}}{\rho_\gamma}\,t_{{\rm e}\gamma} \simeq \frac{3N_{\rm H}(1+f_{\rm He}+X_{\rm e})}{8\rho_\gamma/(m_{\rm e}c^2)}\,t_{\rm T} \simeq 0.31\,t_{\rm T}\,(1+z)^{-1} \simeq 7.3\times10^{19}(1+z)^{-4}\ \mathrm{sec}\,. \tag{3.31}$$

where the estimate was evaluated for $X_{\rm e} = 1+2f_{\rm He}$ (fully ionized) and $f_{\rm He} \approx Y_{\rm p}/[4(1-Y_{\rm p})] \approx 0.079$. Before recombination, the Compton cooling time is about $\simeq 1.6\times10^9$ times shorter than the Comptonization time. This means that electrons and baryons (through Coulomb scatterings) remain in full thermal contact with the photon field until very late. From Fig. (3.8) one can see that thermal decoupling is expected to happen somewhere around $z \simeq 100-200$ [56]. This is when the earliest signals from the 21cm era are produced [43].

Remark about Compton drag. Another very important moment in the cosmic history is when photons no longer can stop electrons and baryons from falling into the dark matter potential wells. The relevant *Compton drag* time-scale is slightly shorter than the Thomson scattering time-scale and is related to the coupling of the CMB dipole with the baryon bulk velocity ($\rightarrow$ linear order momentum exchange). The associated time-scale follows directly from the evolution equation of the baryon velocity, giving $t_{\rm drag} \simeq R\,t_{\rm T}$, where $R = 3\rho_{\rm b}/4\rho_\gamma \simeq 673/(1+z)$ is the *baryon loading* of the fluid. Comparing it with the expansion time-scale, the redshift at which Compton drag stops is determined by $z_{\rm drag} \simeq 136/X_{\rm e}^{2/5}$, which is a little lower than the decoupling redshift.

3.3.4 Bremsstrahlung

Thermal Bremsstrahlung is the first and most obvious suspect for photon production and absorption in the early Universe. It turns out that in our Universe double Compton emission is much more important [19], but nevertheless, at late times BR has to be included for precise computations. We already understand that we only need to worry about electron-proton (or a little more general, electron-ion) Bremsstrahlung, since $\mathrm{e}^-\mathrm{e}^-$ Bremsstrahlung is very inefficient at low temperatures (cf. Fig. 3.2). Considering hydrogen ions as an example, this process has the form

$$e(p) + H^+(h) \longleftrightarrow e(p') + H^+(h') + \gamma(k), \tag{3.32}$$

where the forward process results in BR emission and the backward process describes BR absorption. Without the extra photon this process is basically like a Coulomb scattering event. BR emission and absorption are thus the lowest order radiative correction with the photon number changing.

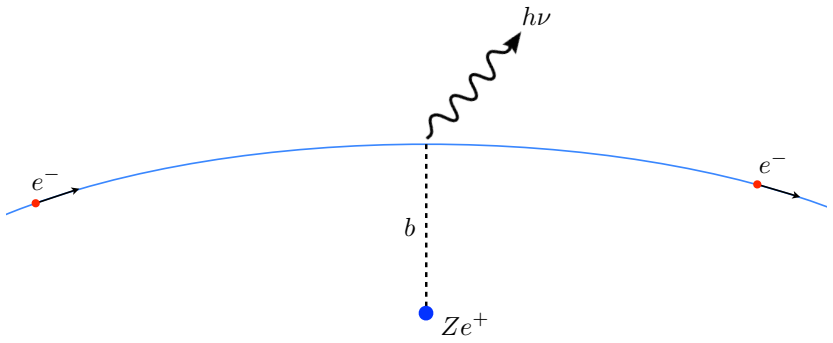

Figure 3.9: Bremsstrahlung process.

Before trying to understand things a bit more rigorously, let's follow the classical estimate using the dipole approximation. Imagine an electron passing a charge Ze^+ at some impact parameter b (see Fig. 3.9 for illustration). At the closest encounter the acceleration of the electron is $a \simeq Ze^2/(m_e b^2)$ and the time it takes to pass the charge is $\Delta t \simeq 2b/v$. Then the change in the velocity of the electron is $\Delta v \simeq 2Ze^2/(m_e b v)$ (if you integrate the force along a straight path at impact parameter b this is actually what you get). Then the total radiated energy in one single encounter is roughly given by

$$\frac{\mathrm{d}E}{\mathrm{d}\nu} \simeq \frac{4e^2}{3c^3}\Delta v^2 \simeq \frac{16Z^2e^6}{3m_e^2c^3v^2b^2}. \tag{3.33}$$

At frequencies $\nu \gg 1/\Delta t \simeq v/(2b)$ [short wavelength limit], hardly any power is emitted, so that $\mathrm{d}E/\mathrm{d}t \approx 0$ in that regime.

Now lets assume there is density N_i of ions with charge Ze^+ and we have N_e electrons. The flux of electrons incident per unit time and area on the ions is $N_e v$, and the cross section at fixed impact parameter is $2\pi b\,\mathrm{d}b$. Then the total emission of energy per unit volume, unit time and unit frequency is

$$\frac{\mathrm{d}E}{\mathrm{d}V\,\mathrm{d}t\,\mathrm{d}\nu} \simeq N_e N_i v \int \frac{\mathrm{d}E}{\mathrm{d}\nu}\,2\pi b\,\mathrm{d}b \simeq \frac{32\pi e^6}{3m_e^2c^3v} Z^2 N_e N_i \int \frac{\mathrm{d}b}{b}. \tag{3.34}$$

Formally, the integral over the impact parameter diverges, but an upper cut-off is introduced at $b_{\max} \simeq v/\nu$ (for a fixed frequency, not much power is emitted there according to the approximations). A lower limit on the impact parameter is introduced when (i) the straight line approximation breaks down ($\Delta v \simeq v$) or (ii) when the classical limit is no longer valid. Overall, these complications can be shoveled into the Bremsstrahlung *Gaunt factor*, $g_{\mathrm{ff}}(v,\nu)$, for which tables exist [e.g., 32]. In this way, we have

$$\frac{\mathrm{d}E}{\mathrm{d}V\,\mathrm{d}t\,\mathrm{d}\nu} \simeq \frac{32\pi^2e^6}{3\sqrt{3}m_e^2c^3v} Z^2 N_e N_i\, g_{\mathrm{ff}}(v,\nu) \tag{3.35}$$

for the BR emission at a single velocity. By averaging over a Maxwell-Boltzmann distribution at a temperature T_e, one can find

$$\frac{\mathrm{d}E}{\mathrm{d}V\,\mathrm{d}t\,\mathrm{d}\nu} \simeq \frac{32\pi^2e^6}{3\sqrt{3}m_e^2c^3} Z^2 N_e N_i \sqrt{\frac{2m_e}{\pi kT_e}}\,\mathrm{e}^{-\frac{h\nu}{kT_e}}\,\bar{g}_{\mathrm{ff}}(T_e,\nu) \propto Z^2 N_e N_i\, T_e^{-1/2}\,\mathrm{e}^{-x_e}. \tag{3.36}$$

Here, we used $\langle 1/v\rangle \simeq \sqrt{\frac{2m_e}{\pi kT_e}}\,\mathrm{e}^{-\frac{h\nu}{kT_e}}$ and that the minimal velocity required for the production of a photon of energy $h\nu$ is $v_{\min} \simeq \sqrt{2h\nu/m_e}$. Extensive tables for the thermally averaged Gaunt factor, $\bar{g}_{\mathrm{ff}}(T_e,\nu)$, can be found in Karzas & Latter [32] and Itoh et al. [30]. Overall, the Gaunt factor varies slowly with photon energy (see

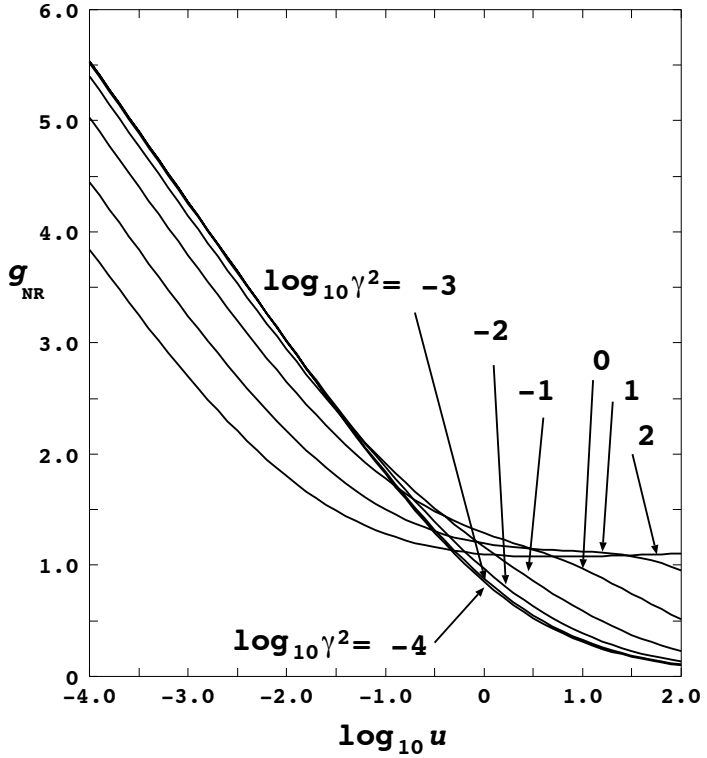

Figure 3.10: Thermally averaged Gaunt factor in the non-relativistic limit. Here, $u = \frac{h\nu}{kT_\mathrm{e}}$ and $\gamma^2 = \frac{Z^2 1.579\times10^5\mathrm{K}}{T_\mathrm{e}}$. The figure is taken from Itoh et al. [30] and a modern version of computations by Karzas & Latter [32].

Fig. 3.10), and the strongest dependence of the photon emission is due to the exponential cut-off at photon energies $h\nu \gg kT_\mathrm{e}$, simply because very few electrons could really emit photons at that energy. For estimates one can use $\bar{g}_\mathrm{ff}(T_\mathrm{e}, \nu) \approx \frac{\sqrt{3}}{\pi} \ln(2.25/x_\mathrm{e})$ for $x_\mathrm{e} \leq 0.37$ and $\bar{g}_\mathrm{ff}(T_\mathrm{e}, \nu) \approx 1$ otherwise.

With Eq. (3.36) the problem is already solved (at least approximately)! To write down the change of the photon distribution function due to BR emission, we only need to convert from change in the energy density to photon occupation, which gives a factor of $\equiv \frac{c^3}{8\pi h\nu^3}$. Here, we assumed that the BR emission process is isotropic. Since photons are social, we also need to multiply by $(1 + f)$ to account for stimulated emission. Then the change in the photon occupation number due to BR emission is

$$\left.\frac{\partial f}{\partial t}\right|_\mathrm{em} \approx \frac{8\pi}{3} \frac{e^6}{m_\mathrm{e} h\nu^3} \frac{Z^2 N_\mathrm{e} N_i}{\sqrt{6\pi m_\mathrm{e} kT_\mathrm{e}}} \mathrm{e}^{-\frac{h\nu}{kT_\mathrm{e}}} \bar{g}_\mathrm{ff}(T_\mathrm{e}, \nu)\,[1 + f(\nu)] = \epsilon_\mathrm{ff}(\nu, T_\mathrm{e})[1 + f(\nu)]. \tag{3.37}$$

For the inverse process (BR absorption) we can use the *detailed balance* argument: in full equilibrium there should be not net emission and absorption. The absorption term has the form $\partial f/\partial t|_\mathrm{abs} = N_\mathrm{e} N_i\, \alpha(T_\mathrm{e}, \nu) f$ and by setting $\partial f/\partial t|_\mathrm{abs} \equiv \partial f/\partial t|_\mathrm{em}$ for $f(\nu) = (\mathrm{e}^{x_\mathrm{e}} - 1)^{-1}$ we find $\partial f/\partial t|_\mathrm{abs} \equiv \epsilon_\mathrm{ff}(\nu, T_\mathrm{e})\, \mathrm{e}^{x_\mathrm{e}}\, f(\nu)$. In total this gives

$$\left.\frac{\partial f}{\partial t}\right|_\mathrm{BR} \approx \epsilon_\mathrm{ff}(\nu, T_\mathrm{e})\,[1 - f\,(\mathrm{e}^{x_\mathrm{e}} - 1)] = \frac{8\pi}{3} \frac{e^6 h^2}{m_\mathrm{e}(kT_\mathrm{e})^3} \frac{Z^2 N_\mathrm{e} N_i}{\sqrt{6\pi m_\mathrm{e} kT_\mathrm{e}}} \frac{\mathrm{e}^{-x_\mathrm{e}}\, \bar{g}_\mathrm{ff}(T_\mathrm{e}, \nu)}{x_\mathrm{e}^3}\,[1 - f\,(\mathrm{e}^{x_\mathrm{e}} - 1)]\,. \tag{3.38}$$

We cheated, since nobody actually told us that away from equilibrium one should have a factor $\simeq \mathrm{e}^{x_\mathrm{e}}$ for the absorption term instead of e^x! However, the argument is that the emission and absorption are driven energetically by the thermal electrons, so that the BR emission and absorption are driven into equilibrium at the electron temperature T_e. Even if $T_\gamma \neq T_\mathrm{e}$, at (very) low frequencies equilibrium will still be reached and it is controlled by the electrons and ions, so we actually need $\mathrm{e}^{x_\mathrm{e}}$ rather than e^x. Notice also, that in the

approximation the energy required to produce the photon comes solely from the electron! The energy of the ion does not change (it only carries away momentum but no energy) by the process.

We can rewrite Eq. (3.38) in terms of the Thomson rate, $t_{\rm T} = (\sigma_{\rm T} N_{\rm e} c)^{-1}$. The Thomson cross section is given by $\sigma_{\rm T} = (8\pi/3) r_{\rm e}^2 = (8\pi/3)[e^2/m_{\rm e}c^2]^2 \simeq 6.65 \times 10^{-25}\,{\rm cm}^2$. If we also use the Compton wavelength, $\lambda_{\rm e} = h/m_{\rm e}c \simeq 2.43 \times 10^{-10}\,{\rm cm}$ and fine-structure constant, $\alpha = 2\pi e^2/hc \simeq 1/137$, this yields

$$\left.\frac{\partial f}{\partial \tau}\right|_{\rm BR} \approx \frac{K_{\rm BR}\,{\rm e}^{-x_{\rm e}}}{x_{\rm e}^3}\,\left[1 - f\,({\rm e}^{x_{\rm e}} - 1)\right] \tag{3.39}$$

$$K_{\rm BR} = \frac{\alpha}{2\pi}\frac{\lambda_{\rm e}^3}{\sqrt{6\pi}\,\theta_{\rm e}^{7/2}}\sum_i Z_i^2 N_i\,\bar{g}_{\rm ff}(Z_i, T_{\rm e}, \nu) \simeq 1.4\times 10^{-6}\left[\frac{\bar{g}_{\rm ff}}{3.0}\right]\left[\frac{\Omega_{\rm b}h^2}{0.022}\right](1+z)^{-1/2}. \tag{3.40}$$

With these expressions we can ask on what time-scale the distribution function is brought into equilibrium with the electrons under BR emission and absorption at any given frequency $x_{\rm e}$. The time-scale is

$$t_{\rm BR} \approx \frac{x_{\rm e}^3\,t_{\rm T}}{K_{\rm BR}(1-{\rm e}^{-x_{\rm e}})} \approx 1.6\times 10^{26}\left[\frac{\bar{g}_{\rm ff}}{3.0}\right]^{-1}\left[\frac{\Omega_{\rm b}h^2}{0.022}\right]^{-1}\frac{x_{\rm e}^3}{1-{\rm e}^{-x_{\rm e}}}(1+z)^{-5/2}\;{\rm sec}\,. \tag{3.41}$$

This expression shows that at higher redshifts BR is more efficient, which of course should not surprise us much because the density increases. But also, the lower frequencies you look at, the faster photons thermalize. To give an example, at $x_{\rm e} \lesssim 10^{-2}$, one can thermalize within less than a Hubble time at $z \gtrsim 10^5$ using BR alone.

Explicit Collision integral. Similar to Compton scattering, the Bremsstrahlung collision term reads

$$\mathrm{C}[f]|_{\rm BR} = \frac{1}{2E}\int \mathrm{D}p\,\mathrm{D}h\,\mathrm{D}p'\,\mathrm{D}h'\,(2\pi)^4\delta^{(4)}(p+h-p'-h'-k)\,|M|^2\,\mathcal{F}(p,h,p',h',k), \tag{3.42}$$

where the statistical factor takes the form

$$\mathcal{F}(p,h,p',h',k) = f_{\rm e}(\boldsymbol{p}) f_{\rm p}(\boldsymbol{h})[1+f(\boldsymbol{k})] - f_{\rm e}(\boldsymbol{p}') f_{\rm p}(\boldsymbol{h}') f(\boldsymbol{k}). \tag{3.43}$$

For isotropic distributions, one can furthermore write $f_{\rm e}(\boldsymbol{p}') f_{\rm p}(\boldsymbol{h}') = f_{\rm e}(\boldsymbol{p}) f_{\rm p}(\boldsymbol{h})\,{\rm e}^{h\nu/kT_{\rm e}}$, so that the collision term directly takes the form $\mathrm{C}[f]|_{\rm BR} \propto I(T_{\rm e}, \boldsymbol{k})[1 - f(\boldsymbol{k})({\rm e}^{x_{\rm e}} - 1)]$. With these expressions one can in principle compute the full problem. The standard simplification is that the ion does not exchange any energy with the electron or the photon, since it is so heavy. It does, however, carry away some of the momentum, because a process of the form $e(p) \longleftrightarrow e(p') + \gamma(k)$ is kinematically not allowed.

3.3.5 Double Compton scattering

In Fig. 3.2, the double Compton emissivity is a couple of orders of magnitude smaller than the emissivity of BR. However, BR emission scales like $\propto N_{\rm e} N_i$, while double Compton depends on $\propto N_{\rm e} N_\gamma$. Due to the huge specific entropy of our Universe this means that double Compton emission actually dominates as a source of photons, at least at early times (due to its temperature dependence which we discuss now).

The DC process has the form

$$e(p) + \gamma(k) \longleftrightarrow e(p') + \gamma(k') + \gamma(k_2). \tag{3.44}$$

The differential cross section for this process was first calculated by Mandl & Skyrme [39] and several useful expressions can be found in the book of Jauch & Rohrlich [31]. Like BR is the first radiative correction to Coulomb scattering, DC is the first radiative correction to Compton scattering, where $\gamma(k_2)$ is usually though of as a *soft photon* with $h\nu_2 \ll h\nu$ and $\nu \simeq \nu'$. In this limit, the photon $\gamma(k')$ plays the role of the scattered

photon and $\gamma(k_2)$ can be distinguished because of its energy. There is no classical analogue like for BR, but in the *soft photon limit* the DC cross section becomes rather simple. In this approximation, Lightman [38] derived the kinetic equation for the DC process which takes a form that is very similar to that of BR. In the first computations of the cosmological thermalization problem only BR was included [54] and later Danese & de Zotti [19] added DC to this, showing that thermalization is more rapid than just with BR.

DC emission in the soft photon limit. To compute the production of photons by the DC process, we can start with resting electrons and assume that the scattering photon does not lead to a large recoil of the electron, $h\nu \ll m_{\rm e}c^2$. In this limit, we have $\nu \approx \nu' + \nu_2$, which means that after the scattering event the electron is basically still at rest and also that the energy is shared between to two outgoing photons. In principle $\gamma(k_2)$ and $\gamma(k')$ are completely equivalent photons, but assuming that $\nu' \simeq \nu$ (this restricts the scattering angles close to forward scattering) one can label the photons and use the *soft photon limit* of the DC cross section. From Jauch & Rohrlich [31], we then have

$$\frac{{\rm d}\sigma}{{\rm d}\nu\,{\rm d}\nu'\,{\rm d}\nu_2} \approx \frac{4\alpha}{3\pi}\sigma_{\rm T}\left(\frac{h\nu}{m_{\rm e}c^2}\right)^2 \frac{\delta(\nu'-\nu)}{\nu_2}, \tag{3.45}$$

where we already averaged over all possible angles of the incoming electron and photon and the scattered photon. This expression shows that for very low energy photons, the DC emission is suppressed by $(h\nu/m_{\rm e}c^2)^2$. Thus, for a distribution of photons (say a blackbody), most of the emission arises from the high frequency tail of the spectrum. To get the net emission in terms of number of photons around ν_2 we have

$$\frac{8\pi\nu_2^2}{c^3}\left.\frac{\partial f(\nu_2)}{\partial t}\right|_{\rm em} \approx cN_{\rm e}\int \frac{{\rm d}\sigma}{{\rm d}\nu\,{\rm d}\nu'\,{\rm d}\nu_2}\frac{8\pi\nu^2}{c^3}f(\nu)[1+f(\nu')][1+f(\nu_2)]\,{\rm d}\nu\,{\rm d}\nu', \tag{3.46}$$

where the factors of $(1+f)$ account for stimulated DC emission. Thus, the DC emission term is

$$\left.\frac{\partial f(\nu_2)}{\partial \tau}\right|_{\rm em} \approx \frac{4\alpha}{3\pi}\int\frac{\nu^2}{\nu_2^3}\left(\frac{h\nu}{m_{\rm e}c^2}\right)^2 f(\nu)[1+f(\nu)][1+f(\nu_2)]\,{\rm d}\nu = \frac{4\alpha}{3\pi}\,\theta_\gamma^2\,\frac{I_{\rm dc}}{x_2^3}[1+f(x_2)] \tag{3.47a}$$

$$I_{\rm dc} = \int x^4 f(x)[1+f(x)]\,{\rm d}x \approx -\int x^4\partial_x f_{\rm bb}(x) = 4G_3^{\rm Pl} = \frac{4\pi^4}{15} \approx 25.98. \tag{3.47b}$$

For the approximation of $I_{\rm dc}$ we assumed that the *seed photons* are given by the CMB blackbody spectrum. This should be a good approximation since the distortions only add a very small correction. This expression also shows that without photons present initially, no DC emission occurs!

By using the detailed balance argument, we can then write

$$\left.\frac{\partial f}{\partial \tau}\right|_{\rm DC} \approx \frac{K_{\rm DC}}{x^3}\,\left[1 - f\,({\rm e}^{x_{\rm e}}-1)\right] \tag{3.48a}$$

$$K_{\rm DC} = \frac{4\alpha}{3\pi}\,\theta_\gamma^2\,I_{\rm dc} \simeq 1.7\times10^{-20}\,(1+z)^2. \tag{3.48b}$$

The DC emission coefficient, $K_{\rm DC}$, is a strong function of temperature, but in the soft photon limit it does not depend on frequency. Comparing with BR, we can find that in our Universe DC emission becomes more important than BR emission at $z \gtrsim 3.7\times10^5$. As we will see, this means that bulk of the thermalization process is controlled by DC emission!

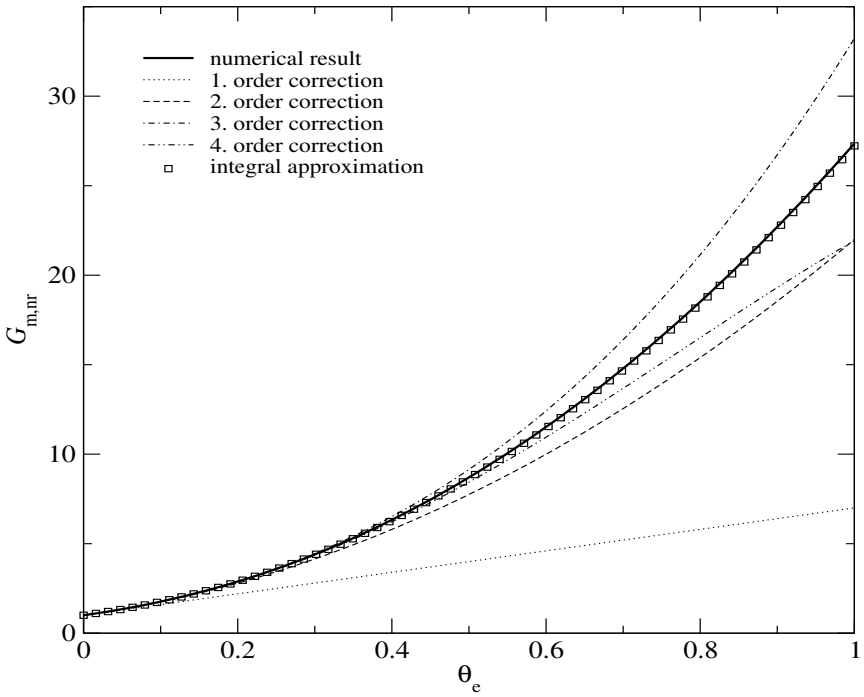

Figure 3.11: Enhancement of the DC emissivity due to thermal motions of the electrons. The approximation Eq. (3.49) works extremely well even to high temperatures. The figure is taken from Chluba et al. [14].

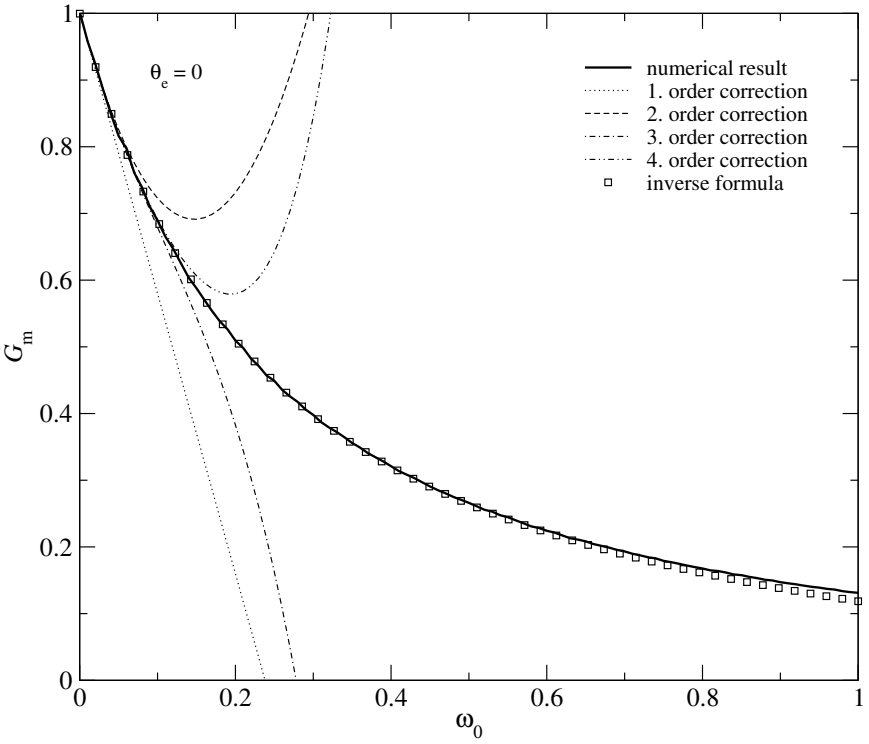

Figure 3.12: Suppression of the DC emissivity for larger incoming photon energy $\omega_0 = h\nu_0/m_e c^2$. The approximation Eq. (3.50) works extremely well even to large energies. The figure is taken from Chluba et al. [14].

Beyond the Lightman approximation – Temperature corrections. For the derivation of Eq. (3.48), we assumed that (i) the electrons are initially at rest and (ii) the incoming (≡ scattering) photon does not loose much of its energy (no recoil ↔ $h\nu \ll m_e c^2$) so that the 'emitted' photon is very soft. One can go beyond these approximations defining *DC Gaunt factors* based on analytic expressions. At early times ($z \gtrsim$ few $\times 10^6$) and when $h\nu_2 \simeq h\nu$ (→ *Gould-factor*), this makes a significant difference.

Let us first consider corrections due to the fact that the electrons can be moving. In the rest frame of the electron, a incoming mono-energetic photon has an energy $\nu_e \simeq \gamma\nu$, so that the DC production rate is expected to be $\gamma^2 = 1/(1-\beta^2)$ times larger if the electron is moving. Taking all angular dependencies into account, you find the photon production rate to be increased by $G(\beta) \simeq (1+\beta^2)/(1-\beta^2)$ [14]. Averaging over a relativistic thermal distribution one finds the enhancement factor

$$G(\theta_e) = \frac{[1+24\theta_e^2]K_0(1/\theta_e) + 8\theta_e[1+\theta_e^2]K_1(1/\theta_e)}{K_2(1/\theta_e)} \approx 1 + 6\theta_e + 15\theta_e^2 + \frac{45}{4}\theta_e^3 - \frac{45}{4}\theta_e^4 + O(\theta_e^3). \tag{3.49}$$

The comparison with the numerical result for the DC enhancement factor caused by moving electrons is illustrated in Fig. 3.11. The approximation Eq. (3.49) clearly works extremely well even to high temperatures.

If we instead crank up the energy of the incoming (scattering) photon, we expect the DC emission rate to decrease just like the Compton scattering cross section decreases in the Klein-Nishina regime. In terms of $\omega = h\nu/m_e c^2 \ll 1$ one can find the correction factor [14]

$$G(\omega) = 1 - \frac{21}{5}\omega + \frac{357}{25}\omega^2 - \frac{7618}{175}\omega^3 + \frac{21498}{175}\omega^4 + O(\omega^5) \approx \frac{1}{1 + \frac{21}{5}\omega + \frac{84}{25}\omega^2 - \frac{2041}{875}\omega^3 + \frac{9663}{4375}\omega^4}. \tag{3.50}$$

The comparison with the numerical result for the DC suppression factor is illustrated in Fig. 3.12. Again the approximation works very well in particular when using the inverse formula that was deduced by inspecting the terms of the Taylor series. For comparison, the suppression of the total Compton scattering cross section is $\sigma \simeq \sigma_T(1-2\omega)$, which shows that the effective suppress of the DC rate is about twice as large.

Obviously, one can also find approximations when both electrons are moving and the energy of the incoming photon increases. Analytic approximation for this case are given in Chluba et al. [14], with enhancement terms due to the electrons motion fighting the suppression for larger photon energy. To include all effects for blackbody photons as source, one again has to perform a Fokker-Planck expansion of the DC collision term. This becomes quite complicated and details can be found in Chluba [7] and Chluba et al. [14]. A useful expression that approximates the reduction of the DC emissivity relative to the Lightman approximation for blackbody radiation with temperature takes the form [7]

$$G_{dc}(\theta_\gamma, \theta_e) = \frac{1}{1 + 19.739\theta_\gamma - 5.5797\theta_e} \overset{\theta_e \approx \theta_\gamma}{\underset{\downarrow}{=}} \frac{1}{1 + 14.16\,\theta_\gamma}. \tag{3.51}$$

A comparison with the numerical result is shown in Fig. 3.13, illustrating the performance of the approximation. It also improves over previous fit given by Svensson [55] given for Wien spectra only, because Eq. (3.51) includes both stimulated DC emission and differences in the electron and photon temperature.

Beyond the soft photon limit. In the previous paragraph we considered corrections in θ_e and $\omega = x\theta_\gamma$. But we still worked in the soft photon limit, $\nu_2 \ll \nu$ and $\nu \simeq \nu'$. Assuming again resting electrons and $h\nu \ll m_e c^2$, one can readily give the general expression for all energies of $0 \le h\nu_2 \le h\nu$. The frequency-modulation of the DC emissivity is captured by the *Gould factor*[3] [24]

$$H_{dc}(\nu_2/\nu) \approx \frac{\nu_2}{\nu} H_G\left(\frac{\nu_2}{\nu}\right) \tag{3.52}$$

where $H_G(w) = [1 - 3y + 3y^2/2 - y^3]/y$ with $y = w[1-w]$. In the limit $\nu_2/\nu \to 0$, one finds $H_{dc}(x) \to 1$ and similarly for $\nu_2/\nu \to 1$ (due to symmetry around $\nu_2/\nu = 1/2$). Again this factor was simply obtained by setting $\beta = 0$ in the full DC cross section, expanding to lowest order in $\omega \ll 1$ (so that $\nu \approx \nu' + \nu_2$) and then performing all the angle integrals.

[3]Note that $H_G(w)$ is 1/2 of $F(w)$ given by Eq. (27) of Gould [24]. The factor of 2 is to avoid double counting of photons.

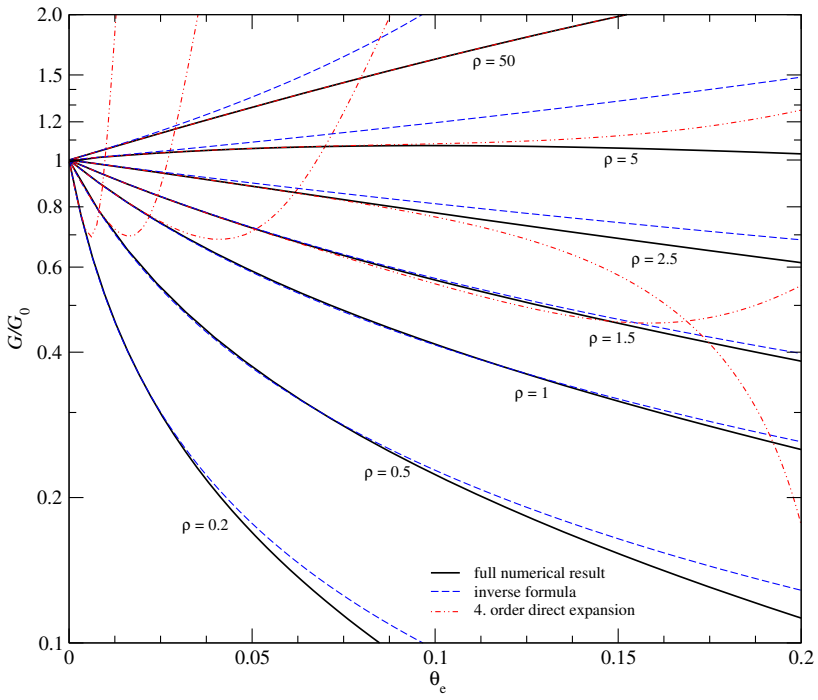

Figure 3.13: Double Compton Gaunt factor for Planckian photons at a temperature θ_γ and electrons at temperature $\theta_e = \rho\,\theta_\gamma$. Approximation Eq. (3.51) represents the full numerical result extremely well, especially for $\theta_\gamma \approx \theta_e$. The figure is taken from Chluba [7].

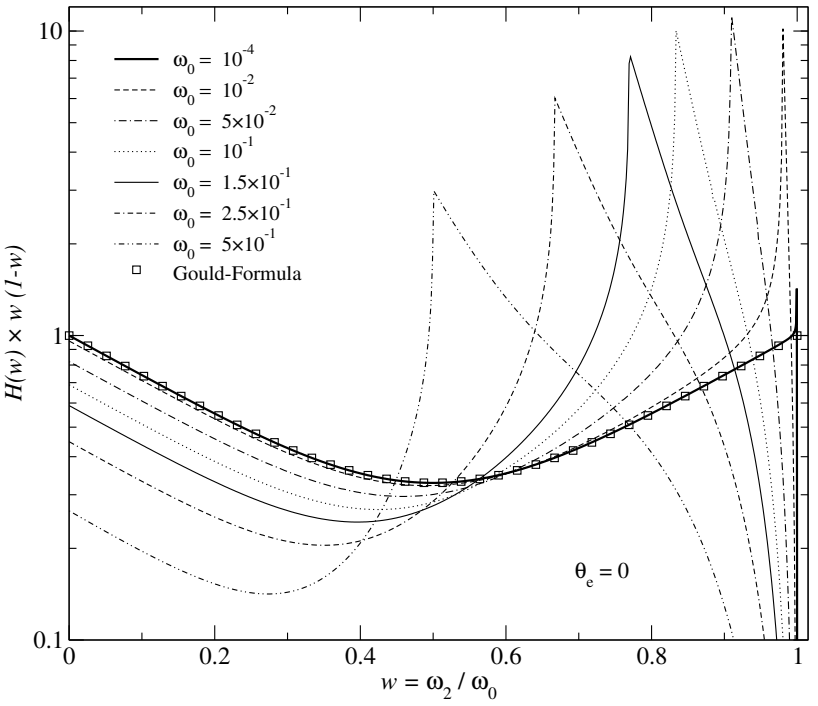

Figure 3.14: Gould factor for different incoming photon energies but $\theta_e = 0$. For larger $\omega_0 = \frac{h\nu}{m_e c^2}$, recoil corrections become important and the high frequency photon transfers energy to the electrons. The cusp is roughly at $w \simeq 1/(1+2\omega_0)$. The figure is taken from Chluba [7].

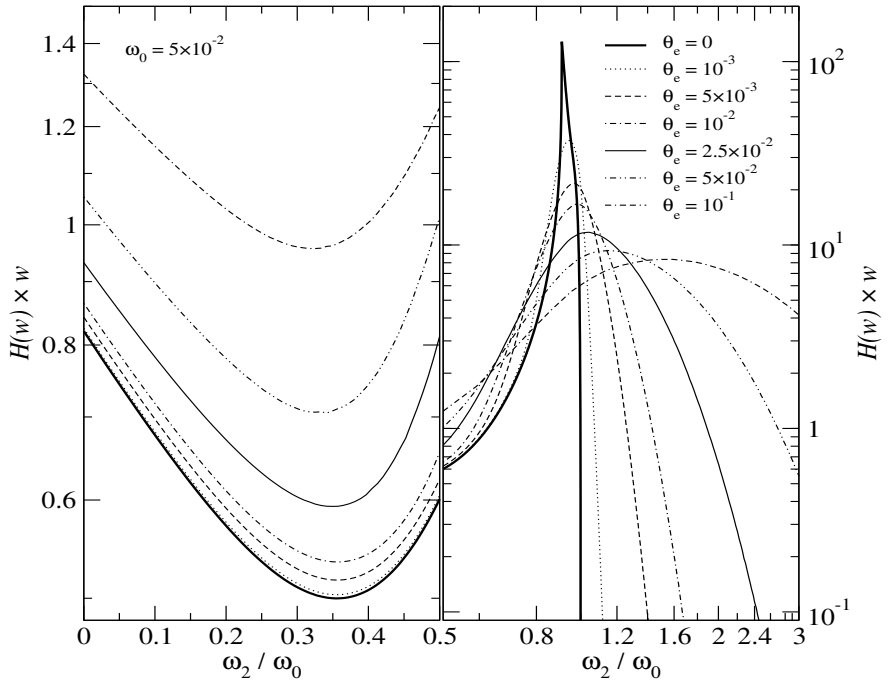

Figure 3.15: Gould factor for different different temperatures and $\omega_0 = 0.05$. For increasing θ_e, electrons transfer some energy to the high frequency photon due to Doppler boosts, leading to scattering correction to the Compton process. The figure is taken from Chluba [7].

In Fig. 3.14, we illustrate the functional shape of the Gould factor. For low incoming photon energy the shape of $H_{\rm dc}$ is clearly represented very well with the Gould formula. However, for larger ω, corrections related to the energy redistribution of the scattering photon become important. In this case, $\nu \neq \nu' + \nu_2$, but some energy is transferred to the initially resting electron. Thus, in particular the range $(1+2\omega)^{-1} \lesssim \nu_2/\nu \lesssim 1$ shows significant structure. However, at $\nu_2 \lesssim \nu/2$ the shape of $H_{\rm dc}$ is very well represented by the Gould formula and the suppression of the DC emissivity can be captured by $G(\omega)$ given in Eq. (3.50), so that overall $H_{\rm dc} \approx \frac{\nu_2}{\nu} H_{\rm G}\left(\frac{\nu_2}{\nu}\right) G(\omega)$.

Similarly, if we allow the electrons to have non-zero temperature, the factor $G(\theta_{\rm e})$ given in Eq. (3.49) allows capturing the enhancement of the DC emissivity at low energies. In this case, Doppler boosts from the electron allow the high frequency photon to gain energy above it initial value (see Fig. 3.16), so that the high frequency tail of the DC spectrum has a more complicated structure. For the thermalization problem this additional redistribution can be neglected.

To account for corrections beyond the soft photon limit on the DC emissivity, we have to modify the DC integral, $I_{\rm dc} = \int x^4 f(x)[1+f(x)]\,{\rm d}x$, over the incoming photon distribution. We know that photons emitted at frequency $x_2 = h\nu_2/kT_\gamma$ are produced by incoming photons at frequency $x \geq 2x_2$ with the stimulated factor $[1+f(x)] \rightarrow [1+f(x-x_2)]$. The modified DC emission integral, assuming small distortions, is thus

$$H_{\rm dc}(x_2) \approx \frac{1}{I_{\rm dc}} \int_{2x_2}^{\infty} x^4 n_{\rm Pl}(x)[1+n_{\rm Pl}(x-x_2)] \left[\frac{x_2}{x} H_{\rm G}\left(\frac{x_2}{x}\right)\right] {\rm d}x \tag{3.53a}$$

$$\approx e^{-2x_2}\left[1 + \frac{3}{2}x_2 + \frac{29}{24}x_2^2 + \frac{11}{16}x_2^3 + \frac{5}{12}x_2^4\right]. \tag{3.53b}$$

The approximation (Exercise 4) was given in Chluba & Sunyaev [17] and represents the numerical result very well. It significantly improves the previous approximation $H_{\rm dc}(x) \approx {\rm e}^{-x/2}$ given by Burigana et al. [4].

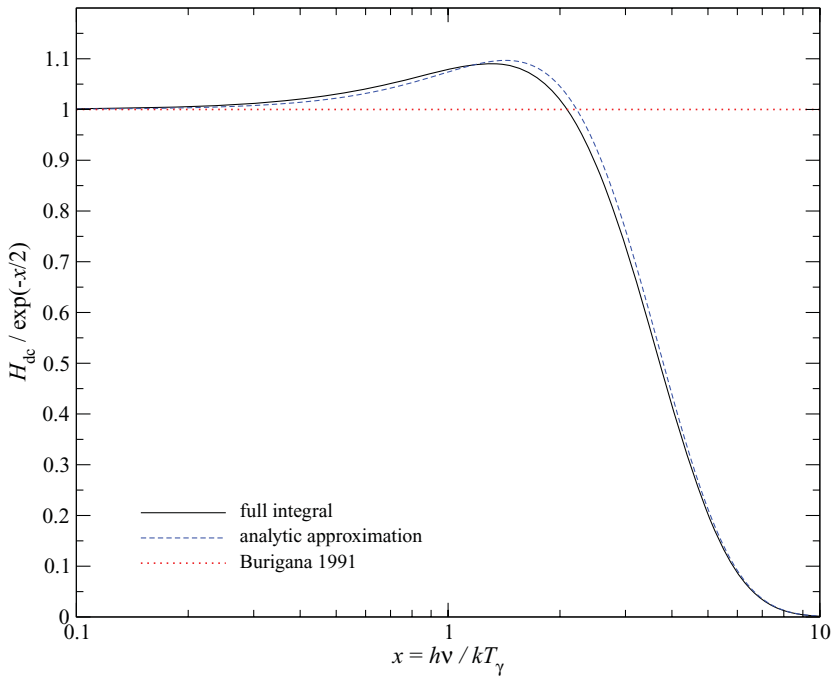

Figure 3.16: Effective double Compton correction factor $H_{\rm dc}(x)$. We compare the result from a full integration of a blackbody spectrum with the approximation given by Eq. (3.53). For comparison, we also show the approximation $H_{\rm dc}(x) \approx {\rm e}^{-x/2}$ given by Burigana et al. [4]. Close to the maximum of the CMB blackbody spectrum the differences are $\sim 20\% - 40\%$ and at high frequencies the expression of Burigana et al. [4] overestimates the DC emission significantly. The figure is taken from Chluba & Sunyaev [17].

3.4 Final set of evolution equations

We now have all the ingredients together to write down the photon and electron evolution equations. For the photons we perform one more step by transforming to $x = h\nu/kT_\gamma$, with $T_\gamma = T_0(1+z)$, instead of p or ν itself. This allows us to absorb the redshifting term, $-Hp\partial_p f$, in Eq. (3.11), so that with ${\rm d}\tau = \sigma_{\rm T} N_{\rm e} c\,{\rm d}t$ we have

$$\frac{\partial f}{\partial \tau} \approx \frac{\theta_{\rm e}}{x^2}\frac{\partial}{\partial x}x^4\left[\frac{\partial}{\partial x}f + \frac{T_\gamma}{T_{\rm e}}f(1+f)\right] + \frac{K_{\rm BR}\,{\rm e}^{-x_{\rm e}}}{x_{\rm e}^3}[1 - f\,({\rm e}^{x_{\rm e}}-1)] + \frac{K_{\rm DC}\,{\rm e}^{-2x}}{x^3}[1 - f\,({\rm e}^{x_{\rm e}}-1)] + S(\tau, x) \quad (3.54a)$$

$$K_{\rm BR} = \frac{\alpha}{2\pi}\frac{\lambda_{\rm e}^3}{\sqrt{6\pi}\,\theta_{\rm e}^{7/2}}\sum_i Z_i^2 N_i\,\bar{g}_{\rm ff}(Z_i, T_{\rm e}, T_\gamma, x_{\rm e}), \qquad K_{\rm DC} = \frac{4\alpha}{3\pi}\,\theta_\gamma^2\, I_{\rm dc}\, g_{\rm dc}(T_{\rm e}, T_\gamma, x) \quad (3.54b)$$

$$\bar{g}_{\rm ff}(x_{\rm e}) \approx \begin{cases} \frac{\sqrt{3}}{\pi}\ln\left(\frac{2.25}{x_{\rm e}}\right) & \text{for} \quad x_{\rm e} \le 0.37 \\ 1 & \text{otherwise} \end{cases}, \qquad g_{\rm dc} \approx \frac{1 + \frac{3}{2}x + \frac{29}{24}x^2 + \frac{11}{16}x^3 + \frac{5}{12}x^4}{1 + 19.739\theta_\gamma - 5.5797\theta_{\rm e}}. \quad (3.54c)$$

where $f = f(\tau, x)$, $I_{\rm dc} = \int x^4 f(1+f)\,{\rm d}x \approx 4\pi^4/15$, $g_{\rm dc} \approx G_{\rm dc}\,H_{\rm dc}{\rm e}^{2x}$ with $G_{\rm dc}$ and $H_{\rm dc}$ taken from Eq. (3.51) and (3.53b), respectively. The DC Gaunt factor, $g_{\rm dc}$, should provide a very good approximation for our purposes. For the BR Gaunt factors, $\bar{g}_{\rm ff}$, we use fits from Itoh et al. [30] in numerical calculations or the above approximation for estimates. We also explicitly added a photon source term, $S(\tau, x)$, although the specific shape depends on the process. This term adds both energy and photons to the photon field.

Equation (3.54) needs to be augmented by an evolution equation for the electron temperature. This equation can be readily derived from Eq. (3.14) adding non-zero collision terms (Exercise 5). It has contributions from the adiabatic expansion of the Universe, which drives $T_{\rm e} \propto a^{-2}$. The adiabatic cooling is counteracted by

Compton heating, which drives the electron temperature always extremely close to the photon temperature until $z \simeq 10^2$ (see Fig. 3.8). It is thus useful to use $\rho_\mathrm{e} = T_\mathrm{e}/T_\gamma$ as a variable. In addition, when spectral distortions are present, the matter cools/heats via DC and BR, but the effect is small and can be neglected. Finally, if some significant energy is released, this will in addition heat the medium. Putting all this together the evolution equation for the electron temperature reads [compare, 17]

$$\frac{\mathrm{d}\rho_\mathrm{e}}{\mathrm{d}\tau} = \frac{\mathrm{d}(T_\mathrm{e}/T_\gamma)}{\mathrm{d}\tau} = \frac{t_\mathrm{T}\dot{Q}}{\alpha_\mathrm{h}\theta_\gamma} + \frac{4\tilde{\rho}_\gamma}{\alpha_\mathrm{h}}[\rho_\mathrm{e}^\mathrm{eq} - \rho_\mathrm{e}] - \frac{4\tilde{\rho}_\gamma}{\alpha_\mathrm{h}}\mathcal{H}_\mathrm{DC,BR}(\rho_\mathrm{e}) - H\,t_\mathrm{T}\,\rho_\mathrm{e}. \tag{3.55}$$

Here, we introduced the heat capacity of the medium[4], $k\alpha_\mathrm{h} = \frac{3}{2}k[N_\mathrm{e} + N_\mathrm{H} + N_\mathrm{He}] = \frac{3}{2}kN_\mathrm{H}[1 + f_\mathrm{He} + X_\mathrm{e}]$; the energy injection rate (per $m_\mathrm{e}c^2$), $\dot{Q}$, which for example could be caused by some decaying particles; and the energy density of the photon field in units of electron rest mass, $\tilde{\rho}_\gamma = \rho_\gamma/m_\mathrm{e}c^2$. We furthermore defined $\rho_\mathrm{e}^\mathrm{eq} = T_\mathrm{e}^\mathrm{eq}/T_\gamma$, where T_e^eq is the Compton equilibrium temperature, Eq. (3.29). The BR and DC heating integral, $\mathcal{H}_\mathrm{DC,BR}$, can be directly computed using the corresponding terms in the photon Boltzmann equation, Eq. (3.54).

It is rather straightforward to solve the photon Boltzmann and temperature equations for a given energy release scenario numerically. One flexible code is[5] CosmoTherm [17], with several scenarios implemented. The departure from equilibrium are created purely by the electron heating term, $\propto \dot{Q}$, and the photon source term, $S(\tau, x)$. One of the great simplifications we will discuss below is that all distortions are expected to be small, so that the problem can be *linearized*. In this case, one can resort to a *Greens function method* [9], which allows us to compute the distortion signal for different energy release scenarios efficiently, as we explain below. Under simplifying assumptions, additional insight can be found analytically, as we explain in the next section.

Exercises

Exercise 1 Prove Eq. (3.14) using the conservation law $T^\mu{}_{\nu;\mu} = 0$ of the energy momentum tensor for the isotropic Universe. You will need the Christoffel symbols for the FRW metric, which you can find in Dodelson [21], but you can also explicitly compute them (if you like).

Exercise 2 Explicitly derive the Kompaneets equation, using Eq. (3.25) and the moments Eq. (3.26).

Exercise 3 Estimate by how much the DC emissivity is reduced at redshift $z = 10^6$ and 10^7. Given that thermalization becomes very slow at $z \simeq$ few $\times\, 10^5$ and very rapid at $z \gg 2 \times 10^6$, how large a correction to the thermalization problem do you expect?

Exercise 4 Can you derive the approximation Eq. (3.53b)? Think about which photons produce most of the emission. Does this allow you to simplify the integral?

Exercise 5 Derive the evolution equation for the electron temperature, Eq. (3.55) starting from Eq. (3.14) for all ordinary matter species. Due to Coulomb interactions protons, electron, hydrogen atoms and helium ions behave as one fluid with the number of particles not changing anymore. Injecting some energy into one of the species means that the energy is shared among all of them. Can you give the explicit form of the term due to DC and BR emission.

[4] We neglected relativistic corrections to the heat capacity of the electrons, which at $z \sim 10^7$ would be of order percent [7].

[5] `www.Chluba.de/CosmoTherm/`

Chapter 4

Simple Analytic Approximations

In this chapter, we discuss simple analytic approximations for the spectral distortions caused by early energy release. We start by introducing the *Compton-y* and *μ-distortions*, which are the *classical* types of distortions first studied by Zeldovich & Sunyaev [59] and Sunyaev & Zeldovich [54]. In the *y*-distortion era ($z \lesssim 5\times10^4$), DC and BR emission and photon transport from low to high frequencies are already inefficient, so that at high frequencies the distortion shape is purely determined by Compton scattering. In contrast, during the *μ*-era ($z \gtrsim 5\times10^4$), thermalization works very well and the amplitude of the distortion evolves significantly. The efficiency of thermalization is described by the *distortion visibility function*, which is close to unity at $z \lesssim 2\times10^6$ but drops exponentially at higher redshifts, as we explain in more detail here.

4.1 Compton-*y* distortion and the thermal Sunyaev-Zeldovich effect

In section 3.3.3, we learned that around $z_{\rm K} \simeq 5\times10^4$ the Comptonization time-scale (transfer of energy from electrons to photons) becomes longer than the Hubble time. It is clear that this marks an important transition in the efficiency of Compton scattering and redistribution of photons. Let us try to quantify this a little better by looking at the photon evolution equation. If we neglect DC and BR emission processes, we have

$$\left.\frac{\partial f}{\partial \tau}\right|_{\rm CS} \equiv \frac{\theta_{\rm e}}{x^2}\frac{\partial}{\partial x}x^4\left[\frac{\partial}{\partial x}f + \frac{T_\gamma}{T_{\rm e}}f(1+f)\right], \tag{4.1}$$

in the expanding Universe, with $f = f(\tau, x)$. This equation has no general analytic approximation, but we can solve it for limiting cases.

4.1.1 Scattering of CMB photons in the limit of small *y*.

Assuming that at $\tau = 0$ we start with $f = f_{\rm bb} = 1/({\rm e}^x - 1)$, then after a very short time $\Delta\tau \ll 1$ we find

$$\begin{aligned}
\Delta f &\approx \frac{\Delta\tau\theta_{\rm e}}{x^2}\frac{\partial}{\partial x}x^4\left[\frac{\partial}{\partial x}f_{\rm bb} + \frac{T_\gamma}{T_{\rm e}}f_{\rm bb}(1+f_{\rm bb})\right]\\
&\approx \frac{\Delta\tau(\theta_\gamma-\theta_{\rm e})}{x^2}\frac{\partial}{\partial x}x^4 f_{\rm bb}(1+f_{\rm bb})\\
&\approx \Delta\tau(\theta_\gamma-\theta_{\rm e})\left[4x f_{\rm bb}(1+f_{\rm bb}) - x^2 f_{\rm bb}(1+f_{\rm bb})(1+2f_{\rm bb})\right]\\
&\approx \Delta\tau(\theta_{\rm e}-\theta_\gamma)\,G(x)\left[x\,\frac{{\rm e}^x+1}{{\rm e}^x-1} - 4\right] \equiv \Delta\tau(\theta_{\rm e}-\theta_\gamma)\,Y_{\rm SZ}(x),
\end{aligned} \tag{4.2}$$

where we used $\partial_x f_{\rm bb} = -f_{\rm bb}(1+f_{\rm bb}) = -{\rm e}^x/({\rm e}^x-1)^2 = -G(x)/x$ and $(1+2f_{\rm bb}) = ({\rm e}^x+1)/({\rm e}^x-1) = \coth(x/2)$. This is the definition of the so called *Compton-y* distortion, $Y_{\rm SZ}(x)$, which arises in the limit of scatterings with

inefficient energy exchange. This distortion of the CMB was first studied by Zeldovich & Sunyaev [59] and then applied to hot electrons residing inside the potential wells of clusters of galaxies, giving rise to the *thermal Sunyaev-Zeldovich (SZ) effect*. The important time-scale is determined by the *Compton-y parameter*

$$y = \int_0^\tau \frac{k(T_\mathrm{e} - T_\gamma)}{m_\mathrm{e} c^2} \,\mathrm{d}\tau' = \int_0^t \frac{k(T_\mathrm{e} - T_\gamma)}{m_\mathrm{e} c^2} \sigma_\mathrm{T} N_\mathrm{e} c \,\mathrm{d}t', \tag{4.3}$$

which depends on the number of scattering (related to τ) and the net energy exchange[1], $\Delta\nu/\nu \simeq 4(\theta_\mathrm{e} - \theta_\gamma)$, per scattering. Clearly, for $T_\mathrm{e} \equiv T_\gamma$ one has $y = 0$ and $\Delta f = 0$, no matter how many scattering actually take place! The solution Eq. (4.2) for the distortion is thus valid as long as $y \ll 1$, which also ensures that the electron temperature does not change much by the scattering.

One possible way to violate this condition even if the number of scattering is tiny ($\tau \ll 1$) is by having a very large difference in the electron and photon temperature. Note, however, that $\theta_\mathrm{e} \ll 1$ is needed since otherwise relativistic corrections to the Compton process appear, which are not accounted for by the Kompaneets equation. For the cosmological thermalization problem, we are always in the situation that the y-parameter is increased beyond unity by increasing the number of scatterings. In this case, Compton scattering pushes electrons and photons into kinetic equilibrium until a μ-distortion is formed (Sect. 4.2).

Assuming that we are in the regime $|y| \ll 1$, there are two cases of interest:

- $y > 0$: so that overall energy is transferred from the electrons to the photons → *Comptonization*
- $y < 0$: where energy flows from the photons to the electrons → *Compton cooling*

For most conditions in our Universe, $y > 0$ is relevant, since most processes tend to heat the matter in the Universe. Therefore *negative y-distortions* are usually not being considered, however, the adiabatic cooling of matter in the expanding Universe (in the absence of heating) allows $T_\mathrm{e} < T_\gamma$, so that $y < 0$ does occur [7, 17].

In Fig. 4.1, we illustrate frequency dependence of the y-distortion for $T_0 = 2.725\,\mathrm{K}$. It has a very characteristic shape, with a deficit of photons in the Rayleigh-Jeans part and an increment of photon in the Wien tail of the CMB spectrum. The limiting behaviors are

$$Y_\mathrm{SZ}(x) = G(x)\left[x\,\frac{\mathrm{e}^x + 1}{\mathrm{e}^x - 1} - 4\right] \approx \begin{cases} -\frac{2}{x} & \text{for} \quad x \ll 1 \\ x(x-4)\mathrm{e}^{-x} & \text{for} \quad x \gg 1. \end{cases} \tag{4.4}$$

This corresponds to $\Delta I/I \simeq \Delta T/T \simeq -2y$ for $x \ll 1$ and $\Delta T/T \simeq (x-4)y$ for $x \gg 1$. The y-distortion vanishes close to $\nu \simeq 217\mathrm{GHz}\,(\equiv x \simeq 3.830)$, which in principle makes it distinguishable from the μ-distortion (Sect. 4.2). One can easily verify that for a y-distortion

$$\Delta N_\gamma = 0 \propto \int x^2 Y_\mathrm{SZ}(x) \tag{4.5a}$$

$$\Delta\rho_\gamma = 4y\,\rho_\gamma^\mathrm{Pl} \propto \int x^3 Y_\mathrm{SZ}(x)\,\mathrm{d}x. \tag{4.5b}$$

Clearly, Compton scattering should not change the number of photons, as reflected by Eq. (4.5a). Equation (4.5b) implies that $4y \equiv \Delta\rho_\gamma/\rho_\gamma^\mathrm{Pl}$ defines the fractional energy exchange of the electrons with the initial blackbody spectrum. Thus, starting from a pure blackbody, by computing $y = (1/4)\Delta\rho_\gamma/\rho_\gamma^\mathrm{Pl} \ll 1$ one can directly give an approximation for the distortion [59]. In detail, it may be a little more involved to compute $\Delta\rho_\gamma/\rho_\gamma^\mathrm{Pl}$ for some process, but all one really needs to know is how much energy was pumped into the CMB by energy exchange with the thermal electrons.

[1] In a sense it would be better to write $y = \frac{1}{4}\int_0^\tau 4\frac{k(T_\mathrm{e}-T_\gamma)}{m_\mathrm{e}c^2}\,\mathrm{d}\tau'$, so that $4y = \Delta\rho_\gamma/\rho_\gamma$ evidently gives the total amount of energy transfer.

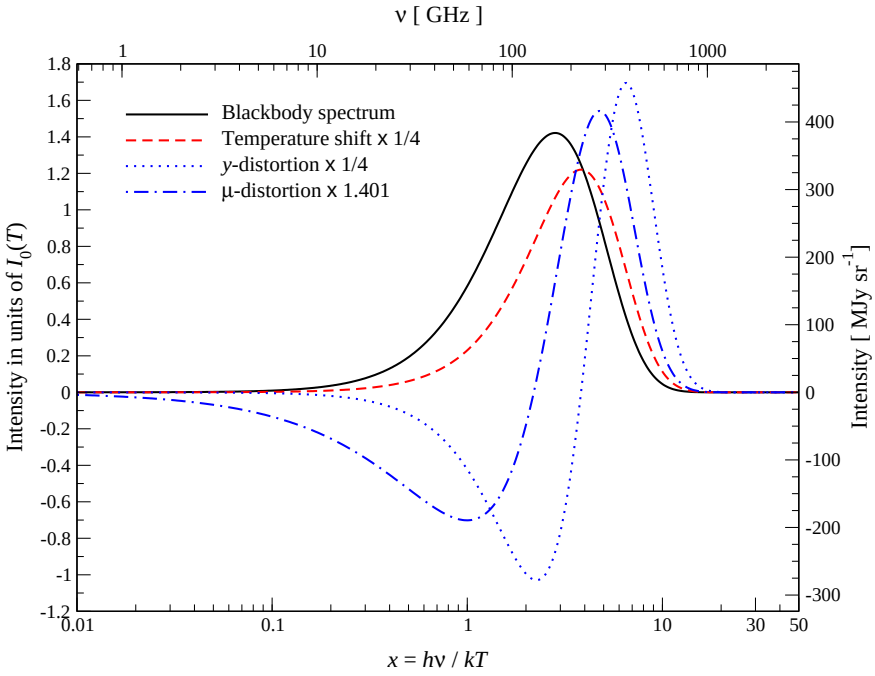

Figure 4.1: Comparison of a Compton y-distortion, $Y_{\rm SZ}(x)$, and μ-distortion, $M(x)$, with the blackbody spectrum and temperature shift, $G(x)$. For convenience, we plot the spectrum as a function of $x = h\nu/kT$ and normalize the left y-axis by $I_0(T) = (2h/c^2)(kT/h)^3 \approx 270\,{\rm MJy\,sr^{-1}}(T/2.725{\rm K})^3$. The y-distortion has its crossover frequency around $x \simeq 3.830\,(\equiv 217{\rm GHz})$, while the μ-distortion has its zero around $x \simeq 2.192\,(\equiv 124{\rm GHz})$. The upper x-axis and right y-axis also give the corresponding frequency and spectral intensity for $T = 2.725\,{\rm K}$.

4.1.2 Thermal Sunyaev-Zeldovich effect

Clusters of galaxies are the largest virialized objects in our Universe, with typical masses $M \simeq (10^{13} - 10^{14}) M_\odot$ ($M_\odot \approx 2\times10^{33}\,{\rm g}$) and up to $\simeq 10^3$ galaxies. Cluster also host a hot plasma with free electrons at temperature $T_{\rm e} \simeq$ few $\times\, 10^7{\rm K}\,(\equiv$ few $\times$ keV) at typical densities $N_{\rm e} \simeq 10^{-3}\,{\rm cm^{-3}}$. We know this already for a while since clusters show a X-ray glow produced by thermal Bremsstrahlung. The hot electrons can scatter CMB photons and create a Compton-y distortion. The typical y-parameter of massive clusters is $y \simeq$ few $\times\, 10^{-5} - 10^{-4}$ with $\theta_{\rm e} \simeq$ few $\times\, 10^{-2}$ and $\tau \simeq$ few $\times\, 10^{-3}$. Because for clusters $T_{\rm e} \gg T_\gamma$, the y-parameter reads

$$y = \int_0^\tau \frac{kT_{\rm e}}{m_{\rm e}c^2}\,{\rm d}\tau' \approx \theta_{\rm e}\,\tau \tag{4.6}$$

and thus directly probes the *integrated electron pressure*, $\bar{P}_{\rm e} \simeq \int N_{\rm e} T_{\rm e}\,{\rm d}l$, through the cluster medium.

One of the great properties of the thermal SZ effect that is it independent of redshift (ignoring evolutionary effects) [53, 44, 5]. The reason is that CMB temperature increases $\propto (1+z)$ with redshift, so that the '*light bulb*' illuminating the hot electrons residing inside the cluster becomes brighter the higher the redshift. The cosmological redshift dimming of the signals, which for example reduces the X-ray fluxes for high redshift clusters, is therefore compensated since the CMB itself is brighter, and no matter what the redshift of the cluster is it will have the same signal relative to the CMB. It is interesting to point out that if we could go back to $z = 1$, in terms of the bolometric luminosity all clusters would be brighter by $2^4 = 16$ (as the CMB itself would), even if we did not change the clusters! The redshift-independence of the SZ signal thus refers to how clusters at different redshifts are seen by the observer but the same cluster signal is brighter if the observer is a higher redshift. The redshift-independence of the SZ signal makes SZ clusters a powerful cosmological probe,

since one can in principle track the growth of structures out to high redshifts ($z \simeq 1-2$) and thus constrain cosmological parameters and the evolution of dark energy [3, 5].

But the thermal SZ effect is even more rich. For a cluster with $kT_\mathrm{e} = 5\mathrm{keV}$, the thermal velocities of the electrons are $v_\mathrm{th} \simeq \sqrt{2\theta_\mathrm{e}}c \simeq 0.14c$. That is quite fast and relativistic corrections become important. In this regime the Kompaneets equation is no longer valid and one has to include higher order corrections [6, 46, 29], which we will discuss later. In addition, if the cluster is moving with respect to the CMB, the Doppler kick adds a change in the CMB temperature towards the cluster by $\Delta I \simeq \beta_\mathrm{c}\tau\, T\partial_T B_\nu(T)$, also knows as *kinematic SZ effect* [53]. This can in principle be used to study large-scale bulk flows in the Universe.

4.2 Chemical potential or μ-distortion

We now understand that for inefficient energy exchange between electrons and photons the shape of the distortion is determined by the y-parameter and has a spectral dependence, $Y_\mathrm{SZ}(x) = G(x)[x\coth(x/2) - 4]$, shown in Fig. 4.1. Let us now consider the other extreme, when many scatterings are taking place and the redistribution of photons in frequency is very efficient. In the early Universe, this regime is found at $z \gtrsim 5\times10^4$ and the distortion is given by the μ-distortion.

4.2.1 Compton equilibrium solution

When many scattering occur, the spectrum is driven towards an equilibrium with respect to Compton scattering. Neglecting emission and absorption processes, the kinetic equation thus becomes quasi-stationary

$$0 \approx \frac{\theta_\mathrm{e}}{x^2}\frac{\partial}{\partial x}x^4\left[\frac{\partial}{\partial x}f + \frac{T_\gamma}{T_\mathrm{e}}\,f(1+f)\right]. \tag{4.7}$$

One solution of this equation is $f_\mathrm{bb} = 1/(\mathrm{e}^x - 1)$ if $T_\mathrm{e} \equiv T_\gamma$, since $\partial_x f_\mathrm{bb} = -f_\mathrm{bb}(1+f_\mathrm{bb})$, as it should be for full equilibrium. However, this is not the general solution of the problem! To find the general solution we have to solve the equation

$$\partial_x f = -\frac{T_\gamma}{T_\mathrm{e}}\,f(1+f). \tag{4.8}$$

The factor T_γ/T_e can be absorbed by redefining the frequency scaling $x \rightarrow x_\mathrm{e}$ so that $\partial_{x_\mathrm{e}} f = -f(1+f)$. This can be integrated to $\ln(1+f) - \ln(f) \equiv x_\mathrm{e} + \mathrm{const}$, or

$$f_\mathrm{eq} = \frac{1}{\mathrm{e}^{x_\mathrm{e}+\mu_0} - 1}, \tag{4.9}$$

where we introduced the integration constant μ_0. This is a *Bose-Einstein spectrum* with constant chemical potential[2] μ_0. Let's pause for a moment. Photons have no rest mass, so the chemical potential should vanish? This statement is only true if we are in full equilibrium, i.e., we have a blackbody at the temperature of the medium. More generally, for fixed photon number the chemical potential can be non-zero.

The chemical potential can in principle be both positive or negative:

- $\mu_0 > 0$: *fewer* photons than in a blackbody at temperature T_e $\rightarrow$ *energy release / photon destruction*
- $\mu_0 \equiv 0$: blackbody at temperature T_e $\rightarrow$ *full equilibrium*
- $\mu_0 < 0$: *more* photons than in a blackbody at temperature T_e $\rightarrow$ *energy extraction / photon injection*

In practice, the solution $\mu_0 < 0$ is unphysical unless μ_0 is actually a function of frequency. The reason is that $x_\mathrm{e} + \mu_0$ can vanish at $x_\mathrm{e} = -\mu_0 > 0$, but this state is never reached or even passed though during the evolution, since instead excess photons would form a Bose-condensate at $x = 0$ with $\mu_0 = 0$ elsewhere [57, 60]. In a real plasma, BR and DC emission will prevent this from happening though [28, 34].

[2] Notice that the sign is different from the normal convention used in thermodynamics.

4.2.2 Definition of the μ-distortion

In the previous paragraph, we showed that $f = 1/(\mathrm{e}^{x_\mathrm{e}+\mu_0} - 1)$ is approached if you have many scatterings in the plasma. But how do we fix the constant μ_0 and what is the definition of the distortion really? Let us assume we start with a blackbody and electrons at temperature $T_\gamma = T_\mathrm{e} = T_i$. Let us change the number and energy density of the photon field by some $\epsilon_N = \Delta N_\gamma / N_\gamma^\mathrm{Pl}(T_i)$ and $\epsilon_\rho = \Delta\rho_\gamma/\rho_\gamma^\mathrm{Pl}(T_i)$, respectively, and then wait until everything has equilibrated by Compton scattering (no DC or BR emission). We then have the conditions

$$N_\gamma^\mathrm{BE} = N_\gamma^\mathrm{Pl}(T_i)(1+\epsilon_N) \equiv \frac{N_\gamma^\mathrm{Pl}(T_f)}{G_2^\mathrm{Pl}} \int \frac{x_\mathrm{f}^2\,\mathrm{d}x_\mathrm{f}}{\mathrm{e}^{x_\mathrm{f}+\mu_0}-1} \tag{4.10a}$$

$$\rho_\gamma^\mathrm{BE} = \rho_\gamma^\mathrm{Pl}(T_i)(1+\epsilon_\rho) \equiv \frac{\rho_\gamma^\mathrm{Pl}(T_f)}{G_3^\mathrm{Pl}} \int \frac{x_\mathrm{f}^3\,\mathrm{d}x_\mathrm{f}}{\mathrm{e}^{x_\mathrm{f}+\mu_0}-1}, \tag{4.10b}$$

where T_f is the final temperature of the electrons in the distorted (Bose-Einstein spectrum) radiation field and $x_\mathrm{f} = h\nu/kT_f$. These two equations allow us to fix T_f and μ_0 as a function of the parameters ϵ_N and ϵ_ρ. The general solution is determined by

$$\left(\frac{(1+\epsilon_\rho)^{3/4}}{G_2^\mathrm{Pl}} \int \frac{x_\mathrm{f}^2\,\mathrm{d}x_\mathrm{f}}{\mathrm{e}^{x_\mathrm{f}+\mu_0}-1}\right)^{1/3} \equiv \left(\frac{(1+\epsilon_N)^{4/3}}{G_3^\mathrm{Pl}} \int \frac{x_\mathrm{f}^3\,\mathrm{d}x_\mathrm{f}}{\mathrm{e}^{x_\mathrm{f}+\mu_0}-1}\right)^{1/4} \tag{4.11a}$$

$$\frac{T_i}{T_f}(1+\epsilon_N)^{1/3} = \left(\frac{1}{G_2^\mathrm{Pl}} \int \frac{x_\mathrm{f}^2\,\mathrm{d}x_\mathrm{f}}{\mathrm{e}^{x_\mathrm{f}+\mu_0}-1}\right)^{1/3}, \tag{4.11b}$$

which is fun to play with but is not as illuminating. Assuming that all changes are small we have

$$N_\gamma^\mathrm{BE} \approx N_\gamma^\mathrm{Pl}(T_f)\left[1-\mu_0\mathcal{M}_2^\mathrm{c}\right] \approx N_\gamma^\mathrm{Pl}(T_i)\left[1+3\frac{\Delta T}{T_i}-\mu_0\mathcal{M}_2^\mathrm{c}\right] \tag{4.12a}$$

$$\rho_\gamma^\mathrm{BE} \approx \rho_\gamma^\mathrm{Pl}(T_f)\left[1-\mu_0\mathcal{M}_3^\mathrm{c}\right] \approx \rho_\gamma^\mathrm{Pl}(T_i)\left[1+4\frac{\Delta T}{T_i}-\mu_0\mathcal{M}_3^\mathrm{c}\right], \tag{4.12b}$$

where $\mathcal{M}_k^\mathrm{c} = kG_{k-1}^\mathrm{Pl}/G_k^\mathrm{Pl}$, so that we have $\mathcal{M}_2^\mathrm{c} \approx 1.3684$ and $\mathcal{M}_3^\mathrm{c} \approx 1.1106$. With the conditions Eq. (4.10), we then find [54, 26]

$$\mu_0 \approx \frac{3}{\kappa^\mathrm{c}}\left[\frac{\Delta\rho_\gamma}{\rho_\gamma}-\frac{4}{3}\frac{\Delta N_\gamma}{N_\gamma}\right] \approx 1.401\left[\frac{\Delta\rho_\gamma}{\rho_\gamma}-\frac{4}{3}\frac{\Delta N_\gamma}{N_\gamma}\right] \tag{4.13a}$$

$$\frac{\Delta T}{T_i} \approx \frac{\mathcal{M}_2^\mathrm{c}}{\kappa^\mathrm{c}}\frac{\Delta\rho_\gamma}{\rho_\gamma}-\frac{\mathcal{M}_3^\mathrm{c}}{\kappa^\mathrm{c}}\frac{\Delta N_\gamma}{N_\gamma} \approx 0.6389\frac{\Delta\rho_\gamma}{\rho_\gamma}-0.5185\frac{\Delta N_\gamma}{N_\gamma} \approx 0.4561\mu_0+\frac{1}{3}\frac{\Delta N_\gamma}{N_\gamma} \tag{4.13b}$$

with $\kappa^\mathrm{c} = 4\mathcal{M}_2^\mathrm{c} - 3\mathcal{M}_3^\mathrm{c} \approx 2.1419$. From Eq. (4.13a) we see that for $\Delta\rho_\gamma/\rho_\gamma \equiv (4/3)\Delta N_\gamma/N_\gamma$ we have no distortion ($\mu_0 = 0$), as we already understood from the adiabatic condition, Eq. (2.15). In this case, only the temperature of the blackbody is increased after scattering redistributed all photons, $\Delta T/T_i \approx \frac{1}{3}\Delta N_\gamma/N_\gamma$.

In Fig. 4.2 we illustrate a Bose-Einstein spectrum with $\mu_0 = 0.5$ and $T_i = T_0 = 2.726\,\mathrm{K}$. Only energy was added to the photons but the number of photons was not changed with respect to the initial CMB spectrum. One can see that in the Rayleigh-Jeans tail of the CMB the Bose-Einstein spectrum shows a deficit of photons, while in the Wien tail more photons than in the CMB blackbody spectrum are present. We have $f_\mathrm{BE} \approx f_\mathrm{bb}$ at $\nu_\mathrm{cr} \approx 124\,\mathrm{GHz}$ although for large chemical potential $\nu_\mathrm{cr} \approx 124\,\mathrm{GHz}\,(1-0.304\,\mu\ln\mu)$ is more accurate [10].

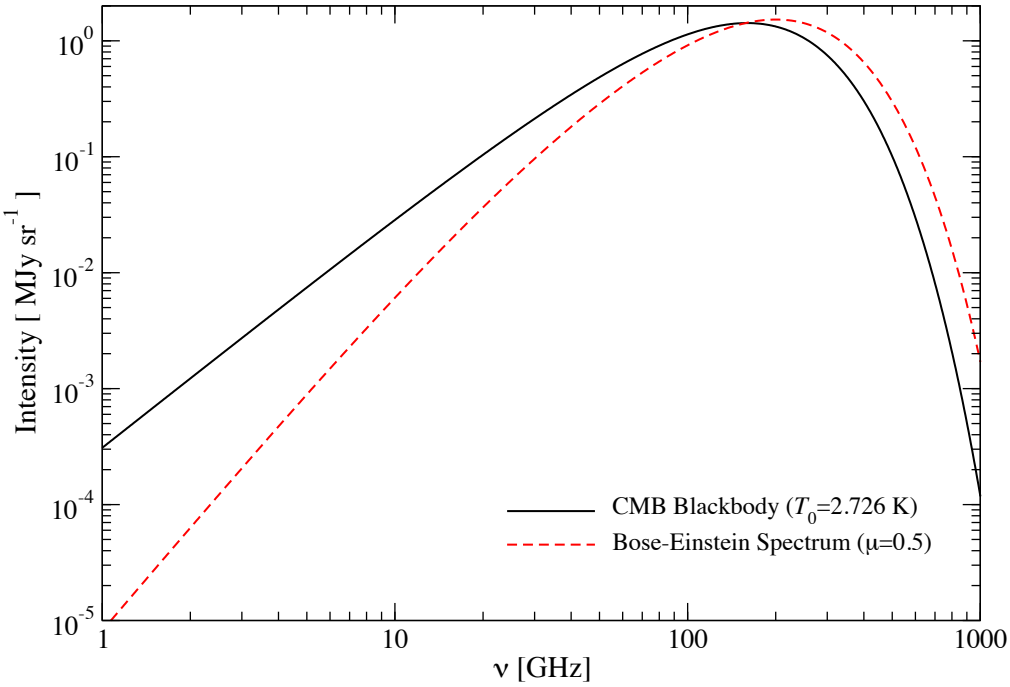

Figure 4.2: Bose-Einstein spectrum for large chemical potential $\mu = 0.5$ and $T_i = T_0 = 2.726\,\mathrm{K}$. Only energy was added to the photon field, but the number of photons was not changed with respect to the initial CMB spectrum. For large chemical potential, the cross over frequency shifts towards higher frequencies according to $\nu_{\rm cr} \approx 124\,\mathrm{GHz}\,(1 - 0.304\,\mu\ln\mu) \approx 158\,\mathrm{GHz}$. The figure was taken from Chluba [10].

But how do we define the distortion? To derive the expressions from above, we used

$$f_{\rm BE} = \frac{1}{\mathrm{e}^{x_{\rm e}+\mu_0}-1} \approx \frac{1}{\mathrm{e}^{x_{\rm e}}-1} - \frac{G(x_{\rm e})}{x_{\rm e}}\mu_0 + \mathcal{O}(\mu_0^2). \tag{4.14}$$

This suggest that $\Delta f = -G(x_{\rm e})\,\mu_0/x_{\rm e}$ could be called the distortion with respect to the blackbody part at temperature $T_{\rm e}$ and in fact this kind of definition has be used frequently. However, since also the final electron temperature, $T_{\rm e} = T_f$, depends on μ_0, this definition does not separate the distortion cleanly. Motivated by the fact that Compton scattering conserves photon number, one natural definition is to fix the μ-distortion such that $\int x^2 M(x)\,\mathrm{d}x = 0$. Integrating Δf gives $\int x^2\Delta f\,\mathrm{d}x = -2\mu_0\int x\,\mathrm{d}x/(\mathrm{e}^x-1) = -2G_1^{\rm Pl}\mu_0 = -\mu_0\,\pi^2/3 \approx -3.2899\,\mu_0$, so that $M(x) = G(x)[\alpha_\mu - 1/x]$ with $\alpha_\mu = 2G_1^{\rm Pl}/3G_2^{\rm Pl} = \pi^2/18\zeta(3) \approx 0.4561$ fulfills $\int x^2 M(x)\,\mathrm{d}x = 0$. If we in addition normalize the relative change of the photon energy density to unity ($\Delta\rho_M/\rho^{\rm Pl} = 1$), we find the spectral shape of the μ-distortion

$$M^*(x) = \frac{3}{\kappa^{\rm c}}M(x) = \frac{3}{\kappa^{\rm c}}G(x)\left[\alpha_\mu - \frac{1}{x}\right] \approx 1.401\,G(x)\left[0.4561 - \frac{1}{x}\right] \approx \begin{cases} -\frac{1.401}{x^2} & \text{for} \quad x \ll 1 \\ 0.6390\,x\,\mathrm{e}^{-x} & \text{for} \quad x \gg 1. \end{cases} \tag{4.15}$$

This implies $\Delta I/I \simeq \Delta T/T \simeq -\mu_0/x$ for $x \ll 1$ and $\Delta T/T \simeq 0.4561\,\mu_0$ at $x \gg 1$. The frequency dependence of $M(x)$ is illustrated in Fig. (4.1) in comparison with the y-distortion and spectrum of a temperature shift. The important feature of a μ-distortion is that it is shifted towards lower frequencies with respect to the y-distortion. This makes is distinguishable and observing a μ-distortion is a clear indication for a signal created in the pre-recombination era, deep into the thermal history of our Universe.

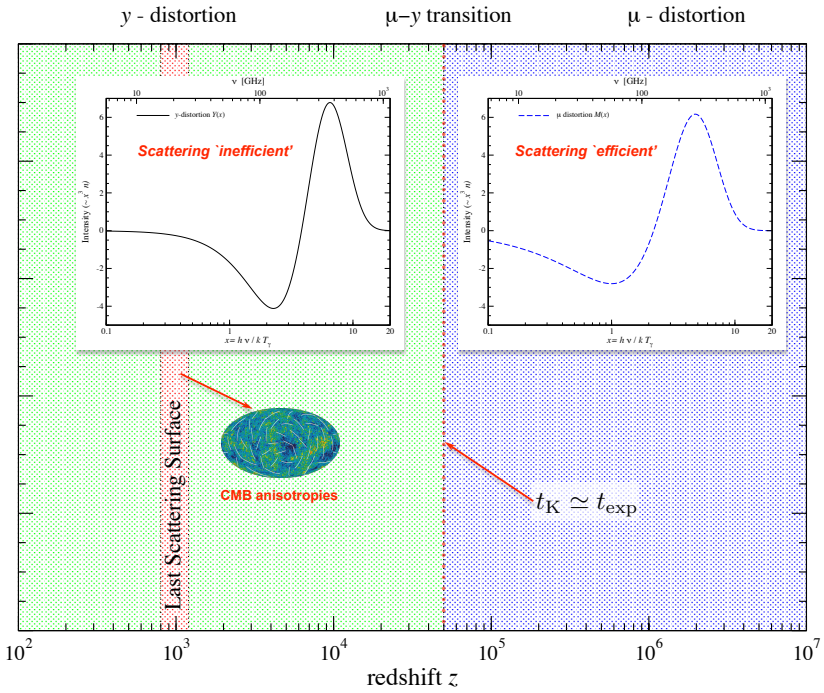

Figure 4.3: Simplest zeroth order picture for the formation of primordial distortions. At low redshifts ($z \lesssim 5 \times 10^4$), a y-distortion is formed, while at high redshifts we expect a μ-distortion. At this point we have not included any photon production and we will see that this strongly attenuates the amplitude of the μ-distortion at $z \gtrsim 2 \times 10^6$.

4.2.3 Simple zeroth order description of primordial distortions

We now have all the pieces for the simplest zeroth order description of primordial distortions together. At late times, ($z \lesssim z_{\rm K} \simeq 5 \times 10^4$), the redistribution of photons by Compton scattering becomes inefficient and a y-type distortion is formed, in the other extreme we have a μ-distortion (see Fig. 4.3) with the approximations

$$y \approx \frac{1}{4} \left. \frac{\Delta\rho_\gamma}{\rho_\gamma} \right|_y \tag{4.16a}$$

$$\mu_0 \approx 1.401 \left[\left. \frac{\Delta\rho_\gamma}{\rho_\gamma} \right|_\mu - \frac{4}{3} \left. \frac{\Delta N_\gamma}{N_\gamma} \right|_\mu \right], \tag{4.16b}$$

so that the total distortion is given by $\Delta f \approx Y_{\rm SZ}\, y + M(x)\, \mu_0$. Here, we indicate that to estimate the distortion one needs to consider the *partial energy release* and *photon production* in the respective y- and μ-era. If photons are injected in the y-era, the distortion is not just a y-distortion, since these extra photons are not redistributed very efficiently, but in the μ-era they are ingested and modify the effective chemical potential. We can, however, treat the problem of photon injection during the y-era approximately (Sect. 4.3).

Two important aspects are still missing. Firstly, we have not included any photon production into the picture but assumed that only Compton scattering changes the photon field. This will be mostly relevant for the evolution of μ-distortions, since not all energy release or photon production eventually is visible as a distortion. That is, the *distortion visibility function* is smaller than unity because thermalization reduces the effective amount of energy release that survives as a distortion. This is implicitly hidden in the definition of $\Delta\rho_\gamma/\rho_\gamma$ and $\Delta N_\gamma/N_\gamma$. We will consider this problem in Sect. 4.5. The second point is that the transition between μ and y distortions is not abrupt but occurs over a range of redshifts where in the intermediate regime the distortion is not only given by the superposition of μ and y-distortion. This makes the distortion signal much richer, as pointed out only recently [17, 33, 9]. We will consider this problem in Sect. 5.1.

4.3 Evolution of the photon distribution by Compton scattering

The thermalization problem with photon production in the y-era ($z \lesssim 5\times10^4$) can be treated approximately using different analytic solutions describing the Compton scattering of photons. No exact solution valid in all regimes was found, but still progress can be made in different limiting cases.

4.3.1 Doppler-dominated scattering

One classic solution of the Compton scattering problem was given by Zeldovich & Sunyaev [59] for cases when recoil terms ($\propto f(1+f)$) can be neglected in the Kompaneets equation. One example is the scattering of CMB photons by hot electrons, since then $T_\gamma/T_\mathrm{e}\simeq10^{-7}$, so that from Eq. (4.1) we have

$$\left.\frac{\partial f}{\partial\tau}\right|_\mathrm{CS}\approx\frac{\theta_\mathrm{e}}{x^2}\frac{\partial}{\partial x}x^4\frac{\partial}{\partial x}f. \tag{4.17}$$

Defining $y_\mathrm{e}=\int\theta_\mathrm{e}\,\mathrm{d}\tau$ and introducing $\xi=\ln x$ we have $\partial_{y_\mathrm{e}}f=\partial^2_\xi f+3\partial_\xi f$. By transforming to $z=\xi+3y_\mathrm{e}$ we arrive at $\partial_{y_\mathrm{e}}f=\partial^2_z f$, which is the simple diffusion equation. Thus, the solution is [59]

$$f(y_\mathrm{e},x)=\frac{1}{\sqrt{4\pi y_\mathrm{e}}}\int f(0,x')\,\mathrm{e}^{-\frac{(\ln[x/x']+3y_\mathrm{e})^2}{4y_\mathrm{e}}}\,\frac{\mathrm{d}x'}{x'}=\int f(0,x')\,G_\mathrm{D}(y_\mathrm{e},x'\rightarrow x)\,\mathrm{d}x'. \tag{4.18}$$

This shows that

$$G_\mathrm{D}(y_\mathrm{e},x'\rightarrow x)=\frac{\mathrm{e}^{-\frac{(\ln[x/x']+3y_\mathrm{e})^2}{4y_\mathrm{e}}}}{\sqrt{4\pi y_\mathrm{e}}\,x'}\equiv\frac{x'^3}{x^3}\,\frac{\mathrm{e}^{-\frac{(\ln[x/x']-3y_\mathrm{e})^2}{4y_\mathrm{e}}}}{\sqrt{4\pi y_\mathrm{e}}\,x'}. \tag{4.19}$$

is the *Green's function* of the Doppler-dominated Comptonization problem, describing how a narrow line broadens and shifts due to the thermal motions of the electrons. Starting with $f(0,x)=A\,\delta(x-x_0)/x^2$, it is straightforward to show that $\rho_\gamma(y_\mathrm{e})=\rho_\gamma(0)\,\mathrm{e}^{4y_\mathrm{e}}$. The positions of the maximum in $N_x=x^2f(y_\mathrm{e},x)$ is $x_0(y_\mathrm{e})=x_0\,\mathrm{e}^{y_\mathrm{e}}$, while for $I_x=x^3f(y_\mathrm{e},x)$ it is at $x_0(y_\mathrm{e})=x_0\,\mathrm{e}^{3y_\mathrm{e}}$. Similarly, the FWHM of the distribution increases as $\Delta\nu/\nu=2\mathrm{e}^{3y_\mathrm{e}}\sinh(2\sqrt{y_\mathrm{e}\ln2})\simeq4\sqrt{y_\mathrm{e}\ln2}$.

The solution is illustrated in Fig. 4.4 for an initially narrow line at low and intermediate frequencies. The approximation, Eq. (4.18), represents the numerical solution very well until recoil terms become important. This leads to a significant deviation of the photon distribution at high frequencies, which for the consider problems starts being important for $y_\mathrm{e}\gtrsim1$ and illustrates the limitations of the approximation.

4.3.2 Recoil-dominated scattering

The other simple solution can be obtained in the limit $h\nu\gg kT_\mathrm{e}$. In this case, Doppler redistribution is negligible and one has

$$\left.\frac{\partial f}{\partial\tau}\right|_\mathrm{CS}\approx\frac{\theta_\gamma}{x^2}\frac{\partial}{\partial x}x^4f(1+f)=\frac{1}{\omega^2}\frac{\partial}{\partial\omega}\omega^4f(1+f), \tag{4.20}$$

with $\omega=h\nu/m_\mathrm{e}c^2$. If we assume $f\ll1$, then the equation can be solved analytically, giving

$$f(\tau,\omega)=\frac{f\left(0,\frac{\omega}{1-\omega\tau}\right)}{[1-\omega\tau]^4}. \tag{4.21}$$

For an initially narrow line, $f_\delta(0,\omega)=A\,\delta(\omega-\omega_0)/\omega^2$, located at ω_0, this just means that the line will move along $\omega_0(\tau)=\omega_0/(1+\omega_0\tau)$, or $f_\delta(\tau,\omega)=A\,\delta[\omega-\omega_0(\tau)]/\omega^2$. At lowest order in $\omega_0\tau$, this means $\Delta\nu/\nu_0\approx-\omega_0\tau$, as we already know from the discussion in Sect. 3.3.3. The solution does, however, not include the broadening

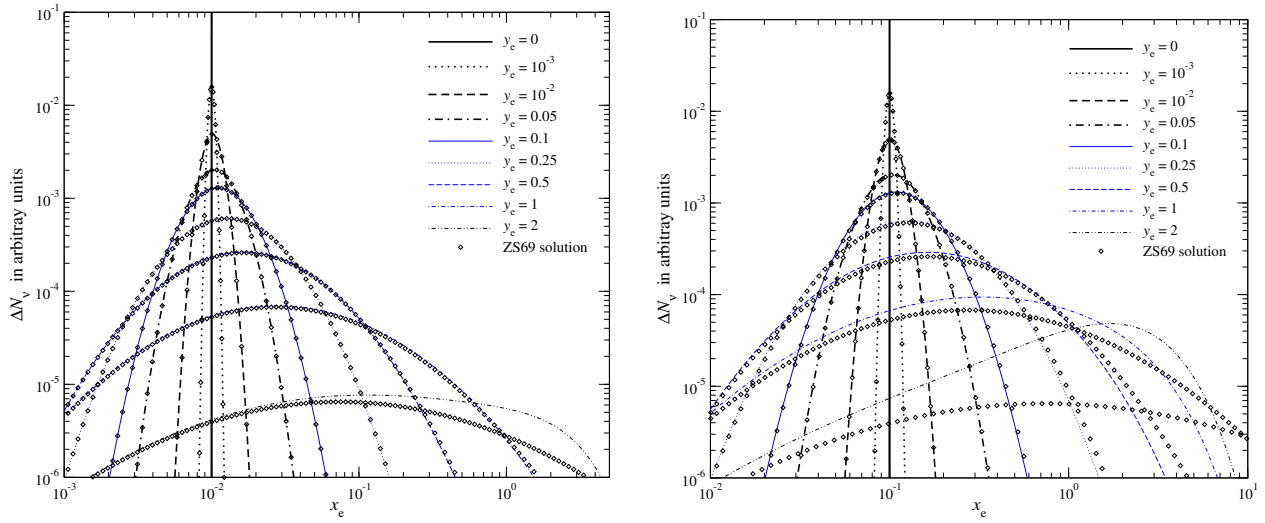

Figure 4.4: Time-evolution of $\Delta N_\nu = \nu^2 \Delta n$ for different values of the y-parameter but neglecting stimulated scattering. The left panel shows the case, for an initially narrow line which was injected at $x_{e,0} = 10^{-2}$, while the right panel shows the solution for injection at $x_{e,0} = 10^{-1}$. In both figures, we present the results as obtained by numerically solving the Kompaneets equation. In addition, we give the analytic solution according to Zeldovich & Sunyaev [59], Eq. (4.18). The figure is taken from Chluba & Sunyaev [15].

of the line by the scattering event. Even for $T_e = 0$, recoil-dominated scattering leads to line broadening $\left\langle \Delta\nu^2/\nu^2 \right\rangle \simeq \frac{7}{5}\omega^2$ [47], which is neglected in the Kompaneets equation, being higher order in $\omega \ll 1$. Including this effect, one has the diffusion equation [47]

$$\left.\frac{\partial f}{\partial \tau}\right|_{\rm CS} \approx \frac{1}{\omega^2}\frac{\partial}{\partial \omega}\omega^4\left(f + \frac{7}{10}\omega^2\partial_\omega f\right). \tag{4.22}$$

Analytic solutions of this equation were discussed by Grebenev & Syunyaev [25] and are relevant for the scattering of hard X-ray lines by cold electrons.

Finally, when stimulated effects dominate ($f^2 \gg f$ and $h\nu \gg kT_e$), the solution of the evolution equation $\partial_\tau f \approx \omega^{-2}\partial_\omega \omega^4 f^2$ is determined by the implicit equation [57, 51]

$$\nu = \phi(s) - \frac{2h}{m_e c^2}\,\tau\, s, \tag{4.23}$$

with $s(\omega, \tau_T) = \omega^2 f(\omega, \tau)$ and where $\phi(z)$ can be found from the initial condition ($\phi(z) \equiv s_0^{-1}(z)$, where $s_0^{-1}(z)$ is the inverse function of $s(\omega, \tau)$ at $\tau = 0$). The non-linear nature of this problem can lead to the appearance of *shock waves* in the photon field, e.g. as explained in Zeldovich & Levich [57] and Zeldovich & Sunyaev [60].

4.3.3 Background-induced stimulated scattering

The previous solutions were all derived for the total photon field. For the evolution of spectral distortions, we are, however, in the situation that the distortion is a small perturbation around the huge CMB blackbody photon bath. In this case, one can rewrite the Kompaneets equation as

$$\left.\frac{\partial f}{\partial \tau}\right|_{\rm CS} \approx (\theta_e - \theta_\gamma) Y_{\rm SZ}(x) + \frac{\theta_\gamma}{x^2}\frac{\partial}{\partial x} x^4\left[\frac{\partial}{\partial x}\Delta f + \Delta f(1 + 2f_{\rm bb})\right], \tag{4.24}$$

where we separated the blackbody (background) and distortion part, $f = f_{\rm bb} + \Delta f$, and kept only linear order terms ($\Delta f \ll 1$ and $(T_e - T_\gamma)/T_\gamma \ll 1$). We can see that there are two relevant time-scales: (i) $y = \int (\theta_e - \theta_\gamma)\, {\rm d}\tau$,

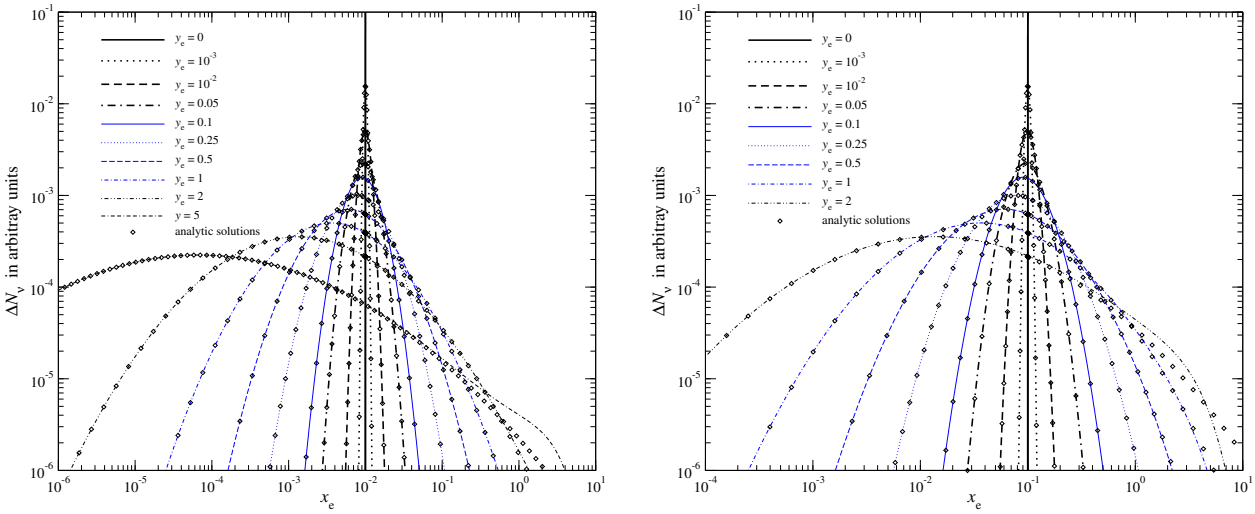

Figure 4.5: Time-evolution of $\Delta N_\nu = \nu^2 \Delta n$ for different values of the y-parameter *including* the effect of stimulated scattering in the blackbody ambient radiation field. The left panel shows the case, for an initially narrow line which was injected at frequency $x_{\rm e,0} = 10^{-2}$, while the right panel shows the solution for injection at $x_{\rm e,0} = 10^{-1}$. In both figures we show the results as obtained by numerically solving Kompaneets equation with $T_\gamma = T_{\rm e}$. In addition, we give the analytic solutions of the linearized problem, Eq. (4.25), according to Eq. (4.26). The figure is taken from Chluba & Sunyaev [15].

which determines how the y-type distortion is sourced by the difference in the electron and photon temperature, and (ii) $y_\gamma = \int \theta_\gamma \, {\rm d}\tau$, which determines how the additional distortion, Δf, broadens and shifts. As long as $y\, y_\gamma \ll 1$, these two parts of the problem can be treated separately.

Thus, let us assume that initially we have a low-frequency frequency feature in the much larger blackbody spectrum with $T_\gamma \simeq T_{\rm e}$. Then, for $f_{\rm bb} \approx 1/x \gg 1$, we may write [15]

$$\left.\frac{\partial \Delta f}{\partial \tau}\right|_{\rm CS} \approx \frac{\theta_\gamma}{x^2}\frac{\partial}{\partial x} x^4 \left[\frac{\partial}{\partial x}\Delta f + \frac{2}{x}\Delta f\right]. \tag{4.25}$$

This equation describes the evolution of the distortion but including the *background-induced stimulated scattering* effect. This case is relevant for example for the evolution of hydrogen and helium recombination lines [45, 16] emitted around $z \simeq 10^3$ in the Rayleigh-Jeans tail of the CMB [15]. Transforming to $\xi = \ln x$ and $s = x^3 \Delta f$, we find $\partial_{y_\gamma} s = \partial_\xi^2 s - \partial_\xi s$. By setting $z = \xi - y_\gamma$, we arrive at $\partial_{y_\gamma} s = \partial_z^2 s$, which has the solution [15]

$$f(y_\gamma, x) = \frac{1}{\sqrt{4\pi y_\gamma}} \int \frac{x'^3}{x^3} f(0, x') \, {\rm e}^{-\frac{(\ln[x/x']-y_\gamma)^2}{4y_\gamma}} \frac{{\rm d}x'}{x'} = \int f(0, x') \, G_{\rm B}(y_\gamma, x' \rightarrow x) \, {\rm d}x', \tag{4.26}$$

with the Green's function

$$G_{\rm B}(y_\gamma, x' \rightarrow x) = \frac{x'^3}{x^3} \frac{{\rm e}^{-\frac{(\ln[x/x']-y_\gamma)^2}{4y_\gamma}}}{\sqrt{4\pi y_\gamma}\, x'}. \tag{4.27}$$

This is very similar to the solution, Eq. (4.19), but with the different shift of the photon caused by stimulated scattering in the blackbody field. Starting with $f(0, x) = A\, \delta(x - x_0)/x^2$, it is straightforward to show that $\rho_\gamma(y_\gamma) = \rho_\gamma(0)\, {\rm e}^{2y_\gamma}$. The positions of the maximum in $N_x = x^2 f(y_\gamma, x)$ is $x_0(y_\gamma) = x_0\, {\rm e}^{-y_\gamma}$, while for $I_x = x^3 f(y_\gamma, x)$ it is at $x_0(y_\gamma) = x_0\, {\rm e}^{y_\gamma}$. Similarly, the FWHM of the photon distribution increases as $\Delta\nu/\nu = 2{\rm e}^{y_\gamma} \sinh(2\sqrt{y_\gamma \ln 2}) \simeq 4\sqrt{y_\gamma \ln 2}$. Overall this means that the blackbody-induced stimulated scattering effect slows down the motion of photons towards higher energies. The photon distribution still gains energy

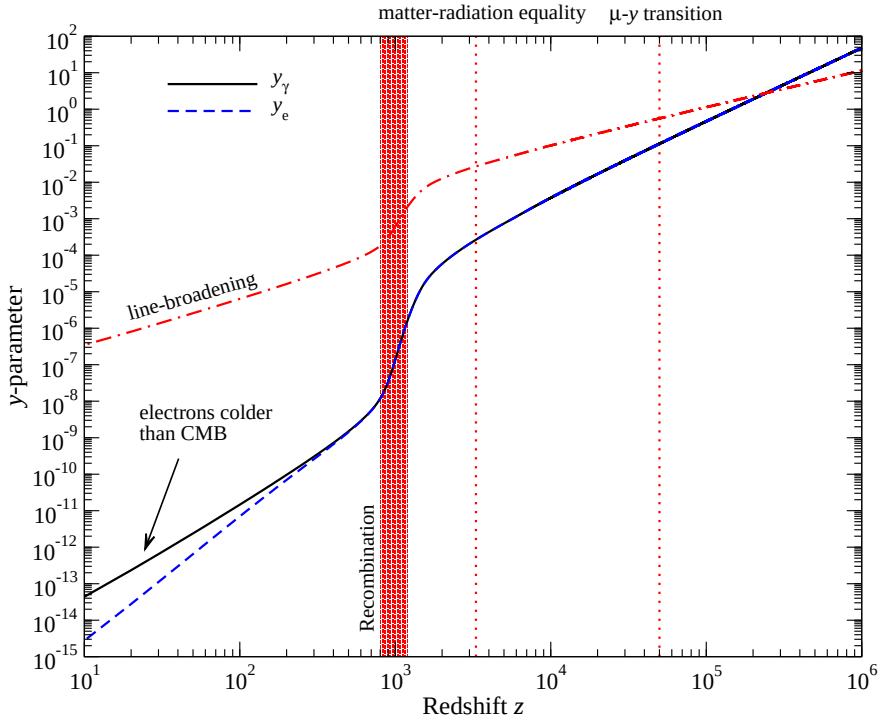

Figure 4.6: Dependence of the y-parameters, y_γ and y_e, on redshift. After recombination the y-parameters drop strongly since the number of free electrons decreases exponentially. At late times, electrons drop out of equilibrium with the photons so that $y_e < y_\gamma$. Around $z_K = 5 \times 10^4$, we have $y_e \simeq y_\gamma \simeq 0.1$. The line-broadening, $\Delta\nu/\nu \simeq 2\sqrt{y_\gamma \ln 2}$, is also illustrated. After recombination it becomes much smaller than $\Delta\nu/\nu \simeq 10^{-3}$.

but only $\Delta\rho_\gamma/\rho_\gamma \simeq e^{2y_\gamma}$ instead of $\Delta\rho_\gamma/\rho_\gamma \simeq e^{4y_e}$ when neglecting stimulated scattering. The line-broadening caused by the Doppler effect is similar to the case without induced scattering. For $N_x = x^2 f$, this is illustrated in Fig. 4.5. In this case, photons move towards lower frequencies rather than higher.

Efficiency of redistribution. At late times, redistribution of photons in energy by Compton scattering becomes very inefficient. To quantify this statement a little more, we can compute the scattering y-parameter, $y_\gamma = \int \theta_\gamma \, d\tau$. At high redshifts ($z \gtrsim 10^4$), it scales like

$$y_\gamma = \int_0^z \theta_\gamma \frac{\sigma_T N_e c}{H(1+z)} \, dz \approx \frac{\sigma_T N_H (1 + 2f_{He}) c}{2H_0 \sqrt{\Omega_r}} \frac{kT_0}{m_e c^2} (1+z)^2 \approx 4.84 \times 10^{-11} (1+z)^2. \tag{4.28}$$

This implies that around $z \simeq 1.4 \times 10^5$ the y-parameter becomes smaller than unity. The dependence of y_γ on redshift is illustrated in Fig. 4.6. It is clear that after recombination redistribution by scattering is already negligible. The amount of Doppler broadening, however, still reaches $\simeq 1\% - 10\%$ between $z \simeq 10^3 - 10^4$. For the calculation of the helium recombination lines it is thus important [45].

The above analysis shows that for scenarios with late photon production, one can practically neglect Compton scattering at $z \leq 10^3$, unless the initial photon energy is very large so that recoil will become significant. In this case, the largest effect will manifest itself as heating of the electrons. At redshifts $z \simeq 10^3 - 5 \times 10^4$, one can apply the analytic solutions discussed above to get an estimate for the distortion, while at $z \gtrsim 5 \times 10^4$ the approximation, Eq. (4.16b), for μ, should become applicable, although we still have to include the effect of photon production on the final amplitude of μ.

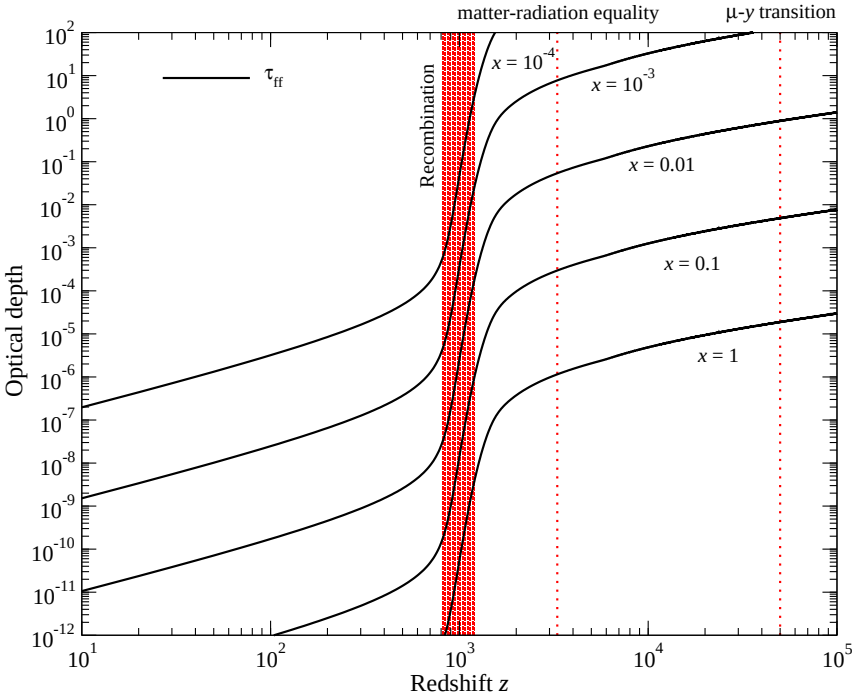

Figure 4.7: Absorption optical depth for BR at different redshifts and frequencies x. At low frequencies, the rough scaling is $\tau_{\rm ff} \simeq x^{-2}$. For $x \simeq 10^{-4}$, the Universe becomes transparent ($\tau_{\rm ff} \simeq 1$) around recombination. For $x \simeq 10^{-3}$ this transition happens around $z \simeq 1700$ and for $x \simeq 0.01$ it is $z \simeq 10^5$.

4.4 Evolution under free-free absorption only

As we just explained, after recombination Compton scattering can be neglected. In this case, the photon distribution only evolves according to BR, since even DC is already inefficient. The kinetic equation for the photons thus reads

$$\frac{\partial f}{\partial \tau} \approx \frac{K_{\rm BR}\, {\rm e}^{-x_{\rm e}}}{x_{\rm e}^3}\big[1 - f\,({\rm e}^{x_{\rm e}} - 1)\big] + S\,(\tau, x), \tag{4.29}$$

where we included a possible photon source term, $S\,(\tau, x)$. The change of the electron temperature by BR emission is very small and can be neglected. Let us also neglect the difference of the photon and electron temperature, so that the evolution equation for a distortion to the CMB blackbody becomes

$$\frac{\partial \Delta f}{\partial \tau} \approx -\frac{K_{\rm BR}(\tau, x)(1 - {\rm e}^{-x})}{x^3}\,\Delta f + S\,(\tau, x). \tag{4.30}$$

Between $z = 0$ and z_i, this equation has the simple solution

$$\Delta f(x, 0) \approx \Delta f(x, z_i)\,{\rm e}^{-\tau_{\rm ff}(x, z_i)} + \int_0^{z_i} {\rm e}^{-\tau_{\rm ff}(x, z')}\,\tilde{S}\,(z', x)\,{\rm d}z \tag{4.31}$$

$$\tau_{\rm ff}(x, z) = \int_0^{z} \frac{K_{\rm BR}(z, x)(1 - {\rm e}^{-x})}{x^3}\,\frac{\sigma_{\rm T} N_{\rm e} c\,{\rm d}z}{H(1+z)}, \tag{4.32}$$

where we introduced the new source function, $\tilde{S}\,(z, x)$, with respect to redshift. The free-free absorption optical depth can be calculated using the result from CosmoRec for the ionization history. We illustrate the result in Fig. 4.7 for several values of x. In the post recombination era ($z \lesssim 10^3$), signals produced at $x \gtrsim 10^{-4}$ ($\equiv 6\,$MHz) are not significantly attenuated by free-free absorption. For percent-level precision, one does furthermore need to include the effect of free-free absorption at $x \lesssim 0.1$ ($\equiv 6\,$GHz) at $z \simeq 10^3 - 10^5$.

4.5 Inclusion of photon production and the distortion visibility function

In the previous sections, we discussed several analytic solutions that allow describing the distortions created by photon injection and heating. However, at early times, Compton scattering and photon emission and absorption have to be considered *simultaneously*. How can we proceed in this case? Matters are simplified because CS is still very efficient when photon production is important. We can thus hope to make progress by solving the problem along a *sequence of quasi-stationary stages* for the chemical potential.

Let us assume that a non-zero constant chemical potential fully characterizes the distortion for the period of interest. In that case from Eq. (4.13a), we can directly deduce

$$\frac{\mathrm{d}\mu_0}{\mathrm{d}\tau} \approx \frac{3}{\kappa^{\mathrm{c}}}\frac{\mathrm{d}\ln a^4\rho_\gamma}{\mathrm{d}\tau} - \frac{4}{\kappa^{\mathrm{c}}}\frac{\mathrm{d}\ln a^3 N_\gamma}{\mathrm{d}\tau}, \tag{4.33}$$

with $\kappa^{\mathrm{c}} \approx 2.1419$. The right hand side describes the increase of the chemical potential by energy release and the reduction by photon production. Since photons and ordinary matter are tightly coupled until $z \simeq 100$, heating of the electrons means heating of the photons, so that one part of the energy release term follows directly from the matter heating rate. Additional photon production [the source term in Eq. (3.54)] contributes to *both* energy release and change of the photon number. DC and BR emission occur mostly at very low frequencies so that they mainly contribute to changing the photon number density.

To make progress, we have to determine the terms on the right hand side of Eq. (4.33) from the photon Boltzmann equation, Eq. (3.54). Pure energy exchange appears only from the Compton scattering term due to interactions with the electrons. Energy injection related to the source term, $S(\tau, x)$, and DC / BR emission terms adds to this. Assuming that no extra source term of photons is present, this means that

$$\frac{\mathrm{d}\ln a^4\rho_\gamma}{\mathrm{d}\tau} \approx 4(\theta_{\mathrm{e}} - \theta_{\mathrm{e}}^{\mathrm{eq}}) + \mathcal{H}_{\mathrm{em}} \approx \frac{\dot{Q}_{\mathrm{e}}^*}{\rho_\gamma}. \tag{4.34}$$

where $\theta_{\mathrm{e}}^{\mathrm{eq}} = kT_{\mathrm{e}}^{\mathrm{eq}}/m_{\mathrm{e}}c^2$ and $\mathcal{H}_{\mathrm{em}}$ describes the effect on the energy density of the photons related to DC and BR emission. This term is small and can be neglected right away, also because it actually cancels identically when computing the equilibrium electron temperature correctly [10]. Here, $\dot{Q}_{\mathrm{e}}^*$ denotes the effective heating rate (≡ energy per volume and Thomson scattering time) of electrons and baryons by the considered process. This rate is slightly smaller than the direct heating rate because the adiabatic cooling of matter always extracts some amount of energy [17, 10], as we will discuss below. Also, at late times after recombination, not all heating of the electrons actually directly reaches the photon field, an aspect that has to be included [17].

For the photon production term in Eq. (4.33), only the source term and the DC / BR emission terms are relevant, since CS conserves the photon number. For simplicity, we again omit the source term. We also know that at low frequencies, the CMB spectrum is pushed into equilibrium with the electrons, so that it is best to describe the distortion with respect to a blackbody at the electron temperature, $f = f_{\mathrm{bb}}(T_{\mathrm{e}}) + \Delta f$. Since the electron and photon temperature are close to each other, at linear order this gives

$$\frac{\mathrm{d}\ln a^3 N_\gamma}{\mathrm{d}\tau} \approx -\frac{1}{G_2^{\mathrm{Pl}}}\int \frac{\Lambda(x, T_\gamma)(1-\mathrm{e}^{-x})}{x}\,\Delta f\,\mathrm{d}x \approx \frac{1}{G_2^{\mathrm{Pl}}}\int \frac{\Lambda(x, T_\gamma)}{x(\mathrm{e}^x-1)}\,\mu(t,x), \tag{4.35}$$

where we used $\Delta f \approx -G(x)\,\mu(t,x)/x$ and defined $\Lambda(x, T_\gamma) = K_{\mathrm{BR}}(x, T_\gamma) + K_{\mathrm{DC}}(x, T_\gamma)\,\mathrm{e}^{-x}$. Now we see a problem: for $x \ll 1$ the integral diverges unless $\mu(t, x)$ vanishes faster than $\Lambda(x)/x^2 \simeq -\ln(x)/x^2$. Assuming constant chemical potential is therefore insufficient here! But there is a simple trick according to Sunyaev & Zeldovich [54]: energetically the high frequency part of the spectrum is important. In that regime, photon production is negligible, so that one can expect $\mu(t, x) \approx \mu_0(t)$ [$x \gtrsim 1$]. That means that Eq. (4.33) should be enough to describe the energetic aspects of the problem, while to obtain an expression for the photon production rate at low frequencies, we do need to look at the kinetic equation again.

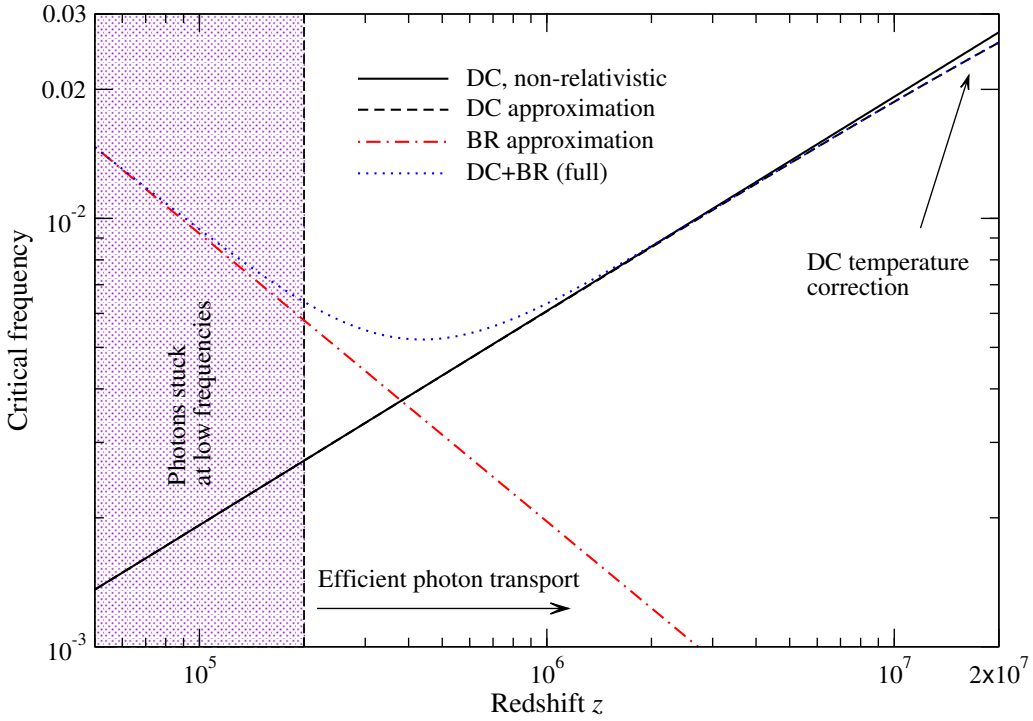

Figure 4.8: Critical frequency, x_c as a function of z. Photon transport is inefficient below $z \simeq 2 \times 10^5$ so that the distortion visibility function quickly approaches unity. DC temperature corrections become noticeable at $z \gtrsim 10^6$. The approximations are from Eq. (4.38) and (4.39). The figure is taken from Chluba [10].

4.5.1 Quasi-stationary solution for the shape of the chemical potential distortion at $x \ll 1$

It is quite straightforward to obtain a solution for the frequency dependence of the chemical potential at $x \ll 1$. We first linearize the problem, assuming that $\mu \ll 1$. We furthermore describe the distortion with respect to the Rayleigh-Jeans spectrum, which is given by a blackbody at the electron temperature, T_e. Finally, we take the limit $x \ll 1$, keeping only leading order terms. Assuming that the solution becomes quasi-stationary, from Eq. (3.54), we find (Exercise 1)

$$0 \approx x^2\mu'' + 2x\mu' - \frac{\Lambda(t,x)/\theta_\gamma}{x^2}\,\mu, \tag{4.36}$$

where we expressed the distortion part in terms of $\mu(t,x)$. This equation was first derived by Sunyaev & Zeldovich [54]. The DC and BR emission coefficients are only weakly dependent on frequency once $x \ll 1$. We can thus replace it by $\Lambda(t,x) \approx \Lambda(t,x_c) \approx \theta_\gamma x_c^2$, where the critical frequency can be determined numerically. Then the equation takes the form [54]

$$0 \approx \partial_x x^2 \partial_x \mu - \frac{x_c^2}{x^2}\,\mu, \tag{4.37}$$

which has the simple solution $\mu(t,x) \approx \mu_0(t)\,\mathrm{e}^{-x_c(t)/x}$. This shows that at $x \gg x_c$, the chemical potential indeed becomes constant, while at low frequencies it vanishes exponentially, with a smooth transition between these regimes around $x \simeq x_c$. The solution thus has the expected limiting behavior, even if strictly speaking it is only valid at low frequencies. Indeed, the correct high frequency behavior is $\mu(t,x) \simeq \mu_0^*(t) + \mathrm{C}(t)\ln x$, where the coefficient, $\mathrm{C}(t)$, is related to the time derivative of the electron temperature [10].

Critical frequency. To complete the problem, we still need to determine the critical frequency, $x_{\rm c}$, in Eq. (4.37). For DC, one can solve the problem analytically, finding [19, 4, 27]

$$x_{\rm c}^{\rm DC} \approx \sqrt{\frac{4\alpha}{3\pi}\,\theta_\gamma I_{\rm dc}^{\rm Pl}} \approx 8.60\times10^{-3}\left[\frac{1+z}{2\times10^6}\right]^{1/2}, \tag{4.38}$$

where corrections due to the DC Gaunt factor were neglected. These can be included following Chluba [10]. The results are illustrated in Fig. 4.8. At high redshifts, the temperature correction reduces the critical frequency notably in comparison with Eq. (4.38). This implies that thermalization should be less efficient, since the frequency at which most photons are produced decreases. At the thermalization redshift $z \simeq 2\times10^6$, the temperature correction to the critical frequency $x_{\rm c}$ is roughly 0.5% and it reaches $\simeq$ 1% at $z \simeq 4\times10^6$. Although this appears to be small, since the critical frequency enters the problem through an integral, the cumulative effect matters so that the correction is amplified and hence significant (see below).

For BR alone, we determined the critical frequency numerically using the expressions from Itoh et al. [30] and assuming a helium mass fraction of $Y_{\rm p} = 0.24$. We find[3]

$$x_{\rm c}^{\rm BR} \approx 1.23\times10^{-3}\left[\frac{1+z}{2\times10^6}\right]^{-0.672} \tag{4.39}$$

to work very well. Comparing with Eq. (4.38), we can see that at the thermalization redshift $z \simeq 2\times10^6$, BR contributes about 10% to the value of the critical frequency. However, the contribution drops rapidly towards higher redshifts (Fig. 4.8). To percent precision, the total critical frequency is $x_{\rm c}^2 \approx (x_{\rm c}^{\rm DC})^2 + (x_{\rm c}^{\rm BR})^2$ [27]. Also, by comparing the redshift dependence of the DC and BR critical frequency, we can see that neglecting DC strongly underestimates the thermalization efficiency.

Approximate photon production term and solution for $\mu_0(t)$. We now can compute the photon production term, Eq. (4.35), using the solution $\mu(t,x) \approx \mu_0(t)\,{\rm e}^{-x_{\rm c}(t)/x}$. It is straightforward to show (Exercise 2) that

$$\frac{{\rm d}\ln a^3 N_\gamma}{{\rm d}\tau} \approx \frac{\theta_\gamma x_{\rm c}}{G_2^{\rm Pl}}\,\mu_0(t). \tag{4.40}$$

Inserting this into Eq. (4.33), and using Eq. (4.34), we find

$$\begin{aligned}\frac{{\rm d}\mu_0}{{\rm d}\tau} &\approx \gamma_\rho\frac{\dot{Q}_{\rm e}^*}{\rho_\gamma} - \gamma_N\,\theta_\gamma x_{\rm c}\,\mu_0\\ \gamma_\rho &= 3/\kappa^{\rm c} \approx 1.401, \quad \gamma_N = 4/(G_2^{\rm Pl}\kappa^{\rm c}) \approx 0.7769,\end{aligned} \tag{4.41}$$

where $\kappa^{\rm c} \approx 2.1419$. Then, by introducing the *thermalization optical depth*

$$\tau_\mu(z) \approx \gamma_N\int_0^z \theta_\gamma x_{\rm c}\frac{\sigma_{\rm T}N_{\rm e}c\,{\rm d}z'}{H(1+z')}, \tag{4.42}$$

and assuming that there is no initial distortion at very early times, we can finally write

$$\mu_0(z) \approx 1.401\int_z^\infty \frac{\dot{Q}_{\rm e}^*}{\rho_\gamma}\frac{{\rm e}^{-\tau_\mu(z',z)}\,{\rm d}z'}{H(1+z')} \tag{4.43}$$

with $\tau_\mu(z,z') = \tau_\mu(z) - \tau_\mu(z')$. The scaling of τ_μ with redshift depends on the photon production process. For any given effective energy release rate, $\dot{Q}_{\rm e}^*$, one can thus directly estimate the final amplitude of the μ-distortion.

[3]Note that again we can evaluate Λ assuming $T_{\rm e} = T_\gamma$.

4.5.2 Single energy release and the distortion visibility function

Assuming only a single energy injection of $\Delta\rho_\gamma/\rho_\gamma$ at some heating redshift z_h, from Eq. (4.43) we find [54]

$$\mu_0(z) \approx 1.401\frac{\Delta\rho_\gamma}{\rho_\gamma}\mathrm{e}^{-\tau_\mu(z_\mathrm{h},z)} = \mu_\mathrm{h}\,\mathcal{J}(z_\mathrm{h},z) \tag{4.44}$$

Here, we defined $\mu_\mathrm{h} = 1.401\Delta\rho_\gamma/\rho_\gamma$. The factor $\mathcal{J}(z_\mathrm{h},z) = \mathrm{e}^{-\tau_\mu(z_\mathrm{h},z)}$ defines the *spectral distortion visibility* between the heating redshift z_h and z. It determines the fraction of energy injected at z_h that is still visible as a distortion at z. For $\mathcal{J}(z_\mathrm{h},z) \simeq 1$, most of the energy is still stored in the distortion, while for $\mathcal{J}(z_\mathrm{h},z) \ll 1$, most of the energy was thermalized and converted into a temperature shift. In this picture, we have the fractional contributions to the photon energy density

$$\frac{\Delta\rho_\gamma}{\rho_\gamma} = \int_z^\infty \frac{\dot{Q}_\mathrm{e}^*}{\rho_\gamma}\frac{\mathrm{d}z'}{H(1+z')} \approx \int_z^\infty \frac{\mathrm{d}(Q_\mathrm{e}^*/\rho_\gamma)}{\mathrm{d}z}\,\mathrm{d}z' \tag{4.45a}$$

$$\left.\frac{\Delta\rho_\gamma}{\rho_\gamma}\right|_\mathrm{dist} = \int_z^\infty \frac{\mathrm{d}(Q_\mathrm{e}^*/\rho_\gamma)}{\mathrm{d}z}\mathrm{e}^{-\tau_\mu(z',z)}\,\mathrm{d}z' \tag{4.45b}$$

$$\left.\frac{\Delta\rho_\gamma}{\rho_\gamma}\right|_T = \int_z^\infty \frac{\mathrm{d}(Q_\mathrm{e}^*/\rho_\gamma)}{\mathrm{d}z}\left(1-\mathrm{e}^{-\tau_\mu(z',z)}\right)\mathrm{d}z' = \frac{\Delta\rho_\gamma}{\rho_\gamma} - \left.\frac{\Delta\rho_\gamma}{\rho_\gamma}\right|_\mathrm{dist}, \tag{4.45c}$$

so that $\mu_0 \approx 1.401\ \Delta\rho_\gamma/\rho_\gamma\big|_\mathrm{dist}$ and $\Delta T/T \approx (1/4)\ \Delta\rho_\gamma/\rho_\gamma\big|_T$, at least for energy released above the Comptonization redshift $z_\mathrm{h} \gtrsim z_\mathrm{K} \simeq 5\times10^4$.

So what does the distortion visibility function look like? To give the distortion visibility function, we need to compute the thermalization optical depth, $\tau_\mu(z)$ in Eq. (4.42). If we only include DC emission, the integral is simple, giving [19, 4, 27]

$$\mathcal{J}_\mathrm{DC}(z_\mathrm{h}) = \mathcal{J}_\mathrm{DC}(z_\mathrm{h}, z=0) = \exp\left(-[z_\mathrm{h}/z_\mathrm{dc}]^{5/2}\right), \tag{4.46}$$

with DC thermalization redshift [e.g., 27]

$$z_\mathrm{dc} \approx 1.98\times10^6\left[\frac{\Omega_\mathrm{b}h^2}{0.022}\right]^{-2/5}\left[\frac{T_0}{2.725\mathrm{K}}\right]^{1/5}\left[\frac{(1-Y_\mathrm{p}/2)}{0.88}\right]^{-2/5}, \tag{4.47}$$

assuming $N_\mathrm{eff} = 3.046$. At $z \gg z_\mathrm{dc}$, thermalization is very efficient and the distortion visibility drops exponentially. If alternatively we only include BR emission, we find [54, 19, 27]

$$\mathcal{J}_\mathrm{BR}(z_\mathrm{h}) = \exp\left(-[z_\mathrm{h}/z_\mathrm{br}]^{1.328}\right) \tag{4.48}$$

with $z_\mathrm{br} \approx 5.27\times10^6$. In the classical result, given first by Sunyaev & Zeldovich [54], the power-law coefficient is $5/4 = 1.25$ because a different approximation for the BR Gaunt factor was utilized. This shows that the thermalization redshift is significantly higher when only BR is included. In addition, the distortion visibility function drops less steeply at $z \gtrsim 5.27\times10^6$.

In Fig. 4.9 we compare the distortion visibility functions for DC and BR only with the numerical result obtained from CosmoTherm [17, 10]. Clearly, DC emission increases the thermalization efficiency significantly. If only BR were taken into account, we would still expect to see some small distortion even from the tail of the electron-positron annihilation era around $z \simeq 2\times10^7$! This would be quite complicated to compute, but luckily the distortion visibility is exceedingly small, even if only DC is included, providing a rough but tiny upper limit. Comparing with the full numerical result, $\mathcal{J}_\mathrm{DC}(z_\mathrm{h})$, provides a very good approximation, which, for simple estimates, is more than sufficient. In Sect. 4.6 we will discuss some improvements for $\mathcal{J}$, but for refined computations it seems more reasonable to simply using the Green's function method described in Sect. 5.

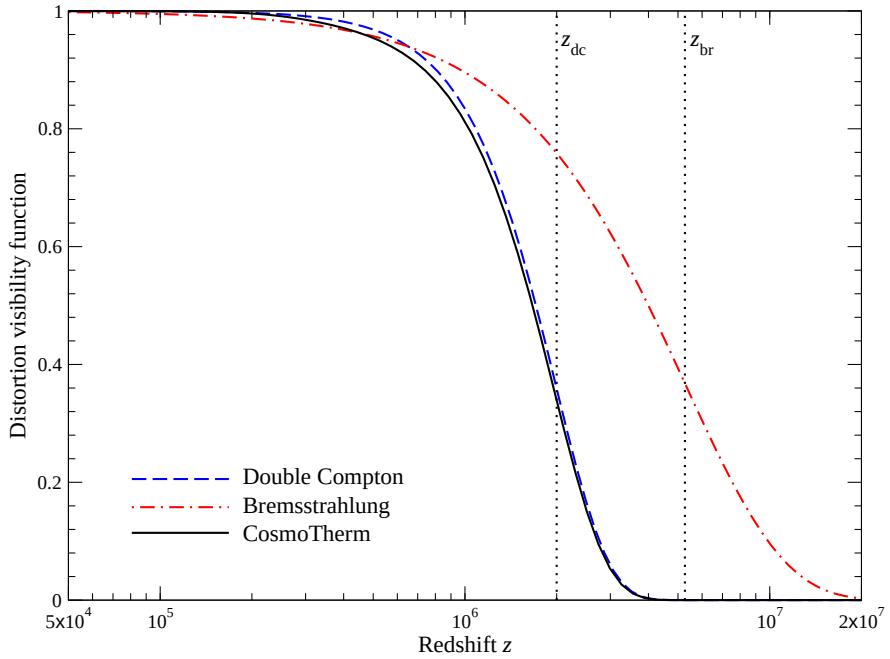

Figure 4.9: Distortion visibility function. We compare $\mathcal{J}_{\rm DC}(z_{\rm h})$, $\mathcal{J}_{\rm BR}(z_{\rm h})$ and the numerical result obtained with CosmoTherm. DC emission significantly change the thermalization efficiency. Deviations from the numerical result can be captured by adding several effects, as discussed in Sect. 4.6.

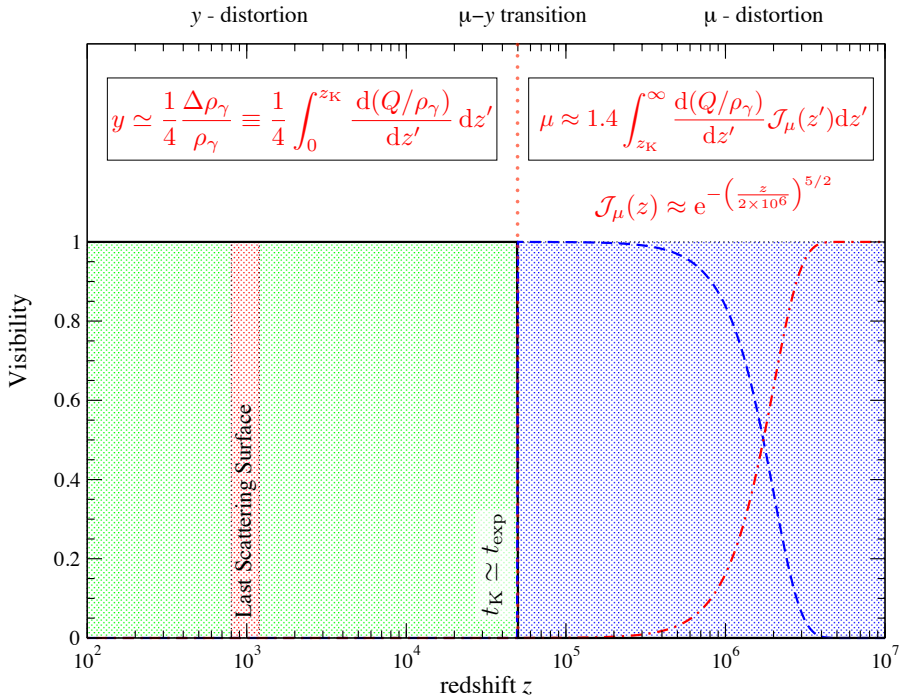

Figure 4.10: Improved picture for the formation of primordial distortions. At low redshifts ($z \lesssim z_{\rm K} \simeq 5\times10^4$), a y-distortion is formed with distortion visibility close to unity, while at high redshifts a μ-distortion appears. The energy release has to be weighted with distortion visibility function which drops exponentially at $z_{\rm dc} \gtrsim 2\times10^6$, leading to a pure temperature shift in that regime from inside the *cosmic photosphere*.

4.5.3 Improved description of primordial distortions

We can now add the first improvement to the picture for the formation of primordial distortions, presented in Sect. 4.2.3 and Fig. 4.3. The transition between μ and y-distortion is still abrupt around $z \simeq z_{\rm K} \simeq 5 \times 10^4$, but the distortion visibility at $z \gtrsim z_{\rm K}$ is no longer unity, which accounts for the effect of thermalization on the distortion amplitude. We can now write the change of the CMB spectrum with respect to the initial blackbody at very early times as $\Delta f \approx Y_{\rm SZ}\, y + M(x)\,\mu_0 + G(x)\,\Delta_T$, where $\Delta_T = \Delta T/T = (1/4)\,\Delta\rho_\gamma/\rho_\gamma\big|_T$. Using the definitions of Eq. (4.45), we may write

$$\frac{\Delta\rho_\gamma}{\rho_\gamma} \approx \int_0^\infty \frac{{\rm d}(Q_{\rm e}^*/\rho_\gamma)}{{\rm d}z}\,{\rm d}z' \tag{4.49a}$$

$$\frac{\Delta\rho_\gamma}{\rho_\gamma}\bigg|_i = \int_0^\infty \frac{{\rm d}(Q_{\rm e}^*/\rho_\gamma)}{{\rm d}z}\,\mathcal{J}_i\,{\rm d}z', \tag{4.49b}$$

where $\mathcal{J}_y(z) \approx \Theta_{\rm H}(z_{\rm K} - z)$, $\mathcal{J}_\mu(z) \approx \Theta_{\rm H}(z - z_{\rm K})\,\exp\left(-[z/z_{\rm dc}]^{5/2}\right)$ and $\mathcal{J}_T(z) \approx 1 - \mathcal{J}_\mu(z)$. Here, $\Theta_{\rm H}(x)$ is the Heaviside step function, $\Theta_{\rm H}(x) = 1$ for $x \geq 0$ and $\Theta_{\rm H}(x) = 0$ otherwise. The visibility functions, $\mathcal{J}_i$, determine the fractions of energy that go into T, μ and y distortion parts. By construction, one has $\sum_i \mathcal{J}_i = 1$ (see Fig. 4.10 for illustration).

In Sect. 5.1, we will discuss the last refinement that takes into account that the transition between μ and y distortions is not abrupt but occurs over a range of redshifts where in the intermediate regime the distortion is not only given by the superposition of μ and y-distortion.

4.6 Refined computation of the distortion visibility function

Exercises

Exercise 1 Derive Eq. (4.36) from the photon evolution equation, Eq. (3.54).

Exercise 2 Derive the approximation Eq. (4.40) for the photon production term. How large are the corrections when you numerically compute the emission term using DC only.

Chapter 5

Computation of the distortions using the distortion Green's function

5.1 Spectral distortion in the transition between the μ and y-eras

Bibliography

[1] André P. et al., 2014, JCAP, 2, 6
[2] Bennett C. L. et al., 2003, ApJS, 148, 1
[3] Birkinshaw M., 1999, Phys. Reports, 310, 97
[4] Burigana C., Danese L., de Zotti G., 1991, A&A, 246, 49
[5] Carlstrom J. E., Holder G. P., Reese E. D., 2002, ARA&A, 40, 643
[6] Challinor A., Lasenby A., 1998, ApJ, 499, 1
[7] Chluba J., 2005, PhD thesis, LMU München
[8] Chluba J., 2013, MNRAS, 436, 2232
[9] Chluba J., 2013, MNRAS, 434, 352
[10] Chluba J., 2014, MNRAS, 440, 2544
[11] Chluba J., Dai L., 2014, MNRAS, 438, 1324
[12] Chluba J., Khatri R., Sunyaev R. A., 2012, MNRAS, 425, 1129
[13] Chluba J., Nagai D., Sazonov S., Nelson K., 2012, MNRAS, 426, 510
[14] Chluba J., Sazonov S. Y., Sunyaev R. A., 2007, A&A, 468, 785
[15] Chluba J., Sunyaev R. A., 2008, A&A, 488, 861
[16] Chluba J., Sunyaev R. A., 2010, MNRAS, 402, 1221
[17] Chluba J., Sunyaev R. A., 2012, MNRAS, 419, 1294
[18] Chluba J., Switzer E., Nelson K., Nagai D., 2013, MNRAS, 430, 3054
[19] Danese L., de Zotti G., 1982, A&A, 107, 39
[20] Dicke R. H., Peebles P. J. E., Roll P. G., Wilkinson D. T., 1965, ApJ, 142, 414
[21] Dodelson S., 2003, Modern cosmology. Academic Press
[22] Fixsen D. J., 2009, ApJ, 707, 916
[23] Fixsen D. J., Cheng E. S., Gales J. M., Mather J. C., Shafer R. A., Wright E. L., 1996, ApJ, 473, 576
[24] Gould R. J., 1984, ApJ, 285, 275
[25] Grebenev S. A., Syunyaev R. A., 1987, Soviet Astronomy Letters, 13, 438
[26] Hu W., 1995, arXiv:astro-ph/9508126
[27] Hu W., Silk J., 1993, PRD, 48, 485
[28] Illarionov A. F., Sunyaev R. A., 1975, Soviet Astronomy, 18, 413
[29] Itoh N., Kohyama Y., Nozawa S., 1998, ApJ, 502, 7
[30] Itoh N., Sakamoto T., Kusano S., Nozawa S., Kohyama Y., 2000, ApJS, 128, 125
[31] Jauch J. M., Rohrlich F., 1976, The theory of photons and electrons. Springer
[32] Karzas W. J., Latter R., 1961, ApJS, 6, 167
[33] Khatri R., Sunyaev R. A., 2012, JCAP, 9, 16
[34] Khatri R., Sunyaev R. A., Chluba J., 2012, A&A, 540, A124

[35] Kogut A. et al., 2011, JCAP, 7, 25
[36] Kompaneets A., 1956, Sov.Phys. JETP, 31, 876
[37] Kouveliotou C. et al., 2014, ArXiv:1401.3741
[38] Lightman A. P., 1981, ApJ, 244, 392
[39] Mandl F., Skyrme T. H. R., 1952, Royal Society of London Proceedings Series A, 215, 497
[40] Penzias A. A., Wilson R. W., 1965, ApJ, 142, 419
[41] Planck Collaboration et al., 2013, ArXiv:1303.5076
[42] Pozdniakov L. A., Sobol I. M., Sunyaev R. A., 1979, A&A, 75, 214
[43] Pritchard J. R., Loeb A., 2008, PRD, 78, 103511
[44] Rephaeli Y., 1995, ARA&A, 33, 541
[45] Rubiño-Martín J. A., Chluba J., Sunyaev R. A., 2008, A&A, 485, 377
[46] Sazonov S. Y., Sunyaev R. A., 1998, ApJ, 508, 1
[47] Sazonov S. Y., Sunyaev R. A., 2000, ApJ, 543, 28
[48] Silk J., Chluba J., 2014, Science, 344, 586
[49] Spitzer L., 1956, Physics of Fully Ionized Gases. Wiley
[50] Stepney S., 1983, MNRAS, 202, 467
[51] Sunyaev R. A., 1970, Astr. Phys. Letters, 7, 19
[52] Sunyaev R. A., Titarchuk L. G., 1980, A&A, 86, 121
[53] Sunyaev R. A., Zeldovich I. B., 1980, MNRAS, 190, 413
[54] Sunyaev R. A., Zeldovich Y. B., 1970, ApSS, 7, 20
[55] Svensson R., 1984, MNRAS, 209, 175
[56] Zeldovich Y. B., Kurt V. G., Syunyaev R. A., 1968, ZETF, 55, 278
[57] Zeldovich Y. B., Levich E. V., 1969, SJETP, 28, 1287
[58] Zeldovich Y. B., Levich E. V., 1970, SJETPL, 11, 35
[59] Zeldovich Y. B., Sunyaev R. A., 1969, ApSS, 4, 301
[60] Zeldovich Y. B., Sunyaev R. A., 1972, Zhurnal Eksperimentalnoi i Teoreticheskoi Fiziki, 62, 153